THE ROLE OF ZOOPLANKTON AND MINERAL BALLASTING IN THE BIOLOGICAL CARBON PUMP

Dissertation

Zur Erlangung des akademischen Grades eines Doktors der Naturwissenschaften

- Dr. rer. nat. -

Fachbereich Geowissenschaften (FB5) der Universität Bremen

Helga Annelies van der Jagt

August 2019

Cover image: a drifting trap deployed at Cape Blanc during RV Poseidon cruise POS495 in February 2016.

Betreuer:

Dr. Morten H. Iversen

Gutachter:

Prof. Dr. Michal Kucera

Dr. Lionel Guidi

Promotionskolloquium: 8 November 2019

SUMMARY

The global ocean is an important carbon sink, and currently stores one-third of the total anthropogenically released CO_2. One of the major processes affecting the oceans functioning as carbon sink is the 'biological carbon pump'. The biological carbon pump describes the transformation of CO_2 into organic matter and its transport to the deep ocean. It is driven by the fixation of CO_2 into organic matter by photosynthesis in the euphotic zone. This organic matter can form aggregates that sink out of the euphotic zone, resulting in a particulate organic carbon (POC) export flux to the deep. During their descent, sinking aggregates are degraded and remineralized, causing POC flux attenuation. On a global scale, ~1% of the primary production in the euphotic zone is sequestered in deep ocean sediments.

The biological carbon pump is strongly affected by ballast minerals and zooplankton activity. Ballast minerals, such as silicate, carbonate and dust, enhance aggregate formation and their subsequent sinking velocities, resulting in higher POC export. On the other hand, zooplankton may feed on sinking aggregates and thereby reduce POC export. In this thesis the quantitative importance of ballast minerals and zooplankton aggregate feeding on the biological carbon pump were studied.

Ballast minerals added to a natural plankton community from the North African Upwelling region enhanced aggregate formation and sinking velocities, leading to a potential ten-fold increase in carbon export (**Manuscript 1**). Aggregates from this region were not able to scavenge any additional ballast minerals, possibly because they were already saturated with ballast minerals (**Manuscript 1**). The presence of ballast minerals could explain up to 91% of the observed variability in POC export in this upwelling region (**Manuscript 2**). Therefore, ballast minerals seemed to control the magnitude of the POC flux in the North African Upwelling region.

Zooplankton can feed on sinking aggregates, but relatively little is known regarding the mechanisms and their quantitative importance for POC export. Two copepod genera *Calanus* and *Pseudocalanus* were observed to detect and feed on *in situ* collected aggregates in three subarctic fjords (**Manuscript 3**). Using *in situ* zooplankton and aggregate abundances in combination with the measured aggregate feeding rates, we calculated that 60-67% of the observed flux attenuation could be explained by *Calanus* and

Pseudocalanus aggregate feeding. This showed that zooplankton aggregate feeding can have a major impact on POC export fluxes in subarctic fjords.

Ballast minerals and zooplankton are of varying importance for POC fluxes between geographical regions, seasons and years (**Manuscript 2**). Simply put, the POC flux magnitude is controlled by primary production and the presence of ballast minerals, whereas their attenuation is controlled by microbial and zooplankton degradation. Especially zooplankton-mediated degradation can cause intense but variable POC flux attenuation on temporal and geographical scales, and may even function as a buffer for POC fluxes at greater depth. In contrast, at some locations high deposition of ballast minerals may significantly enhance POC export (**Manuscript 2**). The understanding of these two contrasting processes is fundamental for improving our understanding of CO_2 sequestration in both today's and future oceans.

ZUSAMMENFASSUNG

Der Ozean ist eine wichtige Kohlenstoffsenke, und speichert derzeit ein Drittel der globalen anthropogenen CO_2-Emissionen. Einer der wichtigsten Prozesse, welche die Ozeane als Kohlenstoffsenke beeinflussen, ist die „biologische Kohlenstoffpumpe“. Die biologische Kohlenstoffpumpe beschreibt die Transformation von CO_2 in organisches Material und dessen Export in die Tiefe. Sie wird durch die Fixierung von CO2 durch Photosynthese in der euphotischen Zone angetrieben. Das fixierte organische Material kann Aggregate bilden, die aus der euphotischen Zone absinken und dadurch einen partikulären organischen Kohlenstoff (POC) -Export in die Tiefe darstellen. Während des Sinkens werden die Aggregate abgebaut und remineralisiert, was zu einer Attenuation des POC-Flusses führt. Schlussendlich wird ~1% der Primärproduktion aus der euphotischen Zone in marinen Sedimenten gebunden.

Die biologische Kohlenstoffpumpe wird stark von Ballastmineralien und Zooplankton beeinflusst. Ballastmineralien wie Silikat-, Karbonat- und Staubpartikel fördern die Aggregatbildung und erhöhen deren Sinkgeschwindigkeiten, was zu einem höheren POC-Export führt. Andererseits kann sich Zooplankton von sinkenden Aggregaten ernähren und dadurch den POC-Export verringern. In dieser Doktorarbeit wurde die quantitative Bedeutung von Ballastmineralien und Zooplankton für die biologische Kohlenstoffpumpe untersucht.

Ballastmineralien, die einer natürlichen Planktongemeinschaft in der nordafrikanischen Auftriebsregion hinzugefügt wurden, erhöhten sowohl die Aggregatbildung als auch die Sinkgeschwindigkeiten, was zu einer möglichen Verzehnfachung des Kohlenstoffexports führte (**Manuskript 1**). Aggregate aus dieser Region konnten jedoch keine zusätzlichen Ballastmineralien aufnehmen, möglicherweise weil ihre Kapazität, weitere Ballastmineralien aufzunehmen, bereits erreicht war (**Manuskript 1**). Das Vorhandensein von Ballastmineralien könnte bis zu 91% der Variabilität des POC-Exports in dieser Auftriebsregion erklären (**Manuskript 2**). Diese Erkenntnisse zeigen, dass Ballastmineralien die Größe des POC-Flusses in der nordafrikanischen Auftriebsregion steuern können.

Zooplankton kann sich von sinkenden Aggregaten ernähren, über die Mechanismen und ihre quantitative Bedeutung für den POC-Export ist jedoch relativ wenig bekannt. Hier

wurde beobachtet, dass die Copepoden-Gattungen *Calanus* und *Pseudocalanus in situ* gesammelte Aggregate in drei subarktischen Fjorden detektieren und beweiden (**Manuskript 3**). Aus *in situ* Zooplankton- und Aggregathäufigkeiten und den gemessenen Aggregat-Beweidungsraten errechneten wir, dass 60-67% der beobachteten POC Export-Attenuation durch *Calanus* und *Pseudocalanus* Aggregat-Beweidungsraten erklärt werden können. Dies zeigt, dass die Beweidung von Aggregaten durch Zooplankton einen großen Einfluss auf den POC-Export in subarktischen Fjorden hat.

Ballastmineralien und Zooplankton sind je nach geografischer Region, Jahreszeit und Jahr von unterschiedlich großer Bedeutung (**Manuskript 2**). Die Größe der POC-Flüsse wird durch Primärproduktion und den Einbau von Ballastmineralien gesteuert, während POC-Attenuation durch mikrobiellen Abbau und Beweidung durch Zooplankton gesteuert wird. Insbesondere die Beweidung von Aggregaten durch Zooplankton kann auf zeitlicher und geografischer Ebene zu einer starken, aber variablen Attenuation des POC-Flusses führen. Im Gegensatz dazu wird an einigen Standorten der POC-Export durch eine hohe Ablagerung von Ballastmineralien stark beschleunigt. Das Verständnis dieser einander entgegengesetzter Prozesse ist von grundlegender Bedeutung für ein besseres Verständnis der CO_2-Sequestrierung im heutigen Ozean.

TABLE OF CONTENTS

Summary iii

Zusammenfassung v

1. Introduction 1

1.1 The biological carbon pump 2

1.2 Zooplankton in the biological pump 7

1.3 Ballast minerals in the biological pump 11

1.4 Regional variations in carbon export 14

1.5 Objectives of this thesis 17

2. Manuscripts 19

Contributions to manuscripts 19

Manuscript 1. The ballasting effect of Saharan dust deposition on aggregate dynamics and carbon export: aggregation, settling and scavenging of marine snow 21

Manuscript 2. Intense zooplankton feeding on aggregates during high primary production decreases variability of export flux to the deep ocean 35

Manuscript 3. Aggregate feeding by Calanus and Pseudocalanus controls carbon flux attenuation in the sub-Arctic 55

3. Discussion 77

3.1 New insights on ballast minerals in the biological carbon pump 78

3.2 New insights on zooplankton in the biological carbon pump 83

3.3 Conclusions 87

Acknowledgements 89

References 91

1. INTRODUCTION

The atmospheric CO_2 concentration has increased from 280 ppm in the 18th century (Wigley 1983; IPCC 2014) to 414 ppm today (average May 2019, source: Mauna Loa Observatory, Hawaii, NOAA ESRL) due to the use of fossil fuels and deforestation. This increased atmospheric CO_2 concentration leads to global warming, sea-level rise and changes in precipitation (IPCC 2014). However, only half of the anthropogenic released CO_2 remains in the atmosphere, as the terrestrial biosphere and the ocean take up the rest (Sabine et al. 2004; Canadell et al. 2007; Sabine and Tanhua 2010). It is estimated that one-third of the total anthropogenic released CO_2 is currently stored in the oceans (Sabine et al. 2004; Sabine and Tanhua 2010).

Dissolved inorganic carbon (DIC) is the largest carbon pool in the ocean. This includes CO_2 (aq), HCO_3^-, and CO_3^{2-}, whose relative abundances are influenced by pH and alkalinity. Atmospheric CO_2 solubility primarily depends on water temperature and the DIC concentration. CO_2 is more soluble in cold water, and therefore more CO_2 dissolves into the cold surface waters of the polar oceans. When this surface water cools down it sinks to the deep ocean, efficiently transporting DIC to the deep. DIC is stored in the deep water until the water mass reaches the surface in warm upwelling regions, where part of the CO_2 is released back to the atmosphere (Fig. 1). This process is known as the “solubility pump”, and plays a major role in the ocean’s carbon storage (Volk and Hoffert 1985; Raven and Falkowski 1999).

The other major “pump” that influences oceanic carbon transport and storage is the “biological carbon pump”. It covers the transformation of DIC into organic matter and the export of this material to the deep ocean (Fig. 1) (Volk and Hoffert 1985). Therefore, the production and sinking of organic material is vital for the ocean’s carbon storage capacity.

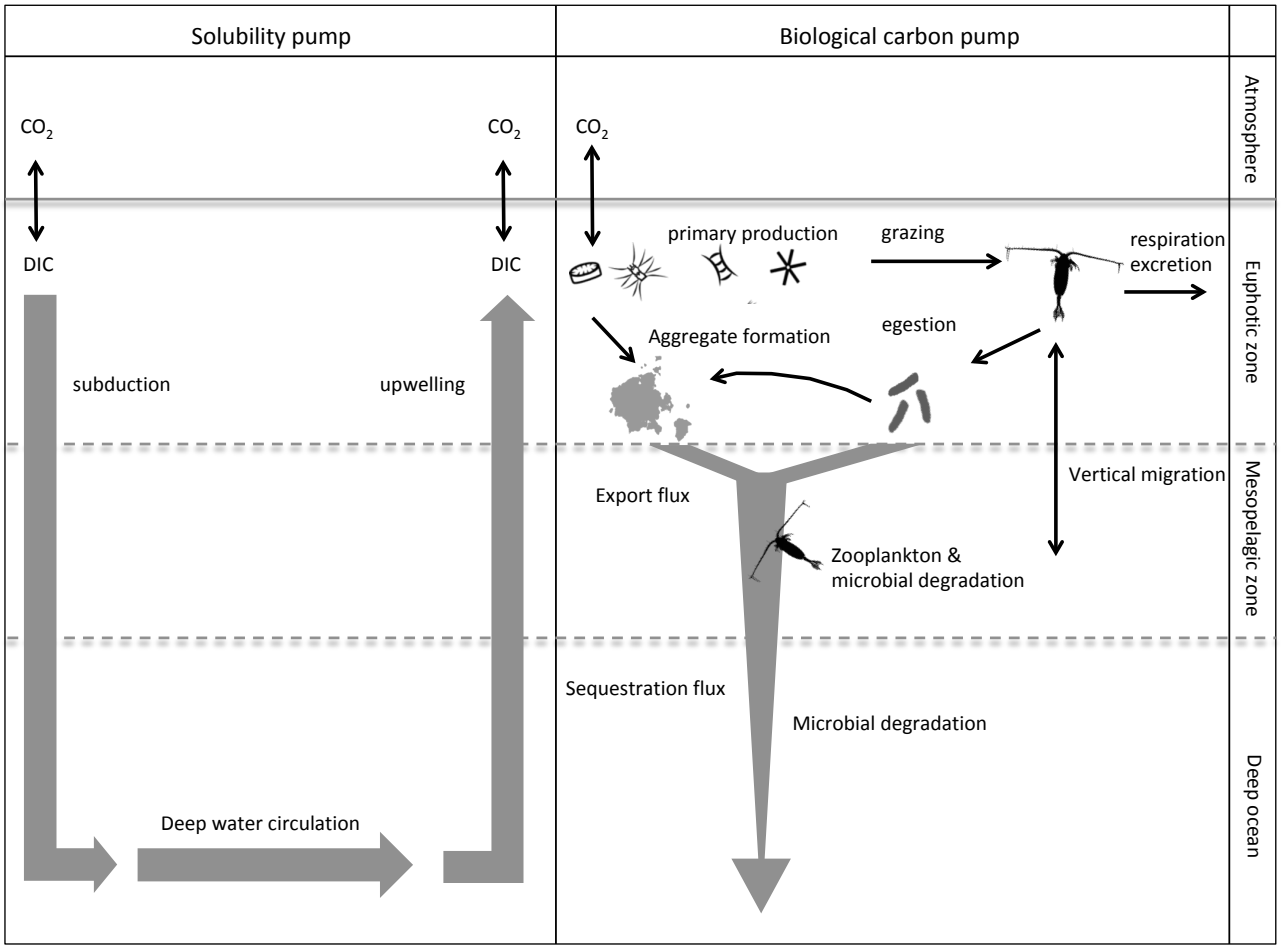

Fig. 1. The ocean's solubility pump (left), where cold water with a high DIC concentration is subducted to the deep ocean and is circulated until the water mass wells up and releases CO_2 in warm regions. The biological carbon pump (right) is driven by the fixation of DIC via photosynthesis in the euphotic zone. Phytoplankton and egested fecal pellets form aggregates that sink out of the euphotic zone and form carbon export. This export flux is degraded and remineralized by zooplankton and microbes in the mesopelagic zone, and thereby strongly attenuated with increasing depth. The organic material that reaches the deep ocean is termed "sequestration flux". Organic matter export in the deep ocean is primarily attenuated via microbial degradation.

1.1 THE BIOLOGICAL CARBON PUMP

The biological carbon pump is driven by the fixation of CO_2 into biomass by primary producers in the euphotic zone. On an annual basis, oceanic primary producers are responsible for the fixation of ~50 Gt carbon (Field et al. 1998). The majority of the net primary production is retained and respired in the surface ocean, only a fraction (5-25%) sinks below the euphotic zone (upper 100 m) (De La Rocha and Passow 2007). Organic matter sinking below the euphotic zone is called the export flux. This flux is driven by three processes: sinking single cells and aggregates (marine snow); advection of organic matter; and transport by vertically migrating zooplankton. Less than 3% of the net primary

production reaches bathypelagic depths (>1000 m), as the rest is degraded and respired in the water column by bacteria, microzooplankton and mesozooplankton (De La Rocha and Passow 2007). The flux of particulate organic carbon (POC) to depths below 1000 m is known as the sequestration flux, as carbon sinking beyond this depth is sequestered in the sea for longer than 100 years (Passow and Carlson 2012). Only 1% of the net primary production is reaching marine sediments, where it can be sequestered for millennia (Ducklow et al. 2001). The depth at which sinking organic carbon is remineralized determines the time carbon is stored in the ocean; shallow remineralization causes immediate exchange of CO_2 with the atmosphere, while deep remineralization stores CO_2 until the water mass is exposed to the atmosphere (Kwon et al. 2009).

The export of carbon and the efficiency of the biological pump vary strongly between regions. High carbon export occurs in coastal and polar regions, whereas export is low in the (sub)tropical oligotrophic gyres (Fig. 2) (Martin et al. 1987; Buesseler 1998; Lutz et al. 2007). These differences in export fluxes are due to variations in primary production, aggregate sinking velocities, and degradation of organic matter.

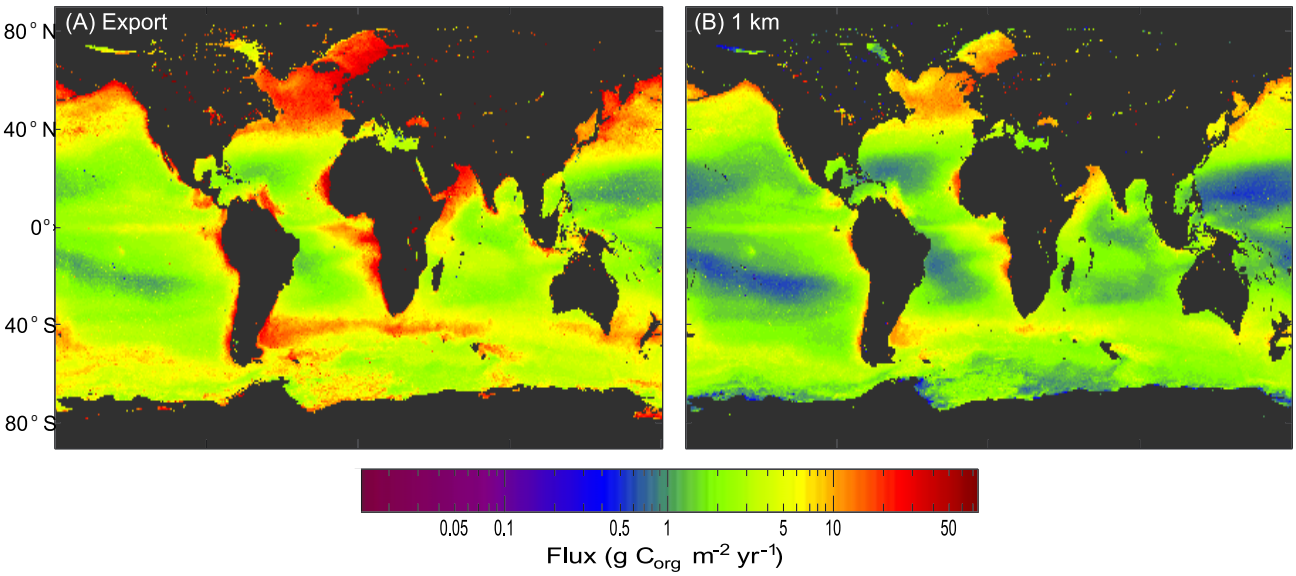

Fig. 2. Estimated annual average particulate organic carbon fluxes. A) Export from the euphotic zone; B) Export at the base of the mesopelagic zone (1 km). (Lutz et al. 2007).

PRIMARY PRODUCTION

Primary production in the euphotic zone is controlled by light and nutrient availability, such as iron, phosphorus and nitrogen (Falkowski et al. 1998). In the euphotic zone, where photosynthesis takes place, these dissolved inorganic nutrients are generally in low supply because of a rapid assimilation into the phytoplankton biomass (McCarthy and Goldman 1979). Below the euphotic zone, dissolved inorganic nutrient concentrations increase as a result of organic matter degradation (Anderson and Sarmiento 1994). Stratification prevents the transport of nutrients from the deep to the surface in large parts of the ocean. However, storms, winter cooling and water upwelling can reduce this stratification and bring deep-water nutrients to the surface (Chavez et al. 2011). Due to these processes, marine primary production is highest in the polar regions and coastal upwelling areas, and lowest in the subtropical oligotrophic gyres where the resupply of nutrients from the deep is limited (Huston and Wolverton 2009).

Within oligotrophic regions, nutrients are efficiently recycled in the surface ocean and <10% of the net primary production is exported below the euphotic zone (~50 m depth) (Pomeroy 1974; Azam et al. 1983; Neuer et al. 2002a). In contrast, coastal and polar regions with high nutrient concentrations often have a high carbon export (Muller-Krager et al. 2005; Chavez et al. 2011), with 30-100% of the net primary production sinking below the euphotic zone in spring (Buesseler 1998). This variability in the export flux between regions is largely due to the differences in food web composition (Legendre and Rivkin 2002) and aggregate dynamics (Buesseler 1998).

AGGREGATE FORMATION

One of the most important processes in the biological carbon pump is the formation and sinking of aggregated organic material. The formation of aggregates occurs mostly in the euphotic zone, where the concentration of source material is highest. Particles can collide and form aggregates via three physical coagulation processes: Brownian motion, fluid shear and differential settling (Burd and Jackson 2009). Brownian coagulation occurs only with particles that are small enough to collide due to Brownian motion, which are usually particles smaller than 1 μm (Burd and Jackson 2009). Larger particles can collide due to fluid shear and faster-settling particles hitting and incorporating slower-sinking ones, which is known as differential settling. Differential settling is the main mechanism behind the rapid change from small to large sinking particles (Burd and Jackson 2009). Whether or not particles that collide in the water column stick together is controlled by their

"stickiness". Stickiness is increased by organic polymers produced by phytoplankton and reworked by microbes (Grossart et al. 2006; Gärdes et al. 2010). Transparent exopolymer particles (TEP) are gel particles of consisting predominantly of polysaccharides (Alldredge et al. 1993; Engel 2000), that enhance physical coagulation of aggregates (Passow 2002; Arrigo 2007).

Besides physical coagulation, aggregates can also form via biological aggregation processes. The most important biological aggregation process is the production of fecal pellets. By ingesting and egesting organic material, zooplankton repackage slow-sinking aggregates into fast-sinking fecal pellets, thus increasing the carbon flux. Fecal pellets of most zooplankton are covered with a so-called peritrophic membrane, which slows disintegration of the pellet. Zooplankton fecal pellets can contribute up to 100% of the carbon flux (Turner 2015). Zooplankton fecal pellets differ strongly in shape, size, density and sinking velocity (Ploug et al. 2008b), and therefore the contribution of fecal pellets to the carbon flux differs between regions with varying zooplankton communities. Some fecal pellets disaggregate easily, making it difficult to determine the contribution of fecal pellets to the downward POC flux (Ebersbach and Trull 2008).

The formation and discard of mucous feeding nets and (appendicularian) houses is an additional biological aggregation process. Appendicularia (pelagic tunicates) feed on nanoplankton using a special feeding net, a 'house', that lets nanoplankton through while keeping larger plankton and detritus outside. When this house is clogged with algae and detritus, the animal discards the house and builds a new one. As appendicularians can discard up to 26 houses per day and they are abundant in both coastal and oceanic waters (Sato et al. 2001), these houses can make up 13-83% of the total POC flux (Alldredge 2005).

SINKING

Aggregates sink out of the euphotic zone when their density is higher than that of the surrounding water. The sinking velocity of aggregates is a crucial parameter, as it determines the time aggregates are exposed to degradation in the water column. Sinking velocities therefore define the maximum depth to which carbon is transported (Boyd et al. 1999). For example, copepod fecal pellets have sinking velocities between 5-220 m d^{-1}, whereas larger salp and pteropods fecal pellets sink with 43-2700 m d^{-1} (reviewed in Turner 2002). Appendicularian houses have sinking velocities of 10-100 m d^{-1} (Alldredge and Gotschalk 1988; Lombard and Kiørboe 2010). Other marine aggregates have sinking

velocities between 5-500 m d^{-1} (Alldredge and Gotschalk 1988; Diercks and Asper 1997; McDonnell and Buesseler 2010).

Aggregate sinking velocities depend on their composition, density, and size (Ploug et al. 2008a; Iversen and Ploug 2010). The incorporation of biogenic and lithogenic minerals, such as silicate, carbonate and Saharan dust, can enhance aggregate sinking velocities (Iversen et al. 2010; Lombard et al. 2013a). For example, diatom aggregates have higher sinking velocities than flagellate colonies of *Phaeocystis spp*. as they contain silica (Reigstad and Wassmann 2007; Wolf et al. 2016). On the other hand, TEP have a lower density than seawater and may therefore reduce aggregate sinking velocities (Azetsu-Scott and Passow 2004).

DEGRADATION

Marine snow is degraded by bacteria, other microbes and zooplankton. The bacterial community composition within aggregates seems to be determined during aggregate formation (Thiele et al. 2015; Mestre et al. 2017), however bacterial colonization also occurs (to a lesser extent) while aggregates are sinking through the water column (Grossart and Simon 1998; Kiørboe et al. 2002; Mestre et al. 2017; Fadeev et al. 2018). Aggregates are highly populated with bacteria and support high bacterial growth activity (Alldredge and Silver 1988; Ploug and Grossart 2000; Ploug et al. 2002). These bacterial hotspots are often colonized by protists, such as ciliates and dinoflagellates, that feed on the aggregate-associated bacterial communities (Silver et al. 1984; Kiørboe et al. 2004). These protists are also known to be significant degraders of marine snow and fecal pellets (Poulsen and Iversen 2008).

Microbial aggregate degradation is controlled by temperature (Iversen and Ploug 2013), hydrostatic pressure (Tamburini et al. 2009), and chemical composition of the aggregates (Armstrong et al. 2002). Measured carbon-specific microbial degradation rates range between 0.01-0.12 d^{-1} (Iversen and Ploug 2013; Morata and Seuthe 2014; Belcher et al. 2016). These observed microbial degradation rates can only partly explain the total observed aggregate degradation. Therefore, other degradation processes, such as zooplankton aggregate feeding, may play an important role in aggregate degradation (Lampitt et al. 1993; Kiørboe 2000).

1.2 ZOOPLANKTON IN THE BIOLOGICAL PUMP

Zooplankton are heterotrophic planktonic organisms, such as jellyfish, pteropods, copepods, amphipods and krill. They can contribute substantially to the downward POC flux through the production of fecal pellets, mucous feeding nets and carcasses (Turner 2002; Alldredge 2005; Sampei et al. 2012). Some species can feed on sinking aggregates and fecal pellets, thereby reducing carbon export (Lampitt et al. 1990; Noji et al. 1991; Iversen and Poulsen 2007). Zooplankton may however also increase the carbon flux by actively transporting carbon to the deep ocean (Vinogradov 1955; Packard and Gómez 2013).

THE ACTIVE CARBON FLUX

Zooplankton can transport carbon to the deep ocean via diel vertical migration (Longhurst and Glen Harrison 1988; Schnetzer and Steinberg 2002). In this process, known as the 'active carbon flux', zooplankton ingest food in the surface waters at night and migrate to the deep during the day. Here, ingested carbon is metabolized and eventually respired as CO_2, excreted as dissolved organic carbon (DOC), or ejected as POC in the form of fecal pellets (Steinberg et al. 2000). This active transport from the euphotic zone to the deep can be significant compared to the passive sinking of aggregates (Vinogradov 1955; Hernández-León et al. 2001; Packard and Gómez 2013). It is estimated to be on average 10-20% of the particulate carbon flux, but can equal the particulate carbon flux when zooplankton biomass is high (Ducklow et al. 2001, 2009; Steinberg et al. 2002). Active transport has been suggested as an important source of carbon for zooplankton and bacteria residing at depth (Steinberg et al. 2008a; Alonso-González et al. 2013).

FEEDING ON MARINE SNOW

Zooplankton cause POC flux attenuation by feeding on sinking material. Some zooplankton are specialized 'flux-feeders' that intercept sinking aggregates (Jackson 1993), while other species colonize sinking marine snow (Steinberg et al. 1994; Green and Dagg 1997; Koski et al. 2005) or ingest fractionated aggregates and fecal pellets (Iversen and Poulsen 2007; Koski et al. 2017) (Fig. 3). Flux feeders, such as pteropods and polychaetes, tend to live below the euphotic zone and intercept settling aggregates with mucous nets (Jackson 1993; Christiansen et al. 2018).

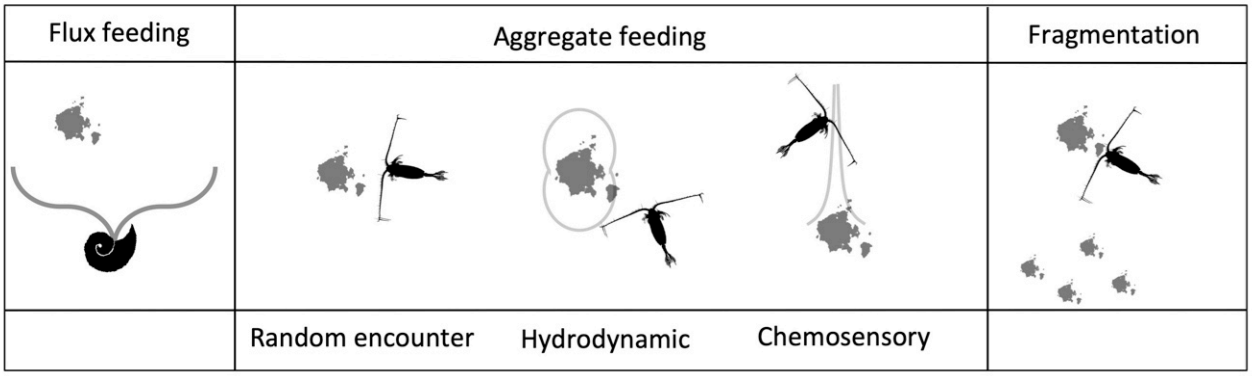

Fig. 3. Zooplankton feed on marine snow with different mechanisms. Flux feeding is done by organisms that live below the euphotic zone and capture sinking aggregates using mucous feeding nets. Aggregate feeding can also occur via different mechanisms. Zooplankton can encounter aggregates randomly, use hydrodynamic cues originating from the sinking aggregates, or recognize a chemical trail of organic solutes leaking from a sinking aggregate. Organisms can also fragment aggregates upon encounter, leading to smaller and slower-sinking aggregates.

Zooplankton without feeding nets, such as copepods and euphausiids, also feed on aggregates and fecal pellets. The copepod genera *Microsetella* and *Oncaea* attach to sinking aggregates and may reside there for minutes to hours while they feed on the aggregated material (Alldredge 1972; Ohtsuka et al. 1993; Koski et al. 2005), *Pseudocalanus* and *Temora* have been observed to reside on aggregates *in situ* (Möller et al. 2012), and *Temora* has been observed to actively feed on aggregates (Lombard et al. 2013b; Koski et al. 2017). These copepods may detect sinking aggregates randomly, recognize their hydrodynamic signals (Visser 2001), or find and follow a chemical trail of organic solutes leaking from sinking aggregates (Kiørboe and Thygesen 2001; Visser and Jackson 2004). The ability to recognize chemical trails increases the chance of finding an aggregate, but has so far only been directly observed for *Temora longicornis* (Lombard et al. 2013b).

There are few studies on aggregate feeding, however, more is known about interactions with fecal pellets. Zooplankton can ingest fecal pellets (cophrophagy), fragment pellets into slow-sinking smaller particles (coprorhexy), or disrupt the pellet membrane so that the pellet unpacks into a more porous aggregate (coprochaly) (Lampitt et al. 1990; Noji et al. 1991; Iversen and Poulsen 2007). Feeding on fecal pellets has been observed for different copepods, such as *Oithona similis, Acartia tonsa, Temora longicornis, Calanus helgolandicus* and *Pseudocalanus elongatus* (González and Smetacek 1994; Poulsen and Kiørboe 2005; Iversen and Poulsen 2007). In these studies, intact fecal pellets were often rejected by copepods, and fecal pellet feeding appeared to be unintentional ingestion of small fecal pellet fragments (Iversen and Poulsen 2007). Therefore, the main effect of

zooplankton fecal pellet degradation seems to be through fecal pellet fragmentation rather than fecal pellet ingestion (Poulsen and Kiørboe 2005; Iversen and Poulsen 2007). Also sinking aggregates can be fragmented by feeding and swimming activity of zooplankton, resulting in smaller slower-sinking aggregates and a longer residence time in the water column, which may lead to higher decomposition (Goldthwait et al. 2004, 2005; Lombard and Kiørboe 2010). Swimming euphausiids can create sufficient shear to disrupt and fragment sinking aggregates (Dilling and Alldredge 2000). Fragmented fecal pellets sink slower and therefore have a higher microbial degradation per meter as they sink through the water column, which may explain high fecal pellet degradation that is often observed in the epipelagic zone (Svensen et al. 2012). It is hypothesized that the main role of zooplankton in POC attenuation is the fragmentation of aggregates into smaller ones and dissolved organic matter, which are subsequently degraded by bacteria (Giering et al. 2014; Mayor et al. 2014). However, there is little known on fragmentation processes happening *in situ*.

ZOOPLANKTON AND FLUX ATTENUATION

Zooplankton has been suggested to control the upper ocean carbon flux attenuation by degrading aggregates (Iversen et al. 2010; Jackson and Checkley Jr 2011), whereas deep flux attenuation seems controlled by microbial degradation (Stemmann et al. 2004). However, the quantitative importance of zooplankton on flux attenuation has proven difficult to measure *in situ*. Zooplankton has been associated with several variations in POC fluxes, including a steep decrease in aggregate abundances at the base of the mixed layer (Lampitt et al. 1993), diel variations in aggregate abundances (Stemmann et al. 2000; Jackson and Checkley Jr 2011), thin layers with high concentrations of copepods and aggregates (Möller et al. 2012), and observed attenuation exceeding microbial remineralisation (Iversen et al. 2010). Studies that aimed to determine the importance of zooplankton relative to bacterial degradation using respiration measurements (Steinberg et al. 2008b) and modelling approaches (Giering et al. 2014), found that zooplankton were responsible for 30-50% and 8-30% of the POC flux attenuation respectively. Giering et al. (2014) concluded that zooplankton was responsible for only a minor part of the POC flux attenuation. These results are in contrast to experimental studies, where several copepod species were observed feeding on sinking aggregates and fecal pellets (Koski et al. 2005; Lombard et al. 2013b; Koski et al. 2017).

Studies on zooplankton aggregate feeding have often used laboratory-formed aggregates and fecal pellets made from phytoplankton cultures (Iversen and Poulsen 2007; Koski et al. 2017). In comparison, *in situ* aggregates tend to contain older material with a lower carbon content (Ploug et al. 2008a) that also varies between regions and seasons (Nowald et al. 2015). It is therefore difficult to translate laboratory studies to the field for determining the quantitative importance of zooplankton in the biological carbon pump.

1.3 BALLAST MINERALS IN THE BIOLOGICAL PUMP

Downward fluxes of biogenic and lithogenic minerals, such as silicate, carbonate and Saharan dust, are often closely correlated to POC fluxes (Armstrong et al. 2002; Francois et al. 2002; Klaas and Archer 2002). These minerals can become incorporated into sinking aggregates and act as ballast. Ballast minerals enhance aggregate formation and increase aggregate density which results in higher sinking velocities, resulting in increased POC export (Hamm 2002; Passow and De La Rocha 2006; Engel et al. 2009a; b; Lee et al. 2009; Iversen and Robert 2015). On the other hand, they may limit POC export by increasing aggregate fragmentation (Hamm 2002).

BIOGENIC MINERALS

Ballast minerals of biogenic origin are silicate and carbonate, which are used by organisms in their skeletal structures. Biogenic silica (BSi) is used by diatoms, radiolarians and silicoflagellates. Carbonate is used by coccolithophores and foraminifera (Fig. 4). Interestingly, the ballasting efficiency of carbonate seems dependent on the producing species: carbonate from coccolithophores is a more efficient ballast mineral than carbonate from foraminifera (Schmidt et al. 2014). Carbonate is estimated to carry 42-76% of the POC flux to the deep ocean (Armstrong et al. 2002; Dunne et al. 2007), making it an important contributor to the biological carbon pump. The white cliffs of Dover show that carbonate was also an important ballast mineral in the past, as they consist almost entirely of sedimented coccolithophore calcium carbonate frustules.

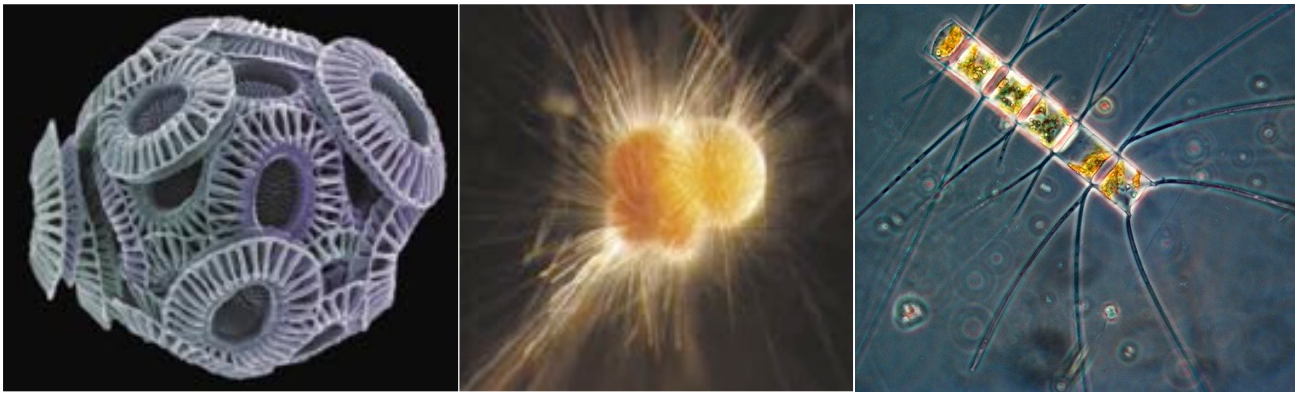

Fig. 4. Biogenic ballast minerals: Coccolithophores and foraminifera use carbonate (Doney 2006), while diatoms use silica (courtesy of Bente Edvardsen).

LITHOGENIC MINERALS

Lithogenic minerals originate from deserts and riverbeds and are transported via the atmosphere and rivers to the surface ocean. Lithogenic ballast minerals are estimated to carry 16-51% of the POC flux to depth (Armstrong et al. 2002; Dunne et al. 2007). An important and well-studied lithogenic ballast mineral is Saharan dust (Fig. 5), increasing POC export in the Mediterranean (Ternon et al. 2010), the Eastern Atlantic Ocean (Fischer et al. 2016) and even the oligotrophic North Atlantic Gyre (Pabortsava et al. 2017). Saharan dust consists of quartz, zircon, clay minerals, carbonates and hematite, and its composition depends on the source region and season (Friese et al. 2016; Korte et al. 2017). Saharan dust input to the surface ocean may vary strongly over time, causing pulses of high POC export (Ittekkot 1993; Ternon et al. 2010; Fischer et al. 2016).

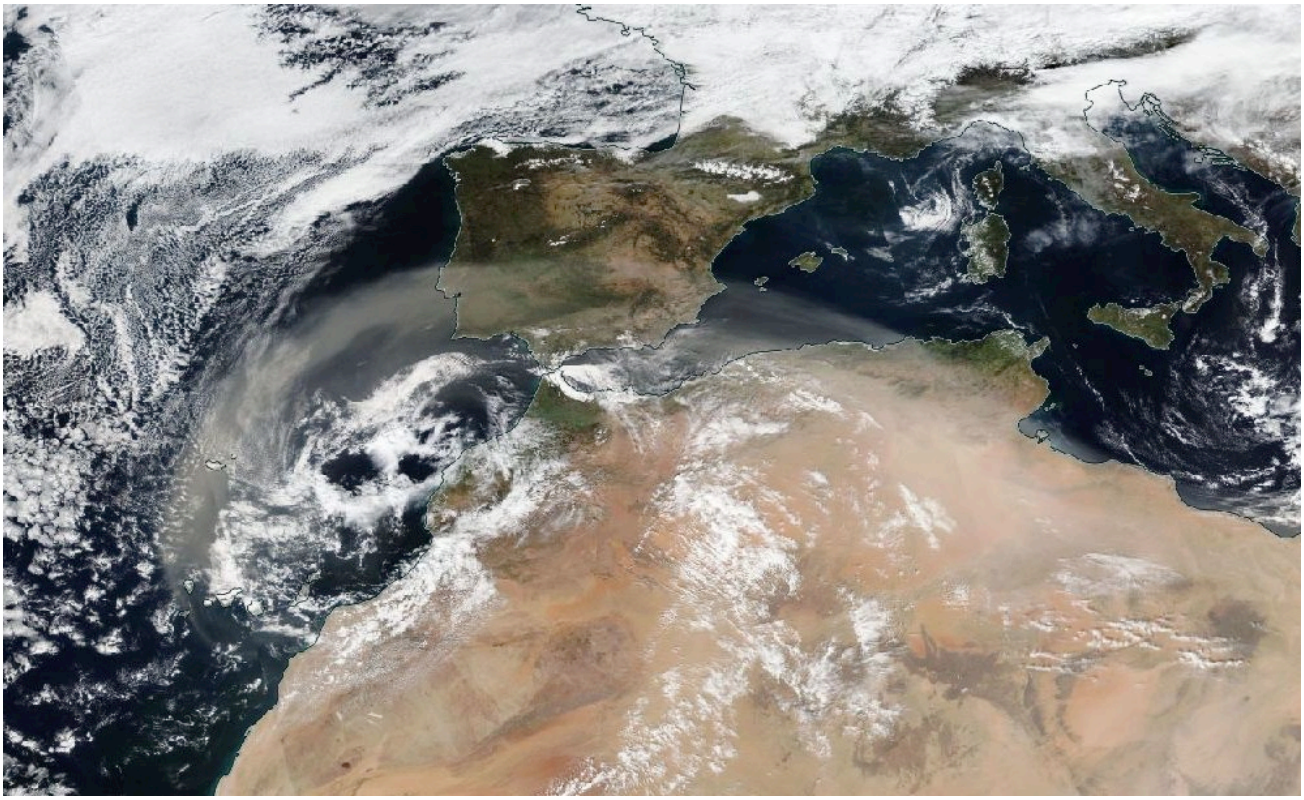

Fig. 5. A Saharan dust storm on 21 February 2017. Source: NASA Earth Observing System Data and Information System (EOSDIS).

BALLAST MINERAL SCAVENGING

Ballast minerals can be incorporated during aggregate formation or are 'scavenged' by aggregates during their descent in the water column. Scavenging rates depend on the concentration of both ballast minerals and sinking aggregates (Stolzenbach 1993). Certain oceanographic regions are known to contain layers with high concentrations of suspended lithogenic materials, known as nepheloid layers. In these nepheloid layers, sinking aggregates can potentially scavenge ballast minerals, although so far little interaction has been reported (Karakas et al. 2006, Iversen et al. 2010).

Ballast mineral scavenging requires a collision between a sinking aggregate and ballast mineral. A sinking aggregate creates a boundary layer, which may limit its scavenging potential (Kiorboe 2008). As an aggregate sinks, the water in its path is deflected around the aggregate, and particles suspended in this water move along the aggregate rather than colliding with it. Porous aggregates may have additional fluid flow through the aggregate, which could significantly increase their scavenging capacity of small particles (Stolzenbach 1993; Li and Logan 1997, 2000). However, so far, a flow through aggregates has only been observed for porous diatom aggregates (Ploug et al. 2002).

Scavenging also depends on aggregate stickiness (Simon et al. 2002; Burd and Jackson 2009). Aggregate stickiness may determine the maximum ballast mineral carrying capacity, as the sticky molecules may become saturated with ballast minerals. In the upper ocean, aggregates may consist out of 95% ballast minerals by weight percentage (Passow 2004), even higher ballast to carbon ratios have been observed in deep sediment traps (Klaas and Archer 2002).

Ballast mineral scavenging rates have so far been studied using laboratory-made aggregates (Hamm 2002), but these differ from aggregates in the field in both composition and porosity (Ploug et al. 2008a). Therefore, the rate at which *in situ* aggregates can scavenge ballast minerals during their descent is currently unknown.

1.4 REGIONAL VARIATIONS IN CARBON EXPORT

The export of carbon and the efficiency of the biological pump vary strongly between locations around the globe. For instance, in the tropical ocean less than 10% of the primary production is exported below the euphotic zone (150 m) (Neuer et al. 2002b), whereas in polar waters the export efficiency can reach almost 100% (Buesseler 1998). This variability in export efficiency is largely due to variations in primary production, sinking velocities, ballast minerals and degradation. The research in this thesis was carried out in two areas, the subarctic fjords of Svalbard and the East Atlantic Upwelling area off Mauritania. Both areas are characterized by strong seasonality with high productivity in spring, which have a high impact on POC export rates.

CAPE BLANC FILAMENT

Eastern Boundary Upwelling Ecosystems (EBUEs) cover 1% of the ocean surface but are responsible for about 15% of the global marine primary production (Behrenfeld and Falkowski 1997; Carr 2002). Wind-driven coastal upwelling brings nutrient-rich water from the deep to the euphotic zone, resulting in high primary production and high POC export (Messié and Chavez 2015).

After the Benguela upwelling, the Northwest African upwelling ecosystem is the second most productive EBUE (Carr 2002). The Northwest African upwelling is driven by the alongshore trade winds and the meeting of the Canary and Mauritanian Currents (Fig. 6). This results in offshore advection of surface waters and the formation of the prominent cold-water “giant Cape Blanc filament” (Van Camp et al. 1991). This filament transports nutrient- and phytoplankton-rich waters up to 450 km offshore (Fischer et al. 2009b), and is a unique feature of the Northwest African upwelling area. Thus, a high amount of aggregates can form far offshore in the North Atlantic open ocean.

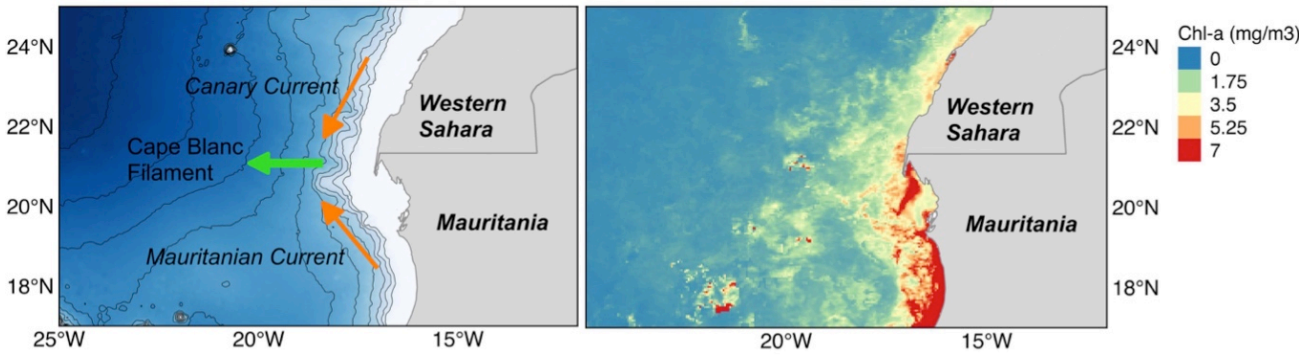

Fig. 6. The "giant Cape Blanc filament" is formed by the meeting Canary and Mauritanian Currents and alongshore trade winds (left), which transports nutrient- and phytoplankton-rich waters far offshore (right). MODIS-A 4 km monthly average chlorophyll-a concentration during winter 2011.

In addition to the offshore transport of phytoplankton, the filament also transports lithogenic minerals from the shelf to the open ocean (Fischer et al. 2009b). Saharan dust deposition events further increases the amounts of ballast minerals, with highest deposition rates during winter (Ratmeyer et al. 1999; Fischer et al. 2009a, 2016; Nowald et al. 2015). During periods of low dust deposition, biogenic carbonate and silica are important ballasters of the POC flux (Fischer et al. 2009a). The high amount of ballast minerals increases the potential for the formation of fast sinking aggregates, which may drastically increase the POC export efficiency in the Cape Blanc filament.

THE ARCTIC OCEAN

Marine ecosystems at high latitudes are characterized by a strong seasonality, where ice cover and polar night results in low productivity in winter and open waters in summer results in high primary production and high POC export (Buesseler 1998; Hill and Cota 2005). High export in polar ecosystems is related to spring blooms of diatoms and other large phytoplankton cells that are quickly removed from the euphotic zone via aggregate formation and settling or via grazing (Smetacek et al. 1984; Buesseler 1998).

Characteristic for the Arctic Ocean is that about one-third of the area is taken up by shelf seas with depths of 100 m or less. These shelf seas are crucial for biogeochemical cycles: for example, the Barents Sea (30% of Arctic shelf) is responsible for 50% of the Arctic primary production (Fig. 7) (Sakshaug 2004; Wassmann et al. 2010). The productivity on the Arctic shelf is strongly influenced by riverine runoff, providing freshwater, nutrients and lithogenic material (Dittmar and Kattner 2003). Due to the persistent reduction of sea ice cover in the last decades, primary production has increased (Pabi et al. 2008), which may result in a higher POC export in the Arctic.

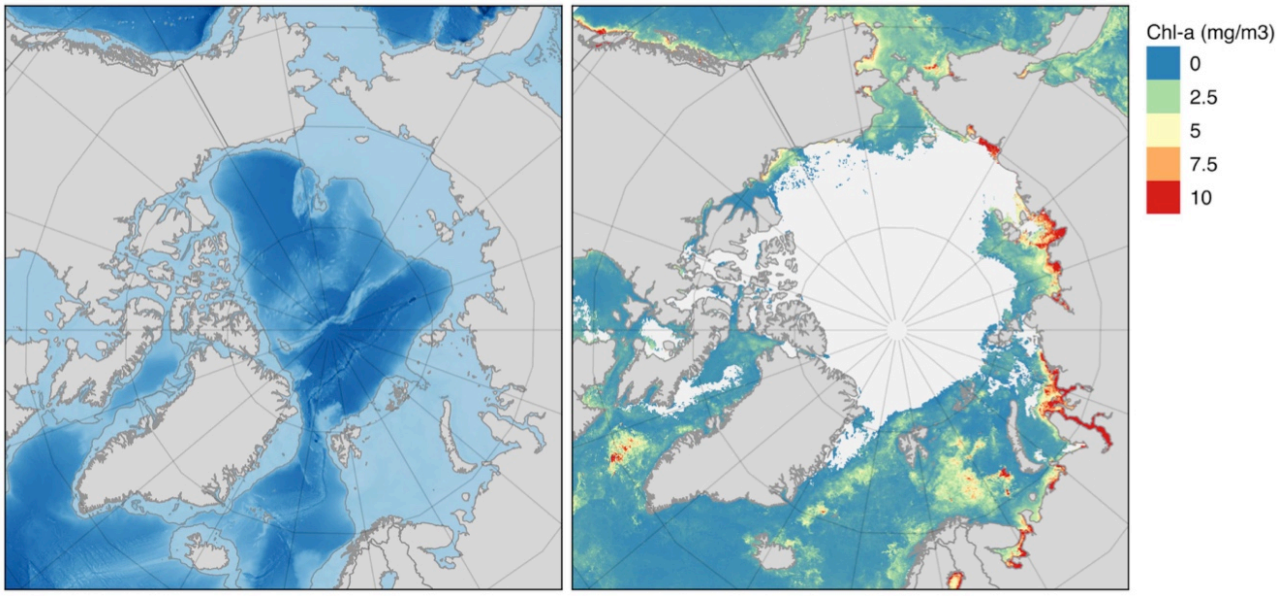

Fig. 7. The Arctic Ocean consists for one-third of shelf seas with shallow depths (left), where the majority of primary production takes place (right). MODIS-A 4 km monthly average chlorophyll-a concentration in summer 2018.

Despite increases in primary production, the Arctic Ocean still accounts for only ± 6% of the total oceanic carbon sequestration (Gruber et al. 2009). POC export fluxes vary strongly between arctic regions, with lowest fluxes in the ice-covered Central Arctic, and highest fluxes on the shelves (Fahl and Nöting 2007; Reigstad et al. 2008). There is strong attenuation of the POC flux in Arctic waters, and only a fraction of the organic material leaving the euphotic zone sinks below 200 m (Noji et al. 1999). Degradation processes seem highest in the upper 100 m of the water column (Wassmann et al. 2003), and there are strong indications that zooplankton play a crucial role in this strong flux attenuation (Olli et al. 2007; Wexels Riser et al. 2008).

1.5 OBJECTIVES OF THIS THESIS

This thesis investigates the role of ballast minerals and zooplankton aggregate feeding in the biological carbon pump. During my PhD, I performed on-board experiments combined with *in situ* measurements in the Cape Blanc filament and along the Arctic coast to investigate ballasting and zooplankton activity, and their quantitative impact on the biological carbon pump. In this thesis, the following research questions are addressed:

BALLAST MINERALS

- *How do ballast minerals influence aggregate formation in a natural plankton community?*
- *Can sinking aggregates scavenge ballast minerals?*
- *How do ballast minerals influence the efficiency of the biological carbon pump?*

ZOOPLANKTON

- *How do zooplankton feed on natural sinking aggregates?*
- *What is the quantitative importance of aggregate feeding by zooplankton on the carbon flux?*

In **Manuscript 1**, I investigated the effect of a Saharan dust deposition on the natural plankton community off Cape Blanc. The main questions were whether aggregates from this area can scavenge additional ballast minerals while they sink, or if ballast minerals are mainly incorporated during aggregate formation in the surface ocean. **Manuscript 2** assessed the influence of ballast minerals and microbial and zooplankton degradation on POC export and attenuation in the upper 400 m in the Cape Blanc filament. **Manuscript 3** described aggregate feeding mechanisms of two copepod genera, *Calanus* and *Pseudocalanus*, and their quantitative importance on POC flux attenuation in three sub-Arctic fjords.

2. MANUSCRIPTS

CONTRIBUTIONS TO MANUSCRIPTS

MANUSCRIPT 1

Helga van der Jagt, Carmen Friese, Jan Berend W. Stuut, Gerhard Fischer, Morten H. Iversen (2018). The ballasting effect of Saharan dust deposition on aggregate dynamics and carbon export: Aggregation, settling, and scavenging potential of marine snow. Limnology and Oceanography **63**: 1386-1394.

Author contributions: Experiment planning and execution by HvdJ and MHI, dust collection and analysis by CF and JBWS, cruise organization by GF, writing by HvdJ under supervision of MHI with contributions from all authors.

MANUSCRIPT 2

Helga van der Jagt, Gerhard Fischer, Clara Flintrop, Lili Hufnagel, Nicolas Nowald, Götz Ruhland, Marco Klann, Stefan Thiele, Jessika Füssel, Helle Ploug, Christine Klaas, Richard Lampitt, Morten H. Iversen (in prep.). Intense zooplankton feeding on aggregates during high primary production decreases variability of export flux to the deep ocean.

Author contributions: sample collection by all authors, measurements by HvdJ, MHI and LH, data analysis by HvdJ and MHI, writing by HvdJ under supervision of MHI with contributions from all authors.

MANUSCRIPT 3

Helga van der Jagt, Ingrid Wiedmann, Nicole Hildebrandt, Barbara Niehoff, Morten H. Iversen (in prep.). Aggregate feeding by *Calanus* and *Pseudocalanus* controls carbon flux attenuation in the sub-Arctic.

Author contributions: Experiment planning and execution by HvdJ and MHI, camera profile analysis by MHI, drift trap analysis by IW, zooplankton counting by NH and HvdJ, data analysis by HvdJ, writing by HvdJ under supervision of MHI with contributions from all authors.

CONTRIBUTIONS TO OTHER MANUSCRIPTS

Iversen MH, Pakhomov EA, Hunt BPV, van der Jagt H, Wolf-Gladrow D, Klaas C (2017). Sinkers or floaters? Contribution from salp pellets to the export flux during a large bloom event in the Southern Ocean. Deep-Sea Res. II **138**: 116-125

Author contributions: HvdJ performed the POC measurements and statistics, and contributed to the writing. MHI, BPVH, EAP and CK performed the experimental work on-board, cruise organization by DWG, writing by MHI and EAP with contributions of all authors.

Miriam Seifert, Mario Hoppema, Claudia Burau, Cassandra Elmer, Anna Friedrichs, Jana K. Geuer, Uwe John, Torsten Kanzow, Boris P. Koch, Christian Konrad, Helga van der Jagt, Morten H. Iversen (2019). Influence of Glacial Meltwater on Summer Biogeochemical Cyles in Scoresby Sund, East Greenland. Front. Mar. Sci. **6**: 412. doi: 10.3389/fmars.2019.00412

Author contributions: HvdJ performed the drift trap deployments, measurements and analyses and contributed to the writing. MS, CB, CE, AF, JKG, UJ, TK, BPK, CK and HvdJ performed sampling, dataset analyzed by MS, MH and MHI with contribution of all authors. Writing by MS under supervision of MH and MHI with contributions of all authors.

MANUSCRIPT 1. THE BALLASTING EFFECT OF SAHARAN DUST DEPOSITION ON AGGREGATE DYNAMICS AND CARBON EXPORT: AGGREGATION, SETTLING AND SCAVENGING OF MARINE SNOW

Helga van der Jagt, Carmen Friese, Jan Berend W. Stuut, Gerhard Fischer, Morten H. Iversen (2018). Limnology and Oceanography. doi:10.1002/lno.10779

ABSTRACT

Lithogenic material such as Saharan dust can be incorporated into organic aggregates and act as ballast, potentially enhancing the marine carbon export via increased sinking velocities of aggregates. We studied the ballasting effects of Saharan dust on the aggregate dynamics in the upwelling region off Cape Blanc (Mauritania). Aggregate formation from a natural plankton community exposed to Saharan dust deposition resulted in higher abundance of aggregates with higher sinking velocities compared to aggregate formation with low dust. This higher aggregate abundance and sinking velocities potentially increased the carbon export ten-fold when the aggregates were ballasted by Saharan dust. After aggregate formation in the surface waters, subsequent sinking through suspended Saharan dust minerals had no influence on aggregate sizes, abundance, and sinking velocities. We found that aggregates formed in the surface ocean off Mauritania were already heavily ballasted with lithogenic material and could therefore not scavenge any additional minerals during their descent. This suggests that carbon export to the deep ocean in regions with high dust deposition is strongly controlled by dust input to the surface ocean while suspended dust particles in deeper water layers do not significantly interact with sinking aggregates.

INTRODUCTION

Carbon export is driven by the formation and sinking of aggregated organic material into the deep ocean. The time period for which carbon is stored in the ocean depends on the depth of remineralization, and only organic matter reaching the bathypelagic will be stored in the ocean for centuries (Lampitt et al. 2008). Fast sinking aggregates remain shorter in the upper ocean, are degraded less and therefore more likely to reach the deep ocean (Iversen and Ploug 2013). Therefore an increased sinking velocity will increase the depth of remineralization and, thus, the carbon export efficiency (Alldredge and Silver 1988; Alldredge and Jackson 1995).

The downward fluxes of biogenic and lithogenic minerals, such as silicate, carbonate and Saharan dust, are often closely correlated to particulate organic carbon (POC) fluxes (Armstrong et al. 2002; Francois et al. 2002; Klaas and Archer 2002). It has been hypothesized that these minerals are incorporated as ballast into aggregates, resulting in increased sinking velocities. This incorporation can take place during the formation of aggregates in the surface and subsurface ocean or when aggregates 'scavenge' dust particles while sinking (Passow and De La Rocha 2006). Incorporation of ballast minerals into aggregates has been observed to enhance aggregate formation, increase size-specific sinking velocities but also to fragment large aggregates into smaller ones (Hamm 2002; Passow and De La Rocha 2006; Engel et al. 2009b; a; Lee et al. 2009; Iversen and Robert 2015). Ballasted aggregates are remineralized at the same rate as non-ballasted aggregates (Ploug et al. 2008b; Iversen and Ploug 2010), but due to their increased size-specific sinking velocities they are likely to be remineralized at greater depth than non-ballasted aggregates. However, most direct studies of the influence of ballast minerals on organic aggregates have been done in the laboratory with phytoplankton cultures (e.g. Hamm, 2002; Passow & De La Rocha, 2006; Iversen & Ploug, 2010).

Ballast minerals can be incorporated into aggregates during aggregate formation in the surface ocean, or when aggregates 'scavenge' suspended minerals during their descent into the bathypelagic. Scavenging depends on the concentration, size and sinking velocity of both aggregates and ballast minerals as well as on the stickiness of the aggregates (Simon et al. 2002; Burd and Jackson 2009). Transparent exopolymer particles (TEP) determine the stickiness of aggregates (Alldredge et al. 1993; Engel 2000), but TEP may become saturated with ballast minerals and therefore lose its stickiness (Passow 2004). Porous aggregates may have fluid flow through them, which could contribute to efficient scavenging of small

suspended or slow-sinking particles (Stolzenbach 1993; Li and Logan 1997, 2000). However, this has only been observed for porous diatom aggregates collected in the Baltic (Ploug et al. 2002) while it is unclear if compact, ballasted aggregates from regions with high concentrations of ballast minerals scavenge lithogenic particles at depth (Iversen et al. 2010), as large sinking particles push water away and this limits the scavenging potential (Kiorboe 2008).

Several studies have observed that detached suspended particles from the shelf and upper slope regions extent horizontally offshore as large slow-sinking plumes of fine particles, that are often referred to as intermediate nepheloid layers (INLs) (Dickson 1986; Hall et al. 2000; Frignani et al. 2002). INLs are a general feature in upwelling regions where intensification of bottom currents and internal waves generate INLs through changes in water density gradients caused by the upwelling (Dickson and McCave 1986). INLs are a prominent feature in the high productive Eastern Boundary Upwelling area off Cape Blanc, Mauritania, where erosion from the shelf sediment generates particle plumes in subsurface layers (Karakas et al. 2006, Nowald et al. 2006, Fischer et al. 2009, Iversen et al. 2010). The INLs are typically observed with optical systems between 200 and 600 m depth near-shore (Nowald et al. 2006, Iversen et al. 2010) while they slowly deepen with sinking velocities of ~5 m d^{-1} as they are advected off-shore via Ekman transport (Karakas et al. 2006). Very little is known about the particle composition of the INLs, except that they are formed from slowly sinking material, which could originate from eroded shelf sediment and/or dust deposition of slow sinking particles near the coast. It has been suggested that there is little interaction between vertically settling marine snow and INLs in the region off Cape Blanc (Karakas et al. 2006, Iversen et al. 2010). On the other hand, several studies have suggested that the vertical flux of organic matter is strongly influenced by Saharan dust deposition to the surface water (Fischer and Karakas 2009; Iversen et al. 2010; Nowald et al. 2015). Especially peak flux events off Cape Blanc seem to follow distinct dust outbreaks during winter and summer (Nowald et al. 2015; Fischer et al. 2016), but it still remains unclear whether these dust outbreaks cause higher aggregate formation in the surface waters or if the deposited dust is scavenged by already formed aggregates.

During a cruise off Cape Blanc, Mauritania we performed on-board incubations, using in-situ collected marine snow, a natural phytoplankton community and Saharan dust. We found that Saharan dust enhanced the formation of aggregates and increased their sinking

velocities. However, we did not find any indications of particle scavenging by already formed aggregates.

MATERIAL & METHODS

We studied the influence of Saharan dust on the formation and settling of aggregates during the RV Poseidon cruise (POS481) from 15 February to 3 March 2015 off Cape Blanc, Mauritania. We performed two experiments to investigate the effect of dust deposition on the formation of aggregates, using a natural plankton community exposed to both high and low concentrations of added Saharan dust. Additionally, we performed one experiment to investigate the scavenging potential of sinking aggregates, by incubating *in situ* collected aggregates with and without added dust.

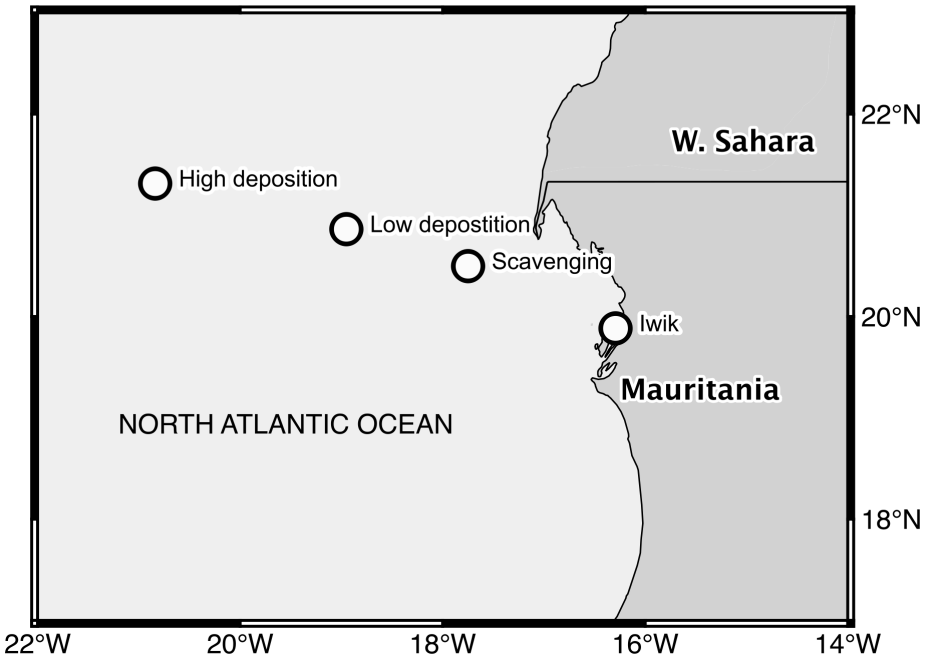

Fig. 8. Overview of the locations of the high dust deposition, low dust deposition and scavenging experiment, and dust collection location Iwik.

Aggregate formation experiments

For the two formation experiments, seawater was collected from the fluorescence maximum depth at 20 m with a CTD-rosette sampler. The collected water was incubated with and without added dust, and repeated for a high and low dust deposition (4.2 and 1.4 mg L^{-1} respectively). The experiment on the effect of high dust deposition was done at 21°18.9´N 20°50.34´W and the experiment on the effect of low dust deposition was done at 20°51.87`N 18°57.08´W (Fig. 8). Both studies were carried out by filling 10 roller tanks

(1.15 L, diameter: 14 cm, depth: 7.5 cm) with fluorescence maximum water, and adding a dust suspension to five of the tanks. The tanks without dust additions received a blank solution of GF/F filtered seawater of the same volume as the dust additions. The roller tanks were placed on a roller table rotating with a speed of 3 RPM for 36 hours in darkness at *in situ* temperature (19 °C) to allow aggregate formation. We collected all the formed aggregates individually and measured their size and sinking velocity in a vertical flow chamber (see Ploug and Jørgensen 1999). Each measured aggregate was frozen individually at -20 °C for further analysis in the home laboratory.

Scavenging experiment

To study how settling aggregates scavenge dust when they sink through the water column, we collected *in situ* marine snow aggregates with a Marine Snow Catcher (MSC). The MSC can sample intact *in situ* formed aggregates, which allows studying the composition, size and sinking velocity of natural aggregates from different water depths (Riley et al. 2012). The aggregates were collected below the fluorescence maximum layer at a depth of 60 m at 20°29.97´N 17°44.98´W. We divided all collected aggregates evenly into eight roller tanks that were filled with GF/F filtered seawater from the MSC, and added the low dust suspension to four of the roller tanks, while the other four received a 1 ml blank solution. The roller tanks were placed on a roller table rotating with 3RPM for 24 hours in darkness to allow dust scavenging by the incubated aggregates. Afterwards, all aggregates were collected individually, and their size and sinking velocities were determined in the flow chamber (Ploug and Jørgensen 1999). Each measured aggregate was frozen individually at -20 °C for further analysis in the home laboratory.

Dust suspensions

To generate the dust suspensions, we collected Saharan dust with modified Wilson and Cooke samplers (Wilson and Cooke 1980; Mendez et al. 2011), which collected wind-transported dust in the Banc d'Arguin National Park in Mauritania (~19°53' N, ~16° 18' W) during 2013 (Friese et al. 2017). These passive samplers are used to collect material transported by wind (dry deposition), and consist of a plastic bottle with an in- and outlet tube that are placed in the wind. Dust particles entering the sampler via the inlet tube settle into the bottle due to a pressure drop caused by a difference in diameter between the inlet tube and bottle, and clean air leaves the bottle via the outlet. The sampling efficiency of a modified Wilson and Cooke sampler is 90% (Goossens and Offer 2000).The sampling bottles were attached to a mast at 290 cm above the ground and were replaced every

month; the collected dust was stored dry and dark. Dust collected in August was used for the high dust deposition experiment, and dust collected in April was used for the low dust deposition and scavenging experiment. We determined the grain-size distribution of the two dust suspensions using a Beckmann Coulter laser particle sizer (LS 13 320) equipped with a Micro Liquid Module (MLM, analytical error of ± 1.26 µm (± 4.00 %), see Friese et al. 2016, 2017). The peak in the particle diameter frequency (given in volume %) was at 30 µm for both samples, which was similar to Saharan dust collected with deep sea sediment traps off Cape Blanc (Friese et al. 2016). Microscopic observations using a Zeiss Axioskop 40 polarizing microscope revealed that the two dust suspensions were of similar composition with the dominant minerals being quartz, carbonate, and clay minerals with minor contributions of hematite and calcite.

The collected dust samples were suspended in 10 ml distilled water and mixed thoroughly before allowing a five seconds resting period to let the fast-sinking particles settle out, and then removing 5 ml of the suspended dust. The resting period was to prevent that the dust suspension would contain very fast-sinking dust particles, which would have settled out individually after deposition. We mixed the dust suspension with GF/F-filtered seawater before adding the solution to the roller tanks. The experiments with high dust deposition contained 4.2 mg dust L^{-1}, and the low dust deposition contained 1.4 mg dust L^{-1}.

Dry weight and POC

We filtered 2L water used for the aggregation experiments onto combusted pre-weighed GF/F filters to determine dry weight and particulate organic carbon (POC). To determine the POC per aggregate for each treatment, one to four aggregates of similar sizes were filtered onto pre-combusted GF/F filters. The filters were gently washed with demineralized water, dried at 40°C for 24 hours and re-weighed to obtain the dry weight before removing inorganic carbon ($CaCO_3$) by fuming with 37% HCl and analyzed with a GC elemental analyzer (Elementar vario EL III) to obtain the POC values. We pooled aggregates into size classes where possible.

Excess density

The excess density was calculated using the Navier-Stokes drag equation, as described in Iversen and Ploug (2010):

$$\Delta\rho = \frac{C_D \rho_w w^2}{\frac{4}{3} g ESD} \quad (1)$$

Where C_D is the dimensionless drag force:

$$C_D = \frac{24}{Re} + \frac{6}{1+Re^{0.5}} + 0.4 \quad (2)$$

And Reynolds number (Re):

$$Re = wESD\frac{\rho_w}{\eta} \quad (3)$$

ρ_w is the density of seawater at 19°C with a salinity of 36 psu (1.0258 g cm^{-3}) , η the dynamic viscosity (1.0610 10^{-2} g cm^{-1} s^{-1}) w the sinking velocity in cm s^{-1}, g the gravitational acceleration (981 cm s^{-2}), and *ESD* the equivalent spherical diameter in cm.

Statistical analysis

Statistics was performed in R (R Core Team et al. 2016). Differences in the relation between ESD versus sinking velocity and excess density between control and treatment were calculated using a linear model that estimated both intercept and slope for each group. The data were log-log transformed prior to analysis to assume linearity. Afterwards, 95% confidence intervals were calculated for each predicted parameter. If the CI's for one of the parameters did not overlap, the groups were determined as significantly different. All other data were first tested for normality using a Shapiro-Wilk Normality Test, after which either a two-sample t-test or a non-parametric Wilcoxon signed-rank test were used.

RESULTS

Aggregate formation and settling after dust deposition

The POC concentrations of the water collected from the fluorescence maximum were 0.17 mg L^{-1} for the high dust deposition experiment and 0.15 mg L^{-1} for the low dust deposition. The total dry weight was 3.14 and 1.29 mg L^{-1} respectively, suggesting that the water used for the high dust deposition contained more inorganic material than that used for the low dust deposition experiment. The aggregates formed during high dust deposition were smaller and sank faster than those formed during low dust deposition (Table 1, Wilcoxon rank sum test, $p<0.01$). Excess density decreased with increasing size for all treatments, due to the fractal nature and porosity of the aggregates (Fig. 10 d-f).

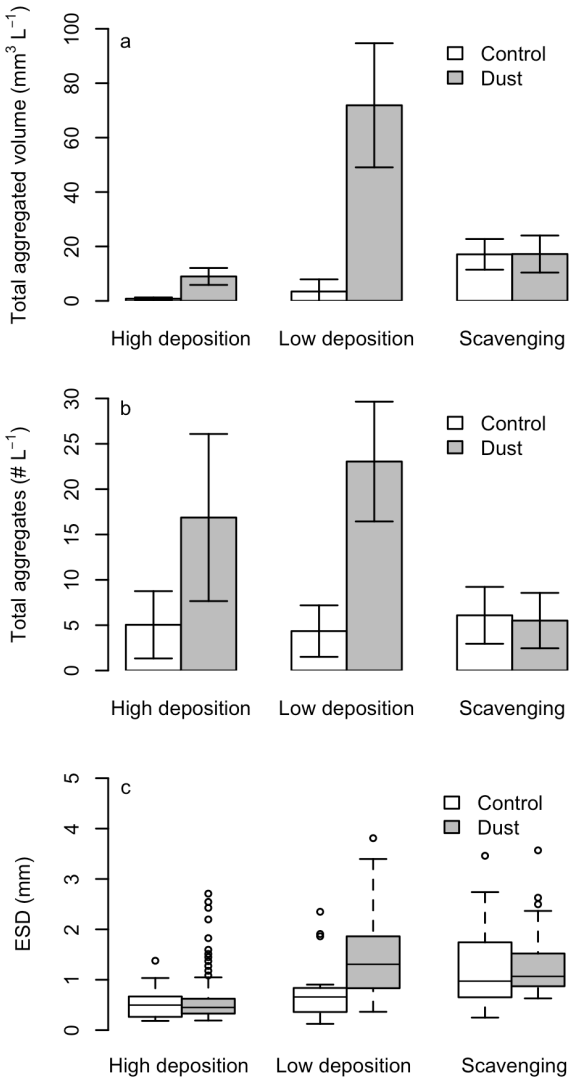

Fig. 9. a) Total aggregated volume per liter for the three experiments, stars indicate significant differences (two-sample t-test, $p<0.01$, $p<0.01$ and $p=0.98$ respectively). Average ± SD; b) Number of aggregates formed per liter, stars indicate significant differences (two-sample t-test, $p=0.04$, $p<0.01$ and $p=0.83$ respectively). Average ± SD; and c) Box-whisker plots of aggregate sizes, star indicates significance (Wilcoxon rank sum test, $P=0.72$, $p<0.01$ and $p=0.53$ respectively).

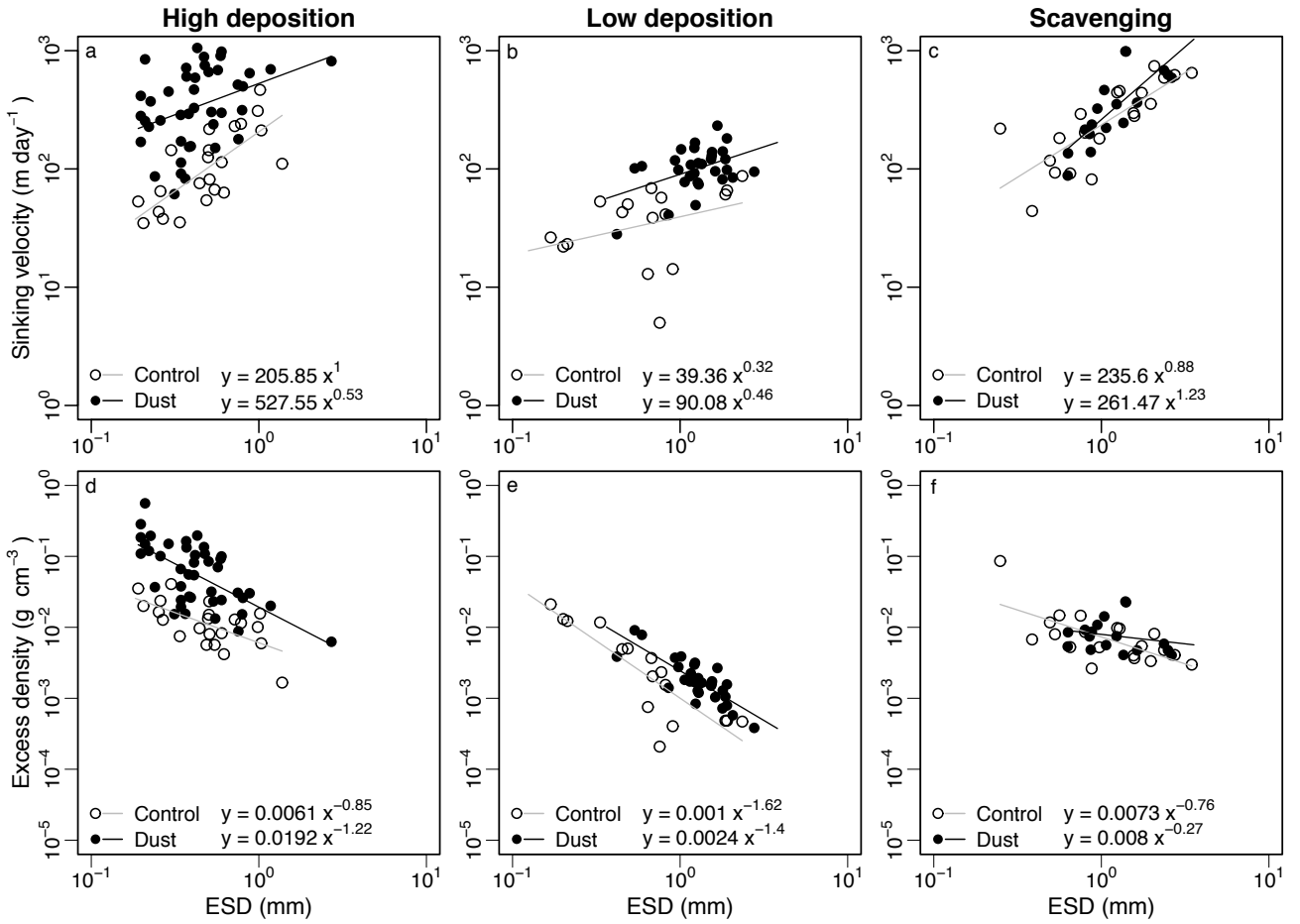

Fig. 10. Size versus sinking velocity and excess density of all measured aggregates, in combination with the fitted regression lines. a and d) Aggregates formed under high dust deposition (linear regression on log- transformed data, $p<0.01$); b and e) aggregates formed under low dust deposition ($p<0.01$); and c and f) *In situ* aggregates sinking through suspended dust ($p=0.53$).

In the high dust deposition experiment, aggregates already formed after 12 h when dust was added, while it took 24 h before the first visible aggregates were observed in the treatments without dust additions. The total aggregated volume and the number of aggregates formed were significantly higher in the dust treatment compared to the control treatment without dust (Fig. 9 a and b, two-sampled t-test, $p<0.01$ and $p=0.04$ respectively). The average equivalent spherical diameter (ESD) of the aggregates formed in the treatment exposed to high dust deposition was not significantly different from the average ESD of the aggregates formed in the control treatment (Fig. 9c, Wilcoxon rank sum test, $p=0.72$). The aggregates formed in the dust treatment had a lower POC to dry weight ratio and a higher dry weight to volume ratio (Table 2), indicating that they contained a higher amount of inorganic mineral particles compared to control aggregates. The size-specific sinking velocities of the aggregates formed with added dust were significantly faster than those formed without dust additions (Fig. 10a, linear regression on log-transformed data, $p<0.01$). Also the excess

density to size relation was different, the excess density of aggregates formed with added dust were significantly higher (Fig. 10d, linear regression on log-transformed data, $p<0.01$).

Table 1. Equivalent spherical diameter (ESD), number of formed aggregates per liter, total aggregated volume and sinking velocity for the high deposition, low deposition and scavenging experiments. Average ± sd.

Experiment		ESD (mm)	Total agg. (# L^{-1})	Total agg. vol. (mm^3 L^{-1})	Sinking velocity (m day^{-1})
High deposition	Control	0.52 ± 0.30	5.04 ± 3.71	0.79 ± 0.48	133 ± 108
	Dust	0.62 ± 0.51	16.87 ± 9.21	8.98 ± 3.11	430 ± 280
Low deposition	Control	1.45 ± 0.78	4.35 ± 2.84	3.43 ± 4.47	42 ± 23
	Dust	0.75 ± 0.61	23.04 ± 6.60	71.88 ± 22.81	109 ± 42
Scavenging	Control	1.29 ± 0.85	6.09 ± 3.14	17.10 ± 5.64	319 ± 210
	Dust	1.40 ± 0.80	5.51 ± 3.05	17.21 ± 6.81	403 ± 280

The low dust deposition experiment showed higher total aggregated volume and numbers of aggregates formed with dust added compared to the aggregates formed without dust additions (Fig. 9a and b, two-sample t-test, $p<0.01$). The aggregates formed in the dust-treatment had higher size-specific sinking velocities than those formed without added dust (Fig. 10b, linear regression on log-transformed data, $p<0.01$), and excess densities were significantly higher (Fig. 10e, linear regression on log-transformed data, $p<0.01$). Contrary to the high dust deposition experiment, the aggregates formed with added dust were significantly larger than those formed without added dust (Fig. 9c, Wilcoxon rank sum test, $p<0.01$). The POC to volume ratio and the POC to dry weight ratio was generally higher for control aggregates (Table 2).

To study the natural occurrence of minerals within the aggregates formed from the incubations without dust additions, we performed microscopic observation using a Zeiss Axioskop 40 polarizing microscope. This showed that the aggregates formed from the *in situ* collected water without dust contained quartz and clay minerals, suggesting that dust was already present in the natural sea water samples.

Size, volume and sinking velocity of scavenging aggregates

We did not observe any difference between *in situ* collected aggregates after incubating them in roller tanks with and without added dust. The total aggregated volume and total amount of aggregates per liter was the same for the treatments with and without dust after 24 h incubation in roller tanks (Fig. 9a and b, and Table 1, two-sampled t-test, $p=0.98$ and $p=0.83$ respectively). We also did not observe any differences between average ESD of the aggregates (Fig. 9c, Wilcoxon signed rank test, $p=0.46$), between the relationship between

size and sinking velocity (Fig. 10, linear regression on log-transformed data, p=0.53) or between the average POC to dry weight ratios between the dust and control treatment after the 24 h of incubation (Table 2).

Table 2. Dry weight and POC values per size class per experiment. Number of measured aggregates (Agg #), average ESD ± sd, POC per volume ratio (POC:V), dry weight per volume ratio (DW:V) and POC per dry weight ratio (POC:DW). n.a.: not available.

Experiment		Agg #	ESD ± sd (mm)	POC:V (µg C mm^{-3})	DW:V (µg mm^{-3})	POC:DW %
High deposition	Control	14	0.33 ± 0.13	n.a.	3696	n.a.
		4	0.98 ± 0.32	9.83	192	5.13
	Dust	10	0.39 ± 0.09	61.42	4495	1.37
		10	0.57 ± 0.27	19.21	1361	1.41
		2	1.71 ± 0.16	4.84	221	2.19
Low deposition	Control	9	0.44 ± 0.27	26.79	1347	1.99
		1	1.86	1.48	58	2.57
	Dust	10	0.91 ± 0.30	5.38	367	1.47
		1	1.64	5.10	n.a.	n.a.
		2	2.13 ± 1.32	0.61	64	0.95
Scavenging	Control	6	0.57 ± 0.24	25.09	3705	0.68
		5	0.96 ± 0.19	4.99	239	2.09
		6	2.06 ± 0.78	1.28	45	2.83
	Dust	5	0.76 ± 0.12	8.63	941	0.92
		3	1.02 ± 0.06	5.06	381	1.33
		4	1.45 ± 0.13	2.28	143	1.59
		3	2.50 ± 0.13	0.82	41	2.00

DISCUSSION

We observed that addition of Saharan dust enhanced aggregate formation from a natural plankton community and resulted in higher aggregate abundance. The formed aggregates had higher size-specific sinking velocities compared to those formed in situations without dust addition. This supports previous observations from laboratory experiments where inclusion of minerals into organic aggregates increased aggregate formation, abundance, and size-specific sinking velocities compared to incubations without minerals (Hamm 2002; Passow and De La Rocha 2006; Iversen and Robert 2015). So far, no studies have observed an influence from ballast minerals on microbial degradation (Ploug et al. 2008, Iversen and Ploug 2010, Iversen and Robert 2015), suggesting that the increased aggregate formation and higher sinking velocities may lead to an increased POC flux in dusty regions. This effect was directly shown in mesocosm experiments in the Mediterranean Sea, where an input of Saharan dust resulted in two to six times higher POC flux (Bressac et al. 2014),

and indirectly with sediment traps recording increased POC fluxes with dust deposition (Ternon et al. 2010; Fischer et al. 2016; Pabortsava et al. 2017). Our results show that dust deposition caused a ten-fold increase in total aggregated volume and two-fold higher size-specific sinking velocities of the dust-ballasted aggregates. On the other hand, the dust-ballasted aggregates had half the amount of volumetric POC compared to non-ballasted aggregates. Still, due to the high aggregate abundance and sinking velocities of the ballasted aggregates, a dust deposition may cause up to ten-fold higher POC flux.

In ballasting experiments conducted with phytoplankton from cultures, mineral ballasting increased aggregate fragmentation and aggregate compactness, resulting in smaller aggregates (Hamm 2002; Passow and De La Rocha 2006; Ploug et al. 2008a). However, in our experiments we did not observe changes in size of the aggregates formed with and without additional dust. Still, there is Saharan dust deposition to the surface waters off Cape Blanc almost year-round (Iversen et al. 2010; Friese et al. 2016; Fischer et al. 2016), and it is therefore likely that the aggregates formed with water from the fluorescence maximum were already ballasted. Nowald et al. (2015) made video observations of settling aggregates in the deep ocean off Cape Blanc and found that *in situ* aggregate sizes remained small throughout the year (mostly with a diameter of ~1 mm) and that Saharan dust deposition only increased aggregate abundance without having any effect on aggregate size. It therefore seems that peak fluxes due to dust deposition off Cape Blanc is driven by the formation of many small and dense aggregates rather than by a few large aggregates (Nowald et al. 2015).

When we exposed *in situ* collected aggregates to suspended Saharan dust, we did not observe any changes in aggregate sizes, abundance, or size-specific sinking velocities, indicating that these aggregates did not scavenge suspended dust. The scavenging potential of an aggregate may be determined by its stickiness, which is in turn controlled by the amount of transparent exopolymer particles (TEP) (Alldredge et al. 1993; Engel 2000). However, TEP may become saturated with particles and lose its stickiness, resulting in a reduced scavenging potential (Passow 2004). It has been suggested that the carrying capacity for minerals by aggregates is limited to 95% of the aggregate's dry weight made up by inorganic components (Passow 2004). We found that organic carbon only contributed with maximum 5% to the total dry weight of the *in situ* formed aggregates, suggesting that the carrying capacity for Saharan dust was already saturated when we exposed them to additional Saharan dust. This would explain why we did not observe scavenging of the

added dust by the *in situ* collected aggregates. Further, this also implies that aggregates formed in surface waters with high dust depositions become ballasted during their formation and may reach their maximum carrying capacity before they sink to the deeper water column. This prevents scavenging of lithogenic material in the deep ocean and could explain the persistence of large nepheloid layers in productive regions such as the upwelling area off Cape Blanc (Fischer et al. 2009b). These nepheloid layers are still observed after large export events during winter and spring (Karakaş et al. 2006), and do not significantly alter aggregate size-distribution and abundance of aggregates that sink through these layers (Iversen et al. 2010). This suggests little interaction between export production and the nepheloid layers.

Two possible, but contrasting, scenarios have been suggested for the future oceans; 1) increasing dust deposition due to future desertification and stronger trade winds (e.g. Naiman, 1976; Shao et al., 2011) and 2) Saharan 'greening' will limit dust emissions from source regions and cause less dust deposition in the future oceans (Fontaine et al. 2011; Lucio et al. 2012). A change in dust deposition may have profound effects on the global ocean due to the fertilizing effect of dust-originating nutrients on primary producers (Jickells et al. 2005; Ridame et al. 2014), especially of iron in high latitude regions. However, the role of dust as ballast material and therefore its effects on the downward carbon flux is often overlooked in global ocean models (e.g. McTainsh and Strong 2007; Maher et al. 2010). We show that the ballasting effect of dust deposition to the surface ocean also has a profound effect on POC export in productive lower latitude regions, while there was no evidence for scavenging of mineral dust by already ballasted aggregates.

ACKNOWLEDGEMENTS

We thank Christiane Lorenzen for the POC measurements and the crew of the R/V Poseidon POS481 for assistance during the cruise. This study was supported by the Helmholtz Association (to HJ and MHI), the Alfred Wegener Institute Helmholtz Centre for Polar and Marine Research (to HJ and MHI) and the DFG-Research Center/Cluster of Excellence "The Ocean in the Earth System" at MARUM (to all). This publication is supported by the HGF Young Investigator Group SeaPump "Seasonal and regional food web interactions with the biological pump": VH-NG-1000.

MANUSCRIPT 2. INTENSE ZOOPLANKTON FEEDING ON AGGREGATES DURING HIGH PRIMARY PRODUCTION DECREASES VARIABILITY OF EXPORT FLUX TO THE DEEP OCEAN

Helga van der Jagt, Gerhard Fischer, Clara Flintrop, Lili Hufnagel, Nicolas Nowald, Götz Ruhland, Marco Klann, Stefan Thiele, Jessika Füssel, Helle Ploug, Christine Klaas, Richard Lampitt, Morten H. Iversen (in prep.).

ABSTRACT

The ocean's biological carbon pump (BCP) is driven by the formation and sinking of aggregated organic material. The efficiency of the BCP is determined by the turnover rate of organic matter during its descent through the water column. We deployed drifting traps over a period of 7 years to study the driving mechanisms of the BCP in the Eastern Boundary Upwelling Region off north-west Africa. The magnitude of the BCP was best correlated to chlorophyll a, i.e. primary production, while the flux of particulate organic carbon (POC) was determined largely by the presence of diatom aggregates and was highest on occasions where diatom aggregates were ballasted by Saharan dust and calcium carbonate from coccolithophores. The magnitude of POC flux at 100 m was proportional to the attenuation of POC flux between 100 and 400 m, i.e. periods with high POC flux at 100 m were characterized by high turnover rates of the sinking organic matter. We found indications that zooplankton abundance and activity rose during periods with high export out of the euphotic zone. The same trend was observed in drifting traps throughout the Atlantic Ocean. We therefore suggest that zooplankton act as a buffer for POC flux to the deep ocean by feeding more intensely on sinking matter during periods with high POC flux.

INTRODUCTION

The ocean's biological carbon pump (BCP) is driven by the formation and sinking of aggregated organic material. This process sequesters atmospheric CO_2 fixed via primary production, and provides energy to deep-sea benthic ecosystems. Together with subduction of dissolved inorganic carbon and active carbon transport by vertical migration of zooplankton (Steinberg et al. 2002; Hansell et al. 2009), these processes are thought to enable the ocean to sequester one-third of the anthropogenic released CO_2 (Sabine et al. 2004; Sabine and Tanhua 2010).

The strength of the BCP, i.e. the magnitude of the particulate organic carbon (POC) flux, is strongly influenced by primary production in the surface ocean(Buesseler and Boyd 2009), however the majority of the primary production is grazed, degraded, and remineralized within the euphotic zone, and only 5-30% sinks below 100 m (Wassmann et al. 2003; De La Rocha and Passow 2007; Buesseler and Boyd 2009). Biogenic and lithogenic minerals, such as silicate, carbonate and terrestrial minerals, enhance POC fluxes (Armstrong et al. 2002; Francois et al. 2002; Klaas and Archer 2002). These minerals are known as ballast minerals, and can be incorporated into sinking aggregates, resulting in increased sinking velocities and higher POC fluxes (Hamm 2002; Passow and De La Rocha 2006; Iversen and Robert 2015; van der Jagt et al. 2018), as well as pulses of high POC export to the deep ocean(Ittekkot 1993; Ternon et al. 2010; Fischer et al. 2016). Biogenic silicate (BSi), mainly derived from diatoms, and calcium carbonate, formed by coccolithophores, foraminifera and pteropods, also increase aggregate sinking velocities and POC fluxes (Klaas and Archer 2002; De La Rocha and Passow 2007, Francois et al. 2002). Therefore the phytoplankton community and ecosystem structure play an important regulatory role in the downward POC flux (Legendre and Rivkin 2002).

Another major determinant of downward POC flux is the attenuation caused by degradation and remineralization of sinking material in the upper ocean (Martin et al. 1987). Flux attenuation in the mesopelagic often exceeds microbial degradation rates, indicating that zooplankton must also be involved (Stemmann et al. 2004; Iversen et al. 2010; Jackson and Checkley Jr 2011). Flux attenuation by zooplankton is increasingly observed in BCP studies. For example, specialized flux feeders, such as pteropods and polychaetes, intercept sinking aggregates (Jackson 1993; Kiørboe et al. 1998; Christiansen et al. 2018). Copepods and euphausiids feed on appendicularian houses, fecal pellets and marine snow (Schnetzer and Steinberg 2002; Koski et al. 2005, 2017; Iversen and Poulsen 2007; Lombard et al. 2013b),

and additionally can break up fecal pellets and marine snow into smaller slower-sinking aggregates (Lampitt et al. 1990; González and Smetacek 1994; Iversen and Poulsen 2007). On the other hand, zooplankton might also decrease flux attenuation via production of fast-sinking fecal pellets (Dagg 1993; Buesseler and Boyd 2009) and by active transport of carbon during diel vertical migration (Packard and Gómez 2013).

The aim of the present study was to determine the role of ballast minerals and biological controls on export fluxes in the Eastern Boundary Upwelling region off northwest Africa (Cape Blanc, Mauritania). A multi-decade moored sediment trap system means that seasonal deep ocean POC fluxes are well defined in this region (Nowald et al. 2015; Fischer et al. 2016), however controls on export fluxes in the upper water column have rarely been investigated (Iversen et al. 2010; Thiele et al. 2015; van der Jagt et al. 2018). During eight cruises from 2011 to 2017, we deployed 18 free-drifting sediment traps to assess the downward POC flux in the upper 400 m of the water column off Cape Blanc, Mauritania. Biogeochemical flux measurements were combined with satellite data, CTD casts and aggregate type assessments from gel traps to determine the impact of ballast minerals and biological degradation processes on POC fluxes in the mesopelagic.

MATERIAL AND METHODS

Sediment traps

In total we deployed 18 free-drifting surface-tethered sediment traps (KC Denmark A/S), consisting of stainless steel sediment trap stations with 4 tubes (Ø 11 cm, 70 cm long) positioned between 100 and 400 m (Table 3). Prior to deployments, the tubes were filled with GF/F filtered seawater, and NaCl was added to increase the salinity with 2 to 6‰ to enhance trapping efficiency. One tube per depth contained an insert with a viscous ethanol-based gel (Tissue-Tek) to sample particles without destroying their original size, structure, and shape. Upon recovery the collected samples were poisoned with $HgCl_2$ and stored at 4°C. At the home laboratory samples were wet-splitted with a rotating McLane splitter and large swimmers were removed.

Of the 18 drifting traps, one was deployed in spring (DF02) (Thiele et al. 2015), two in summer (DF18 and DF19), and fifteen in winter (Table 3). Most traps were deployed close to the long-term deep ocean sediment trap CB_{eu} (20°50'N, 18°44'W) (Nowald et al. 2015), including spring, summer and winter traps (Fig. 11). Two winter and one summer drifting trap were deployed near the long-term deep ocean sediment trap CB_{meso} (21°17'N, 20°50'W) (Fischer et al. 2016), which is located further off shore (Fig. 11). Of the remaining five winter

drifting traps, one was deployed in between CB_{meso} and CB_{eu}, the others were deployed closer to shore.

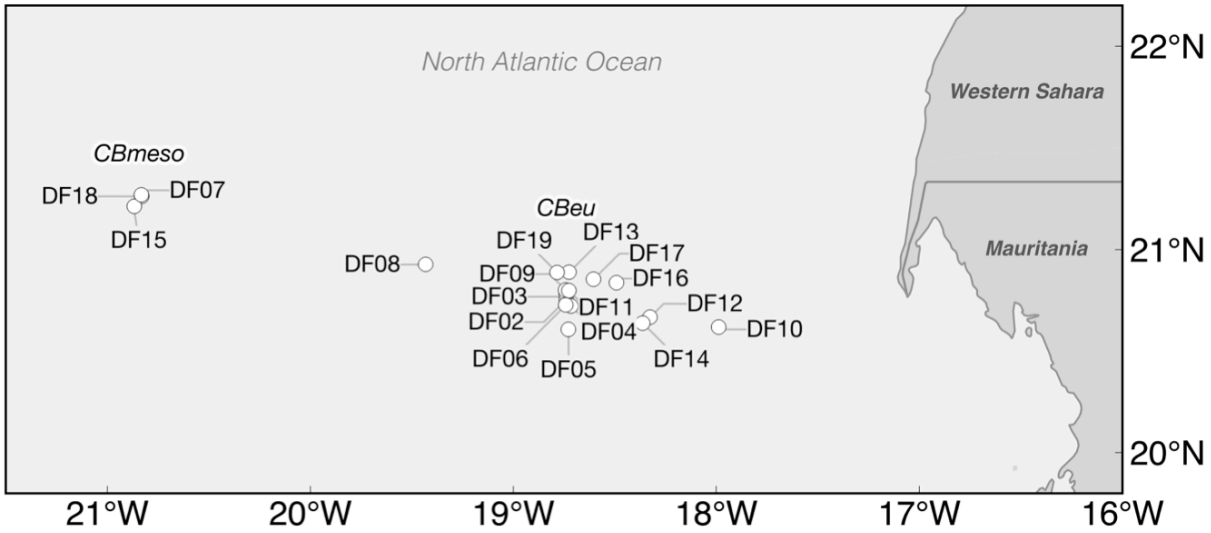

Fig. 11. Locations of the deployed sediment traps. The three westernmost traps were deployed close to the deep-sea sediment trap CBmeso, whereas the majority of the traps were deployed close to deep-sea trap CBeu. DF10 was deployed closest to the coast.

Biogeochemical analysis

For all traps we determined total particulate mass (TPM), particulate organic carbon (POC), particulate organic nitrogen (PON), particulate inorganic carbon (PIC), and biogenic silica (BSi). For mass, POC, PON and PIC, two samples of 1/5 wet splits were filtered on combusted pre-weighed GF/F filters, dried for 48 h at 50°C, and reweighed to determine the total dry particulate mass (TPM). One of the filters was then fumed with HCl for 24 h to remove PIC and dried for 24 h. Both filters were analysed with a GC elemental analyser (EURO EA). PIC was determined by subtracting organic carbon from total carbon. For determining BSi, 1/5 wet splits were filtered onto cellulose acetate filters (0.8 µm) and analysed after Koroleff (Koroleff 1983).

Lithogenic fluxes were estimated as:

$$lithogenic = TPM - CaCO_3 - SiO_2 - 2\times POC \quad (1)$$

where we assume that all PIC is in the form of $CaCO_3$, all BSi is in the form of SiO_2, and total organic matter is equal to twice the amount of POC (Hedges 1992).

The percentage of ballast fluxes (ballast%) was calculated as:

$$ballast\% = \frac{TPM-2\times POC}{TPM} \times 100 \quad (2)$$

where we assume that the total organic matter is equal to twice the amount of POC (Hedges 1992).

Table 3. Overview of all deployed sediment traps, sorted in the ballast clusters. The biogeochemical fluxes POC, PON, PIC, BSi and lithogenic are in mg m-2 d-1. (Proto)Zooplankton fluxes of pteropods, foraminifera, and radiolaria, determined from the number of individuals counted in the gels, in 10^3 ind. m^{-2} d^{-1}.

					Biogeochemical fluxes						(Proto)Zooplankton fluxes		
	Cruise	Date	Trap	Depth	POC	PON	PIC	BSi	Litho	C/N	Ptero	Foram	Radio
					mg m^{-2} d^{-1}						10^3 ind. m^{-2} d^{-1}		
Cluster 1: No Ballast	MSM18	29.04.11	DF02	100	43.7	6.5	27.7	6.3	54	7.8	NA	NA	NA
			DF02	400	18.0	2.1	0.0	11.0	150	9.8	NA	NA	NA
	POS495	22.02.16	DF13	100	54.5	8.5	14.3	58.7	50	7.5	0.7	7.2	0.3
			DF13	200	61.7	8.7	0.0	36.3	181	8.2	0	2.5	2.3
			DF13	400	31.9	3.0	8.2	38.7	62	12.5	0	1.0	0.7
	POS508	26.01.17	DF15	100	58.1	7.1	3.1	24.3	81	9.5	0	0.9	4.7
			DF15	200	25.9	3.9	21.2	12.0	22	7.8	0.3	0.2	1.4
			DF15	400	20.2	2.2	12.8	13.7	44	10.8	0	0.5	0
	POS508	29.01.17	DF16	100	49.1	6.4	0.0	42.8	123	8.9	1.9	7.7	0.6
			DF16	200	56.3	6.6	8.0	58.2	105	9.9	1.6	3.8	1.3
			DF16	400	66.3	7.6	0.0	54.0	185	10.2	0	2.9	2.9
	POS508	02.02.17	DF17	100	74.0	10.0	12.5	55.0	58	8.6	1.1	25.0	0.8
			DF17	200	55.8	7.4	12.1	51.1	27	8.8	0	1.1	1.3
			DF17	400	47.8	5.9	13.3	45.1	78	9.5	0	1.5	0.4
Cluster 2: BSi-ballasted	POS481	23.02.15	DF11	150	83.1	9.8	14.3	171.0	27	9.9	0	0.6	0.4
			DF11	200	76.1	8.9	7.1	154.1	36	10.0	0.4	0.7	0.6
			DF11	400	43.7	3.9	8.4	67.5	20	13.0	0	0.1	0.1
	POS481	26.02.15	DF12	150	82.3	10.7	5.2	179.5	33	9.0	0	0.8	0.7
			DF12	200	75.5	9.9	24.4	193.5	0	8.9	0	0.5	1.7
			DF12	400	56.6	6.7	5.7	146.4	72	9.8	0	1.2	0.2
	POS495	25.02.16	DF14	100	77.8	10.9	23.0	126.3	0	8.3	0.6	4.2	0.8
			DF14	200	53.2	6.8	14.1	108.0	37	9.1	0	6.7	2.2
			DF14	400	52.8	5.3	2.5	115.1	174	11.6	0	4.4	1.7
Cluster 3: PIC & Lithogenic-ballasted	POS445	26.01.13	DF05	100	67.8	7.9	239.0	51.2	380	10.0	0.8	1.6	0.2
			DF05	200	67.8	5.7	254.5	34.6	528	13.9	0.2	3.6	0.4
			DF05	400	45.9	3.8	112.9	28.7	140	13.9	0.2	0.8	0.4
	POS445	27.01.13	DF06	100	63.0	6.9	114.3	28.3	169	10.6	1.1	4.9	0.1
			DF06	200	72.0	6.1	70.8	34.5	336	13.8	1.9	15.2	0.6
			DF06	400	25.2	3.6	113.7	17.1	0	8.2	0.3	2.5	0
	POS464	06.02.14	DF07	150	46.7	4.8	6.6	4.9	243	11.4	1.0	0.1	0.8
			DF07	200	39.7	5.0	24.8	5.4	113	9.3	1.2	1.7	0.4
			DF07	400	51.1	5.9	109.4	11.5	137	10.1	0.1	0.8	0.1
	POS464	08.02.14	DF08	100	44.2	5.6	16.1	41.5	32	9.2	1.1	1.5	0.3
			DF08	200	55.2	6.8	184.5	25.3	386	9.5	0.7	0.1	1.1
			DF08	400	26.3	3.9	57.6	15.5	0	7.9	0	0.5	0.8
Cluster 4: BSi, PIC & Lithogenic-ballasted	POS425	22.01.12	DF03	100	170.2	27.4	69.2	130.0	993	7.2	NA	NA	NA
			DF03	400	42.8	4.5	29.9	29.9	103	11.0	NA	NA	NA
	POS425	24.01.12	DF04	100	191.6	33.7	42.7	127.9	1746	6.6	NA	NA	NA
			DF04	400	60.4	8.2	29.6	61.8	541	8.6	NA	NA	NA
	POS464	11.02.14	DF09	100	79.8	10.3	28.1	91.7	117	9.1	0.9	6.7	0.8
			DF09	200	97.9	12.4	244.0	111.3	114	9.2	0	1.2	0.9
			DF09	400	49.7	6.0	44.0	52.1	38	9.7	0	0.6	1.4
	POS464	14.02.14	DF10	100	170.9	18.5	0.0	159.5	446	10.8	0.9	0.9	0.4
			DF10	200	184.7	22.1	59.4	231.8	166	9.8	0	0	3.9
			DF10	400	114.4	16.1	43.0	190.6	222	8.3	0	0	2.6
Other	M140	28.08.17	DF18	100	35.0	4.4	7.4	NA	132	9.3	NA	NA	NA
			DF18	200	31.9	3.3	4.3	NA	517	11.4	NA	NA	NA
			DF18	400	17.3	1.8	11.6	NA	27	11.2	NA	NA	NA
	M140	31.08.17	DF19	100	37.7	4.2	5.8	NA	136	10.5	NA	NA	NA
			DF19	200	38.0	4.1	0.0	NA	144	10.8	NA	NA	NA
			DF19	400	36.7	3.9	6.0	NA	221	10.9	NA	NA	NA

Gel analysis

Gel samples were directly photographed on board, to minimalize disturbances and contamination. We examined all photographs to identify the main particle and aggregate types, and identified fresh and fragmented copepod and krill fecal pellets, small/large dense/porous aggregates, pteropods, radiolarians, foraminifera, large single diatom frustules and large diatom chains. All foraminifera, radiolarians and pteropods were counted per gel and their fluxes were determined by dividing the number of observations with the area of the gel sampler and the duration of the trap deployment.

Environmental parameters using CTD, Secchi disk and satellite

For each trap deployment and recovery we made a vertical profile with the ship-board CTD (Seabird SBE-19). We determined water temperature (T, °C), oxygen concentration (O, μmol L^{-1}), and mixed layer depth (z_{mld}). If several profiles were obtained during a trap deployment, averages were taken for each value. We determined the Secchi disk depth for most deployments or recoveries of the drifting traps, which is a measure for light penetration. Chlorophyll *a* concentrations were obtained from the MODIS-Aqua satellite (4 km resolution), where we used the weekly average for each trap deployment.

Statistics

Statistical analyses were done in R (R Core Team et al. 2016). We analysed the data per deployment depth, to avoid dependency of the data. As the data did not follow a normal distribution, only non-parametric tests and tests on log-transformed data were used. Spearmans ρ was used to determine correlations between POC fluxes versus environmental parameters and ballast fluxes.

A multiple linear regression between POC and the explanatory variables PIC, BSi and lithogenic was fitted on the log-transformed data, and the adjusted R^2 was used as a measure for how well the variation in the explanatory variables explained differences in the POC flux. Additionally, linear regressions between POC and environmental parameters on log-transformed data were used.

We statistically clustered the traps based on the three ballast mineral fluxes. We determined the third quartile for each ballast flux at 100 m, 200 m and 400 m, and labelled traps with fluxes above this threshold as a ballasted trap. Traps could be labelled as non-ballasted, PIC, BSi or lithogenic ballasted, or a combination thereof. We did not have ballasting from PIC alone and, thus derived four clusters: 1.) traps that were not ballasted (DF02, 13, 15, 16, 17), 2.) traps ballasted with BSi alone (DF11, 12, 14), 3.) traps ballasted with lithogenic

material and PIC (DF05, 6, 7, 8), and 4.) traps ballasted with all three ballast fluxes (DF03, 4, 9, 10).

RESULTS

POC and PON fluxes decreased with increasing depth (Fig. 12). PON fluxes had higher attenuation compared to POC fluxes, resulting in an increased C/N ratio with increased depth. Average PIC and BSi fluxes were lower at 400 m compared to 100 m, but were highest at 200 m (Fig. 12). In both cases this was caused by three traps that had higher fluxes at 200 m compared to 100 m (DF05, DF08 and DF09 for PIC; DF10, DF11 and DF12 for BSi). The average lithogenic flux decreased with increasing depth. Lithogenic fluxes had highest variation of all fluxes (Fig. 12). In general, drifting traps deployed further offshore collected less material than drifting traps deployed closer to the coast. Especially POC and BSi fluxes were up to 3-fold higher at CB_{eu} than at CB_{meso}.

POC and PON fluxes

POC fluxes at 100 m significantly differed from fluxes at 400 m (Wilcoxon paired rank sum test, $p<0.01$). The strongest attenuation between 100 and 400 m was observed in DF03 and DF04 in winter 2012 (>68%), which also exhibited the highest measured POC fluxes at 100 m. POC and PON fluxes were tightly coupled at 100 m, 200 m and 400 m ($\rho=0.93$, $\rho=0.76$ and $\rho=0.94$ respectively). PON fluxes at 100 m ranged from 4.2 mg m^{-2} d^{-1} (DF19) to 33.7 mg m^{-2} d^{-1} (DF04), with a median of 8.1 mg m^{-2} d^{-1} (Table 3). PON fluxes at 400 m ranged between 1.8 mg m^{-2} d^{-1} (DF18) and 16.1 mg m^{-2} d^{-1} (DF10), with a median of 6.8 mg m^{-2} d^{-1}. Organic C:N ratios ranged from 6.6 (DF04 100 m), to 13.9 (DF05 400 m) (Table 3). Generally, the C:N ratio increased with increasing depth, with a strongest increase at trap DF13, from 7.5 at 100 m to 12.5 at 400 m.

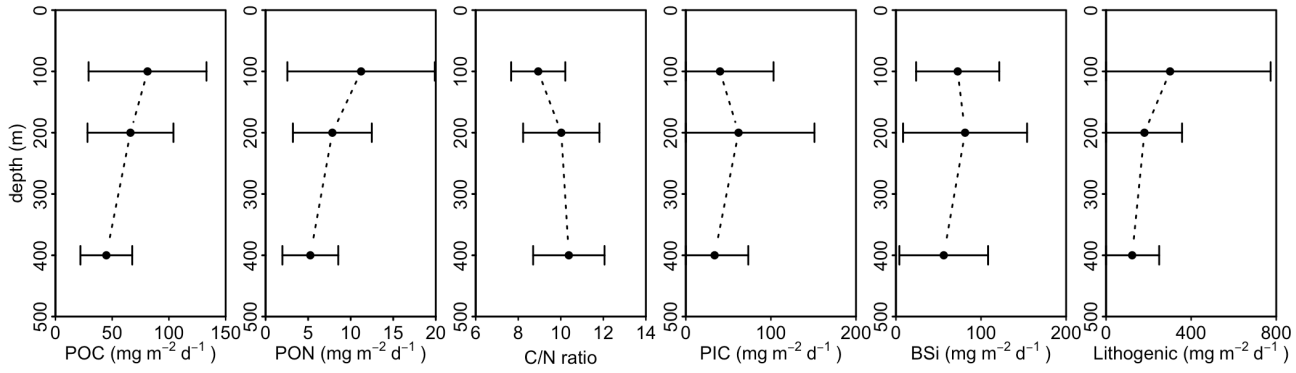

Fig. 12. Average biogeochemical fluxes in mg m^{-2} d^{-1} over depth. From left to right: POC, PON, C/N ratio, PIC, BSi, and lithogenic fluxes. Averages ± SD.

Correlating POC fluxes to chlorophyll, oxygen and temperature

POC fluxes during winter (DF03-DF17) were correlated to environmental parameters obtained from CTD profiles and satellite data (See Table S1). POC fluxes at 100 m showed a strong correlation with the chlorophyll *a* concentration obtained from satellite (ρ=0.70), and a moderate correlation with the surface temperature and oxygen concentration obtained from CTD casts (T_s, ρ=-0.42; O_s, ρ=-0.47). The correlation with chlorophyll *a* could explain 61% of the variability in POC fluxes at 100 m (regression on log-transformed data, adjusted R^2), whereas oxygen and temperature could explain less than 20% of total variability. At 200 m, POC fluxes correlated with T_s and temperature at 100 m (T_s and T_{100}, ρ=-0.79 and -0.60), Secchi disk depth (z_{Secchi}, ρ=-0.71), mixed depth layer (z_{MLD}, ρ=-0.66), and chlorophyll *a* concentration (ρ=0.69). Chlorophyll *a* could explain 38% of the variability in POC fluxes at 200 m, T_0 and T_{100} could explain 62% and 35%, whereas all other parameters could explain less than 20% of total variability. At 400 m, POC correlated strongest with T_{400} and O_{400} (ρ=-0.66 and -0.62) and moderately with chlorophyll *a* concentrations (ρ=0.40). Temperature and oxygen intercorrelated (ρ=0.70), and explained 44% and 53% of the variation in POC fluxes at 400 m respectively, while surface chlorophyll *a* explained 18% of total variance.

Correlating POC fluxes to ballast fluxes

The lithogenic, BSi and PIC ballast fluxes were a major component of total particulate mass (TPM) flux. The contribution from these fluxes to TPM flux at 100 m ranged from 58% (DF15, January 2017) to 95% (DF05), with a median of 73%. Their contribution to TPM flux increased with increasing depth, within a range of 69% (DF16, January 2017) to 93% (DF05) and a median of 81% at 400 m. Lithogenic fluxes at 100 m ranged from 0.0 to 1746 mg m^{-2} d^{-1} (DF14, DF04), with a median of 123.0 mg m^{-2} d^{-1}, and at 400 m from 0.0 to 540 mg m^{-2} d^{-1} (DF06, DF04), with a median of 90.2 mg m^{-2} d^{-1} (Table 3). PIC fluxes at 100 m ranged from 0.0 to 239 mg m^{-2} d^{-1} (DF10, DF05) with a median of 16 mg m^{-2} d^{-1}, and at 400 m from 0.0 to 114 mg m^{-2} d^{-1} (DF02, DF06), with a median of 13 mg m^{-2} d^{-1} (Table 1). BSi fluxes at 100 m ranged from 6.27 mg m^{-2} d^{-1} to 159.5 mg m^{-2} d^{-1} (DF02, DF10) with a median of 55.0 mg m^{-2} d^{-1}, and at 400 m from 11.0 mg m^{-2} d^{-1} to 190.6 mg m^{-2} d^{-1} (DF02, DF10), with a median of 41.9 mg m^{-2} d^{-1} (Table 3). The variability of lithogenic and PIC fluxes decreased with increasing depth, whereas the variability of BSi fluxes increased with increasing depth (Fig. 12).

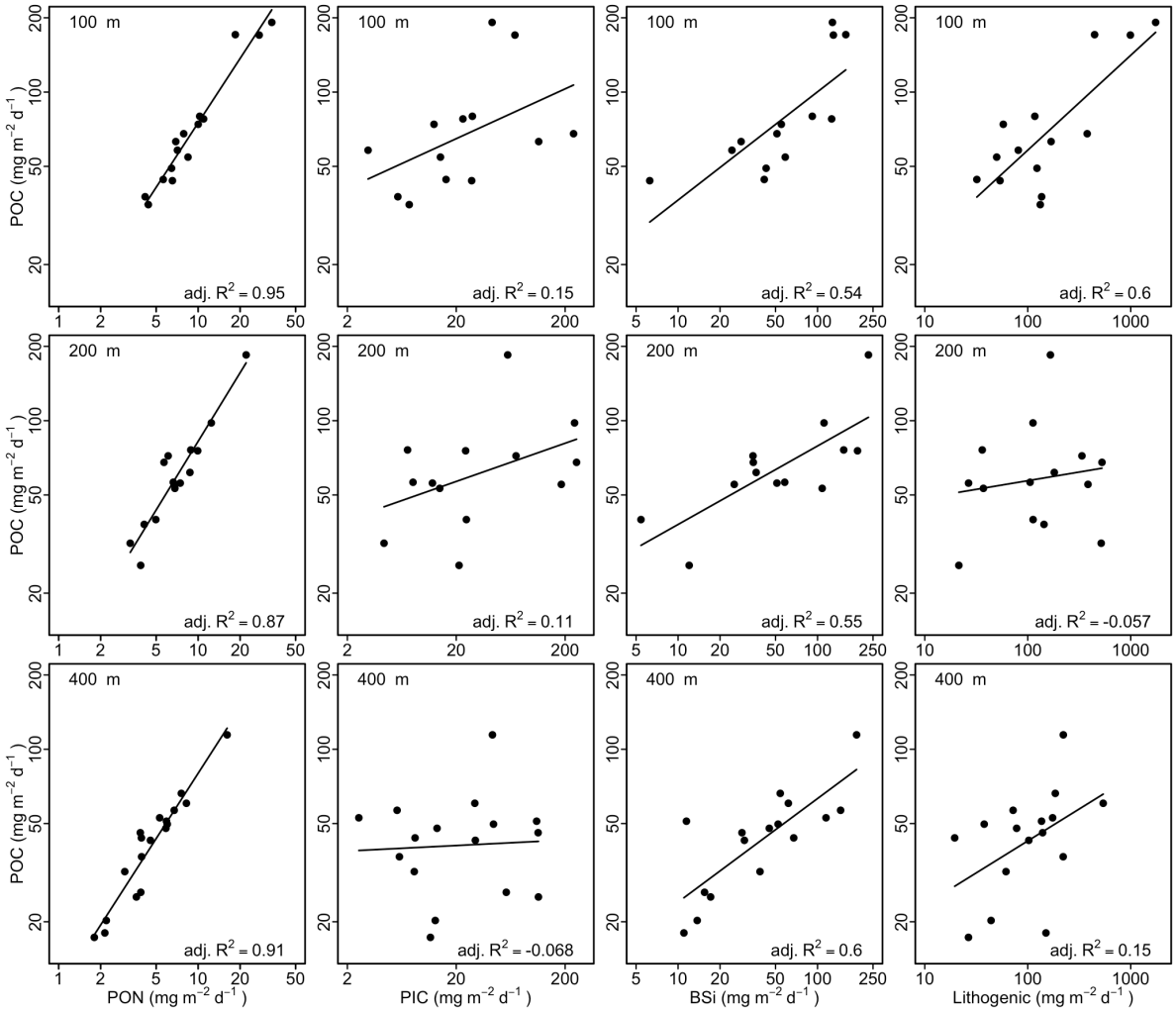

Fig. 13. PON, PIC, BSi and lithogenic fluxes vs. POC fluxes at 100, 200 and 400 m, with fitted regression lines (regression on log-transformed data).

Linear regressions on log-transformed data showed that, of the ballast fluxes, the BSi flux correlated strongest with POC flux at 100 m, 200 m, and 400 m (ρ = 0.86, 0.75 and 0.76) and was able to explain 54-60% of the variability in POC flux (Fig. 13). Lithogenic fluxes correlated moderately with POC fluxes (ρ = 0.42, <0.1 and 0.59) and could explain 60% of the variation in POC at 100 m, but <1% and 15% at 200 and 400 m, respectively (Fig. 13). PIC had the weakest correlation to POC flux of all three ballast mineral fluxes (ρ = 0.33, 0.39 and <0.1) and PIC alone could explain 15% of the variability in POC fluxes at 100 m, 11% at 200 m and <1% at 400 m (Fig. 13). The combination of BSi and lithogenic flux combined could explain 83%, 78% and 60% of the POC flux at 100, 200, and 400 m, respectively. When combined, the PIC, BSi and lithogenic fluxes explained 91%, 75%, and 83% of the observed variability in POC fluxes at 100 m, 200 m and 400 m, respectively. The gel trap analyses showed that this was due the highest POC flux occurring when large diatom aggregates were ballasted by coccolithophores and Saharan dust.

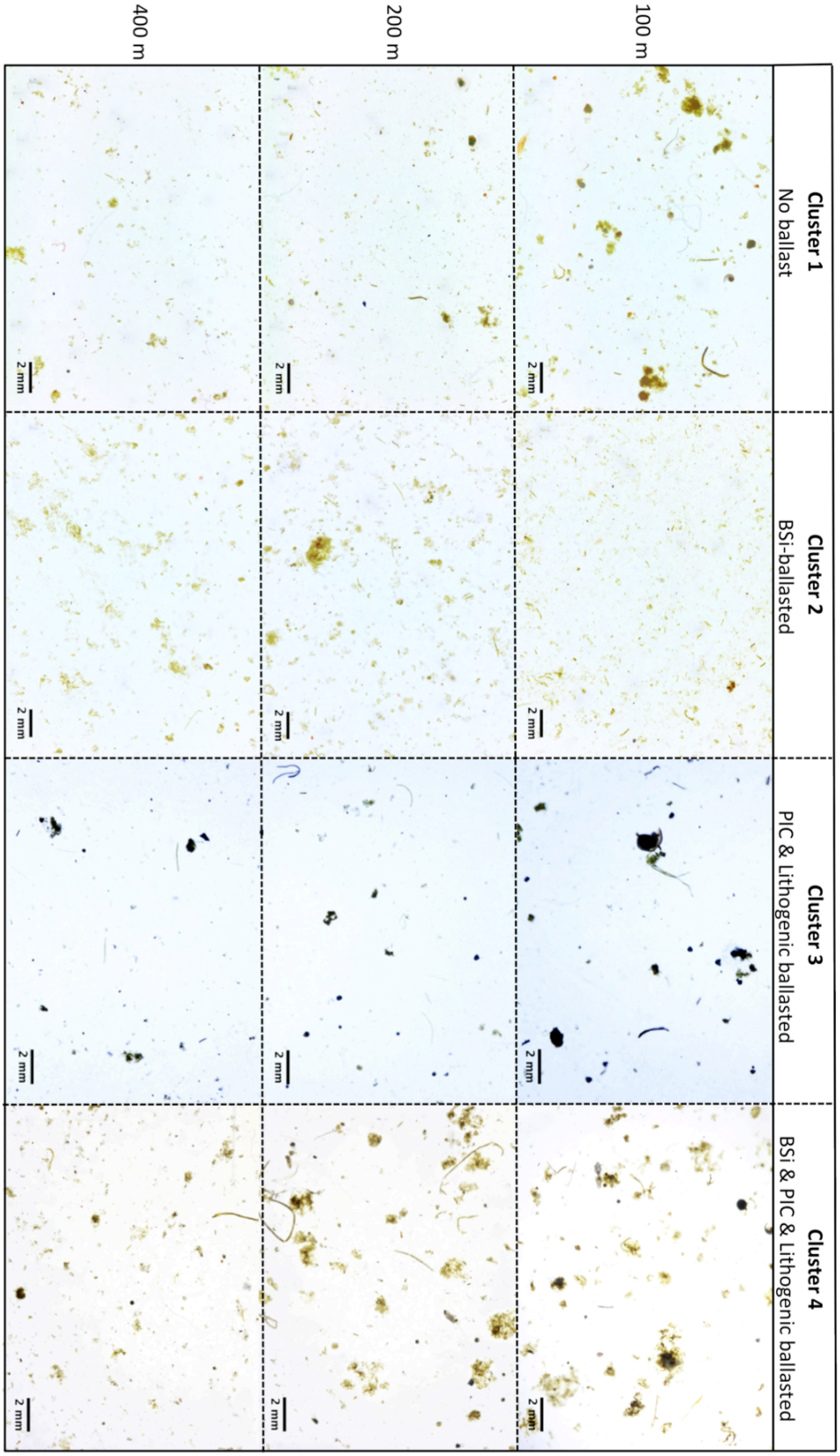

Fig. 14. Gel traps from each cluster, at 100 m, 200 m, and 400 m. a.) No ballast: DF13 contained mostly brown aggregates and fecal pellets at 100 m, and small aggregates at 200 and 400 m; b.) BSi-ballasted: DF12 contained large porous green aggregates and fecal pellets; c.) Lithogenic and PIC: DF05, containing dense brown aggregates, fecal pellets, a pteropod and a radiolarian; d.) Lithogenic, BSi and PIC: DF09, containing large round green aggregates and fresh fecal pellets at 100 and 200 m, and small aggregates at 400 m.

Ballast clusters

We statistically clustered the traps based on the three ballast mineral fluxes, and derived four clusters: 1.) traps that were not ballasted (DF02, 13, 15, 16, 17); 2.) traps ballasted with BSi alone (DF11, 12, 14); 3.) traps ballasted with lithogenic material and PIC (DF05, 6, 7, 8); and 4.) traps ballasted with all three ballast fluxes (DF03, 4, 9, 10). We characterized the dominant aggregate types and (proto)zooplankton occurrence in the gel traps and observed that aggregate types were comparable between traps of the same ballast cluster. Cluster 1 traps (no ballasting) contained small brown-coloured aggregates (<0.5 mm) and fresh and degraded euphausiid and copepod fecal pellets, indicating high grazing on and degradation of the sinking material.

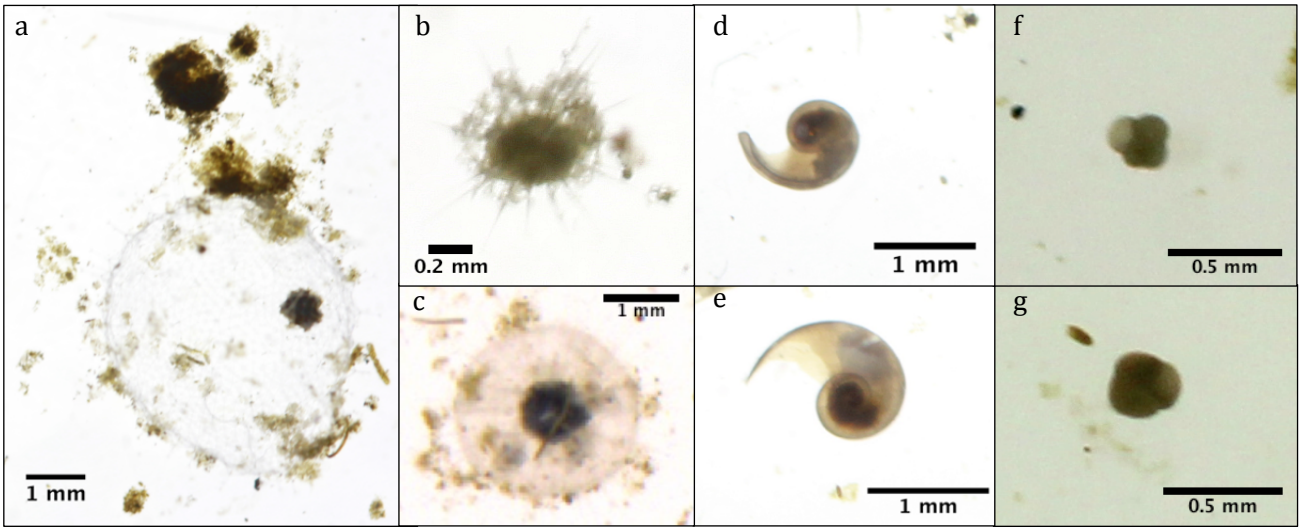

Fig. 15. Examples of radiolarians, pteropods and foraminifera found in the gels. a-c.) Radiolaria (a and c Spumellaria, b Acantharia) with aggregates and fecal pellets; d-e.) pteropods; f-g.) foraminifera.

The small aggregates were densely packed and consisted mainly of degraded fecal material (Fig. 14), indicating that zooplankton must have been abundant during those periods. Additionally, these traps had high abundances of foraminifera, radiolarians and pteropods (Table 3, Fig. 14, Fig. 15). Cluster 2 traps (BSi ballasting) mainly contained large green porous aggregates (>2 mm) and fresh euphausiid and copepod fecal pellets at 100 m (Fig. 14). In contrast, at 200 m and 400 m small aggregates dominated and only few large aggregates occurred. Fecal pellets in the deep traps consisted of both fresh and degraded pellets, while at 100 m predominantly fresh euphausiid and copepod fecal pellets were observed.

Some traps contained large single diatom frustules or diatom chains. Cluster 2 traps contained relatively few pteropods, foraminifera, and radiolarians. Cluster 3 traps (lithogenic and PIC ballasting) were characterized by small dense brown-coloured

aggregates (<0.5 mm), and fresh and degraded fecal pellets (Fig. 14, Table 3). The aggregates contained degraded fecal material and looked very similar to aggregates in cluster 1. The number of aggregates decreased with increasing depth, but the sinking material at all depths seemed equally degraded. Zooplankton was present in all traps, with foraminifera and pteropods being especially abundant at 200 m. Cluster 4 traps (all ballasting) were dominated by both porous and dense large green phytodetritus aggregates (Fig. 14, Table 3). These large aggregates were more densely packed than the large aggregates observed for cluster 2. Fecal pellets were both fresh and degraded at 400 m, suggesting either a high settling velocity or fecal pellet production at depth. Half of the traps contained pteropods, where the other traps contained radiolarians at 100 m and 200 m.

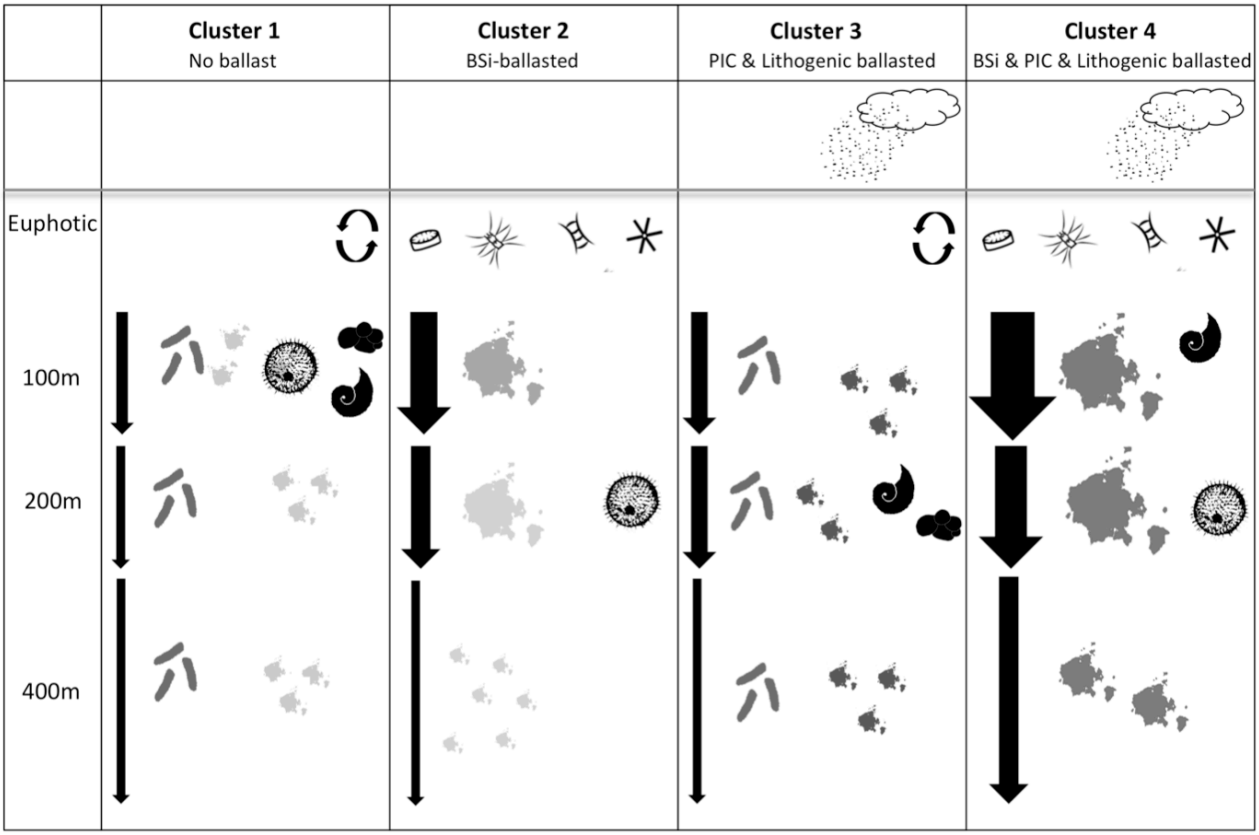

Fig. 16. Overview of the four ballasting regimes at Cape Blanc. 1) Under the no ballasting regime, particulate material is highly recycled in the euphotic layer. Dominant particles are fecal pellets and small aggregates, and radiolarians, pteropods and foraminifera at 100 m. POC fluxes (black arrows) are relatively low. 2) Under a BSi-ballasted regime, diatoms dominate the euphotic zone, aggregates at 100 and 200 m are large and porous, and disaggregate into small aggregates at 400 m. POC fluxes at 100 m and 200 m are high, and decrease at 400 m. 3) When the system is ballasted with PIC and lithogenic minerals, recycling is high in the euphotic layer, and fecal pellets and small dense aggregate dominate the flux. Pteropods and foraminifera are dominant at 200 m. POC fluxes are moderate at 100 m and 200 m, and low at 400 m. 4) When the system is ballasted by BSi, PIC and lithogenic minerals, diatoms seem to dominate the euphotic layer, and large aggregates dominate the flux at 100 and 200 m, where smaller aggregates dominate 400 m. Pteropods occur at 100 m and radiolarians occur at 200 m. POC fluxes at 100 m and 200 m are highest, and decrease at 400 m.

The average POC flux per cluster varied. Cluster 1 had the lowest POC fluxes, followed by cluster 3, cluster 2 and cluster 4 (Table 3, Fig. 16). Sample size per cluster was low (n=3-5), and therefore differences between clusters were not significant, except for the difference between cluster 1 and 4 at 100 m (Wilcoxon rank sum test, p=0.016). Average transfer efficiency, here defined as the fraction of POC at 100 m that reaches 400 m, was 67 ± 40 % for cluster 1, 68 % for cluster 2, 56 ± 14 % for cluster 3, and 47 ± 21 % for cluster 4.

Flux attenuation can be estimated by defining the fraction of POC at 100 m that does not reach 400 m (this was calculated as: 1 - (POC_{400} / POC_{100})). We observed that there was a trend for higher flux attenuation during periods with high POC flux at 100 m (Fig. 17, Table S2). This was not only the case for the Eastern Boundary Upwelling region off northwest Africa studied here, but also for drifting traps deployed in the Sub-Arctic (Fram Strait as part of the FRAM project *FRontier in Marine Monitoring*), at the Porcupine Abyssal Plain (PAP Observatory), and in the Southern Ocean (as part of the RV Polarstern cruise ANT-XXVIII/3) (Fig. 17, Fig. 18, Table S2).

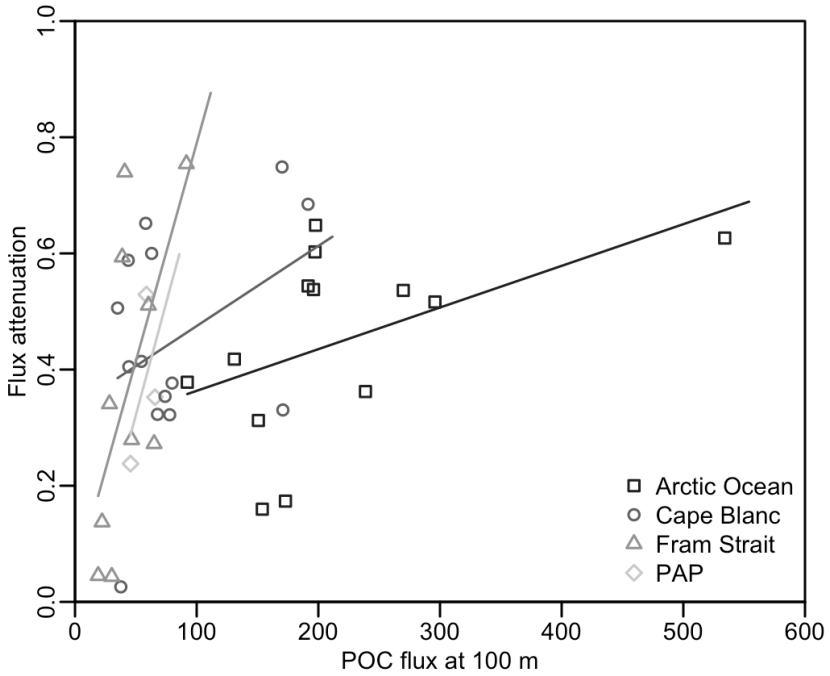

Fig. 17. Flux attenuation (1 – (POC_{400}/POC_{100}) plotted against POC flux at 100 m. Higher POC flux at 100 m often coincided with high attenuation between 100 and 400 m.

DISCUSSION

We deployed drifting traps off Northwest Africa in the tropical East Atlantic Ocean over a 7-year period. The sediment trap deployments stretched over three seasons, over which time four distinct ballasting regimes could be identified: i) a non-ballasted system, characterized by high recycling in the euphotic zone and subsequently low POC fluxes of highly degraded material; ii) a BSi-ballasted system, with large porous diatom aggregates at 100 m and primarily small porous aggregates at 200 m and 400 m. POC fluxes were high at 100 m and attenuated strongly between 100 and 200 m; iii) a PIC- and lithogenic-ballasted system, dominated by small aggregates and characterized by low POC fluxes; and iv) a BSi-, PIC- and lithogenic-ballasted system, with the highest POC fluxes at all depth, that were dominated by large ballasted diatom aggregates.

Downward POC flux was strongly correlated to ballast mineral fluxes. Furthermore, chlorophyll concentrations correlated well to the POC export at 100 m, showing that newly produced organic matter sank rapidly out of the euphotic zone. Of all ballast fluxes, BSi was the best predictor for POC flux, and could explain 54% at 100 m and 60% at 400 m. The correlation between POC flux, BSi flux, and chlorophyll indicated that at 100 m, POC flux was strongly influenced by settling diatoms. The gel traps showed that these diatoms were sinking in the form of aggregated material, i.e. as marine snow. Interestingly, fluxes of lithogenic and PIC ballast minerals seemed to enhance POC export only when BSi fluxes were also high. This was due to diatom aggregates scavenging coccolithophores and Saharan dust, which ballasted the aggregates and increased the size-specific sinking velocities of the aggregates (Hamm 2002; Passow and De La Rocha 2006; Iversen and Robert 2015; van der Jagt et al. 2018).

POC flux was positively correlated with flux attenuation, with high fluxes associated with stronger attenuation (Fig. 17, Table S2). POC flux is attenuated via biological processes, such as microbial degradation and zooplankton grazing as well as aggregate fragmentation by zooplankton, causing the aggregates to sink slower and, thus, have more time for degradation in the surface ocean (Turner 2015). Microbial remineralisation of sinking aggregates is independent of aggregate type, size, and ballasting (Ploug et al. 2008a; Iversen and Ploug 2010; Iversen et al. 2010) and carbon-specific turnover primarily varies as a function of temperature (Iversen and Ploug 2013; Marsay et al. 2015). It is therefore unlikely that microbial degradation alone could have caused the observed variability in flux

attenuation. Instead, it is more likely that differences in zooplankton grazing were responsible for the increased flux attenuation during times of high POC flux.

Previously, zooplankton have been hypothesised to be gatekeepers for the movement of organic matter to the mesopelagic (Jackson and Checkley Jr 2011) and the presence of copepod and euphasiid fecal pellets in all the drifting traps suggests that this could be the case in the Eastern Boundary Upwelling off North-West Africa. Furthermore, pteropods, which have previously been proposed as flux feeders (Jackson 1993), were collected in all traps at 100 m and 200 m. While we did not observe individuals attached to aggregates directly, often the guts of the pteropods were full, indicating that they were feeding before being trapped. Additionally, we often observed radiolarians and foraminifera in the traps, both of which have been suggested to control POC fluxes to control downward carbon fluxes (Lampitt et al. 2009; Fehrenbacher et al. 2018; Belcher et al. 2018). Radiolarians were observed with aggregated material attached to their exoskeleton, suggesting that they were capturing material to feed on, although it cannot be ruled out that they had become entangled in sinking aggregates. The majority of foraminifera collected in the gel-traps were not attached to aggregates, therefore it appears unlikely that these organisms were feeding on aggregates.

Previous studies have indicated that zooplankton are responsible for POC flux attenuation in the Arctic (Wexels Riser et al. 2001), the North Atlantic (Lampitt et al. 1993), the tropical East Atlantic (Iversen et al. 2010), and the Southern Ocean (Lam and Bishop 2007), and have suggested that zooplankton may function as a “biological filter” or “retention filter” of the POC flux in the mesopelagic (Wexels Riser et al. 2001). We compared flux attenuation and magnitude derived from drifting trap data at locations as diverse as the Fram Strait (Arctic Ocean), the Porcupine Abyssal Plain (temperate North Atlantic), and the Southern Ocean (Wolf et al. 2016; Iversen et al. 2017; Roca-Martí et al. 2017), and showed that higher fluxes at 100 m are in general related to higher attenuation between 100 and 400 m (Fig. 17, Fig. 18, Table S2). Thus, periods with high primary production cause high POC export at 100 m, but at the same time high attenuation between 100 and 400 m, likely due to stimulation of the zooplankton community and high aggregate feeding. This suggests that zooplankton may control the magnitude of the POC flux from the base of the euphotic zone to the deep sea at all latitudes in the Atlantic Ocean, despite differences in algal and zooplankton communities.

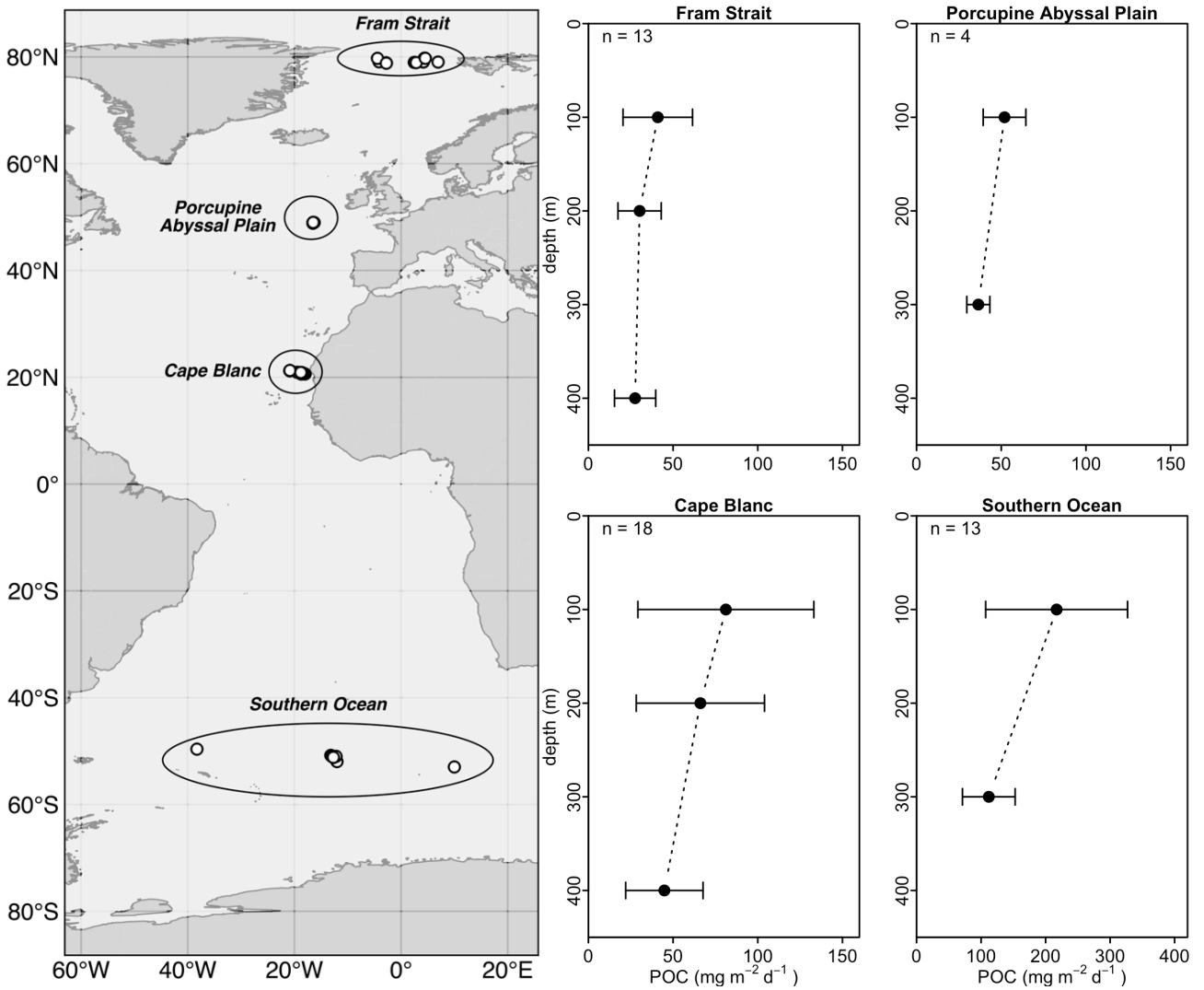

Fig. 18. Deployment locations (left) and POC fluxes (right) of 13 drifting traps deployed between 2013 and 2017 in the Fram Strait, 4 drifting traps deployed in 2014 at the Porcupine Abyssal Plain, 18 drifting traps deployed between 2011 and 2017 off Cape Blanc, and 13 drifting traps deployed in 2011 in the Southern Ocean. Average ± sd, and relative standard deviation (RSD). Note the different scaling of the x-axis for the Southern Ocean.

ACKNOWLEDGEMENTS

We thank the crew of F.S. Poseidon and F.S. Maria S. Merian for their assistance during the cruises. Special thanks to Christiane Lorenzen for the biogeochemical measurements, Marco Klann his assistance during the many cruises, and Michal Kucera for fruitful discussions. This study was supported by the Helmholtz Association, the Alfred Wegener Institute Helmholtz Centre for Polar and Marine Research and the DFG-Research Center/Cluster of Excellence "The Ocean in the Earth System" at MARUM. This publication is supported by the HGF Young Investigator Group SeaPump "Seasonal and regional food web interactions with the biological pump": VH-NG-1000

SUPPLEMENTARY INFORMATION

Table S1. Overview of the environmental parameters used for correlation and regression analyses. Secchi disk depth determined with a Secchi disk, mixed layer depth (MLD), temperature, salinity and oxygen concentrations obtained from CTD casts, and weekly averaged chlorophyll-a concentration obtained from MODIS-Aqua satellite (4 km resolution).

	Secchi disk	CTD				Sattelite
Trap	**Secchi depth (m)**	**MLD (m)**	**Temperature (°C)**	**Salinity (PSU)**	**Oxygen (mL L^{-1})**	**Chl.a (mg m^{-3})**
DF02	NA	NA				0.929
0			NA	NA	NA	
100			NA	NA	NA	
200			NA	NA	NA	
400			NA	NA	NA	
DF03	NA	97.5				2.966
0			19.8	36.6	185.3	
100			19.4	36.8	173.3	
200			17.6	36.6	125.1	
400			12.1	35.7	77.5	
DF04	NA	90				3.360
0			19.3	36.8	192.5	
100			18.8	36.8	162.1	
200			15.6	36.3	116.7	
400			11.5	35.5	59.0	
DF05	NA	95				1.038
0			18.8	36.5	229.6	
100			18.1	36.3	164.8	
200			15.4	36.0	103.8	
400			12.4	35.6	92.4	
DF06	NA	100				0.824
0			18.8	36.4	229.1	
100			18.7	36.4	201.0	
200			15.4	36.0	102.5	
400			12.4	35.6	95.1	
DF07	18	95				0.436
0			19.6	36.5	240.0	
100			17.7	36.4	158.0	
200			14.8	35.8	94.2	
400			12.5	35.6	109.5	
DF08	15	80				1.222
0			18.8	36.2	246.2	
100			17.2	36.2	125.5	
200			15.2	36.0	117.4	
400			12.2	35.6	121.1	
DF09	13	57.5				0.868
0			17.2	36.0	219.5	
100			15.9	36.0	100.4	
200			14.8	36.0	123.1	
400			11.7	35.5	96.4	
DF10	11	50				1.174
0			16.8	36.1	217.0	
100			15.5	35.9	94.7	
200			14.1	35.8	95.6	
400			10.8	35.4	62.8	
DF11	9	52.5				1.327
0			17.3	35.6	292.2	
100			17.1	36.3	144.9	
200			14.9	36.0	108.9	
400			12.0	35.6	92.7	
DF12	NA	50				1.921
0			16.6	36.4	186.6	
100			15.5	36.2	138.2	
200			14.8	35.9	97.2	
400			11.9	35.5	70.7	
DF13	9	62.5				0.898
0			19.3	36.1	188.5	
100			15.7	35.7	121.5	
200			14.7	35.8	107.2	
400			11.9	35.5	78.2	

	Secchi disk	CTD				Sattelite
Trap	**Secchi depth (m)**	**MLD (m)**	**Temperature (°C)**	**Salinity (PSU)**	**Oxygen (mL L^{-1})**	**Chl.a (mg m^{-3})**
DF14	12	125				0.881
0			17.8	36.1	168.9	
100			17.2	36.1	228.4	
200			14.0	35.7	107.3	
400			11.4	35.4	78.5	
DF15	17	90				0.547
0			21.1	36.5	313.0	
100			19.0	36.2	181.0	
200			14.8	35.9	125.5	
400			12.2	35.6	124.5	
DF16	14	70				1.027
0			19.5	36.2	311.2	
100			17.2	36.1	111.3	
200			14.3	35.8	113.4	
400			11.6	35.4	79.6	
DF17	13	60				0.690
0			19.5	36.3	261.5	
100			16.2	36.0	110.9	
200			14.3	35.8	123.3	
400			11.2	35.4	80.2	
DF18	NA	NA				0.137
0			NA	NA	NA	
100			NA	NA	NA	
200			NA	NA	NA	
400			NA	NA	NA	
DF19	NA	NA				0.493
0			NA	NA	NA	
100			NA	NA	NA	
200			NA	NA	NA	
400			NA	NA	NA	

Table S2. Overview of the drifting sediment traps deployed in the Fram Strait, at the Porcupine Abyssal Plain and in the Southern Ocean. POC fluxes are in mg C m^{-2} d^{-1}.

	Cruise	Date	Latitude	Longitude	Trap	Depth	POC flux
Fram Strait	MSM29	08.07.13	78°47.16'N	5°19.98'E	FDF01	100	30.2
						300	28.9
	PS93.2	26.07.15	79°3.90'N	4°10.79'E	FDF02	100	32.1
						200	34.5
						400	45.1
	PS93.2	30.07.15	78°51.74'N	2°44.99'W	FDF03	100	22.2
						200	51.6
						400	19.2
	PS93.2	03.08.15	79°45.33'N	4°24.48'E	FDF04	100	46.5
						200	26.0
						400	33.5
	PS99	26.06.16	79°4.88'N	4°6.41'E	FDF05	100	65.0
						200	43.5
						400	47.3
	PS99	30.06.16	78°52.26'N	2°45.88'W	FDF06	100	32.1
						200	40.9
						400	41.8
	PS99	03.07.16	79°43.49'N	4°23.99' E	FDF07	100	60.3
						200	43.0
						400	29.5
	PS107	27.07.17	79°03.86'N	4°12.65'E	FDF09	100	91.5
						200	16.7
						400	22.5
	PS107	29.07.17	78°58.34'N	2°29.85'E	FDF10	100	25.4
						200	24.5
						400	28.6
	PS107	30.07.17	78°55.64'N	2°51.78'E	FDF11	100	28.3
						200	14.2
						400	18.7
	PS107	03.08.17	78°49.08'N	2°44.56'W	FDF12	100	19.0
						200	21.2
						400	18.2
	PS107	08.08.17	79°44.05'N	4°34.00'E	FDF13	100	38.8
						200	13.5
						400	15.8
	PS107	13.08.17	79°01.98'N	6°57.81'E	FDF14	100	40.8
						200	33.2
						400	10.6
Porcupine Abyssal Plain	M108	13.07.14	48°50.07'N	16°31.16'W	DF11	100	37.8
						300	41.0
	M108	16.07.14	48°59.94'N	16°29.93'W	DF12	100	45.6
						300	34.7
	M108	18.07.14	48°58.53'N	16°16.31'W	DF13	100	58.6
						300	27.6
	M108	20.07.14	48°59.51'N	16°28.00'W	DF14	100	65.7
						300	42.6
Southern Ocean	ANT_XXVIII3	21.01.12	53°0.35'S	10°0.81'E	84	100	295.8
						300	143.1
	ANT_XXVIII3	29.01.12	51°59.89'S	11°59.85'W	86	100	196.0
						300	90.6
	ANT_XXVIII3	02.02.12	50°50.11'W	13°9.88'W	87	100	197.7
						300	69.5
	ANT_XXVIII3	03.02.12	51°12.25'S	12°40.20'W	91	100	197.3
						300	78.4
	ANT_XXVIII3	05.02.12	51°11.97'S	12°39.91'W	98	100	130.9
						300	76.2
	ANT_XXVIII3	06.02.12	51°12.12'S	12°40.04'W	99	100	173.0
						300	143.0
	ANT_XXVIII3	08.02.12	51°12.16'S	12°39.31'W	114	100	269.8
						300	125.1
	ANT_XXVIII3	12.02.12	51°12.51'S	12°38.39'W	128	100	150.7
						300	103.6
	ANT_XXVIII3	14.02.12	51°11.89'S	12°39.88'W	136	100	92.3
						300	57.4
	ANT_XXVIII3	14.02.12	51°0.86'S	12°10.01'W	137	100	295.8
						300	143.1
	ANT_XXVIII3	15.02.12	51°0.17'S	12°59.77'W	139	100	196.0
						300	90.6
	ANT_XXVIII3	16.02.12	51°11.94'S	12°40.43'W	140	100	197.7
						300	69.5
	ANT_XXVIII3	01.03.12	49°40.05'S	38°16.25'W	174	100	153.9
						300	129.4

MANUSCRIPT 3. AGGREGATE FEEDING BY *CALANUS* AND *PSEUDOCALANUS* CONTROLS CARBON FLUX ATTENUATION IN THE SUB-ARCTIC

Helga van der Jagt, Ingrid Wiedmann, Nicole Hildebrandt, Barbara Niehoff, Morten H. Iversen (in prep.).

ABSTRACT

Up to 95% of the primary production in the ocean is recycled within the upper few hundred meters of the water column and less than 1% of the organic matter produced in the surface ocean is exported to the sea floor. Marine snow and fecal pellets in the upper water column are often recycled at rates exceeding those measured for microbial degradation, suggesting zooplankton might be important for upper ocean flux attenuation. However, direct evidence of interactions with zooplankton and settling aggregates are still rare. We investigated the role of zooplankton aggregate feeding in upper ocean flux attenuation by determining aggregate ingestion rates and feeding behavior on settling aggregates of the dominant sub-Arctic filter-feeding copepods *Calanus sp.* and *Pseudocalanus sp.* Both genera were observed to detect and feed on aggregates, however only *Pseudocalanus* seemed to actively and intentionally feed on settling aggregates while *Calanus* seemed to fragment aggregates and primarily ingest the small fragments. Using *in situ* zooplankton and aggregate abundances in combination with the measured aggregate feeding rates, we calculated that 60-67% of the observed flux attenuation at three subarctic locations could be explained by *Calanus* and *Pseudocalanus* aggregate feeding. When including microbial degradation, we were able to explain 77% of the observed flux attenuation. Our results show that mesozooplankton seem the key organisms for flux attenuation in the sub-Arctic, by directly ingesting and fragmenting settling marine snow.

INTRODUCTION

The export of particulate organic carbon (POC) from the euphotic zone to the deep ocean is an important process in the global carbon cycle, as it governs the oceanic sequestration of atmospheric carbon dioxide (Siegenthaler and Sarmiento 1993). This export is driven by the formation and sinking of aggregates, and attenuated by bacterial- and zooplankton-mediated degradation (Buesseler and Boyd 2009). Downward POC fluxes often follow a power function, showing high flux attenuation in the upper ocean, which gradually decreases with increasing depth, resulting in a nearly constant flux in the deep ocean (Martin et al. 1987). This low flux attenuation in the deep ocean has been attributed temperature-limited and pressure-reduced microbial remineralisation (Iversen and Ploug 2013; Tamburini et al. 2013; Marsay et al. 2015). Flux attenuation in the upper few hundred meters often exceeds measured microbial remineralisation rates, indicating that zooplankton likely controls flux attenuation in the upper ocean (Stemmann et al. 2004; Iversen et al. 2010; Jackson and Checkley Jr 2011).

Zooplankton cause POC flux attenuation by feeding on the sinking material. Specialized flux feeders, such as pteropods and polychaetes, feed below the euphotic zone on sinking aggregates captured by their mucous feeding nets (Jackson 1993). Zooplankton without these feeding nets, such as copepods and euphausiids, also feed on aggregates and fecal pellets. The copepod genera *Microsetella* and *Oncaea* attach to sinking aggregates and may reside for minutes to hours while they feed on the aggregated material (Alldredge 1972; Ohtsuka et al. 1993; Koski et al. 2005), *Pseudocalanus* and *Temora* have been observed on aggregates *in situ* (Möller et al. 2012), where so far only *Temora* has been observed to feed on aggregates (Lombard et al. 2013b; Koski et al. 2017). These copepods may detect sinking aggregates randomly, recognize their hydrodynamic signals (Visser 2001), or find and follow a chemical trail of organic solutes leaking from sinking aggregates (Kiørboe and Thygesen 2001). The ability to recognize chemical trails increases the chance of finding an aggregate, and has so far been only observed for *Temora longicornis* (Lombard et al. 2013b). Additionally, copepods can break up fecal pellets and marine snow into smaller slower-sinking aggregates on which they may feed, which has been observed for *Calanus* and *Pseudocalanus* (Iversen and Poulsen 2007). This may result in relatively higher microbial degradation and thus a further attenuation of the POC flux (Lampitt et al. 1990; Mayor et al. 2014).

The quantitative importance of zooplankton on flux attenuation has proven difficult to measure *in situ*. Zooplankton has been associated with several variations in POC fluxes, including a steep decrease in aggregate abundances at the base of the mixed layer (Lampitt et al. 1993), diel variations in aggregate abundances (Stemmann et al. 2000; Jackson and Checkley Jr 2011), thin layers with high concentrations of copepods and aggregates (Möller et al. 2012), and observed attenuation exceeding microbial remineralisation (Iversen et al. 2010). Studies that aimed to determine the importance of zooplankton relative to bacterial degradation using respiration measurements (Steinberg et al. 2008b) and modelling approaches (Giering et al. 2014), found that zooplankton were responsible for 30-50% and 8-30% of the POC flux attenuation respectively, the latter concluding that zooplankton was responsible for only a minor part of the POC flux attenuation. Instead, zooplankton has been suggested to fragment sinking aggregates, thereby reducing sinking velocities and increasing microbial remineralization (Giering et al. 2014; Mayor et al. 2014). These results are in contrast to experimental studies, where several copepod species were observed feeding on sinking aggregates and fecal pellets (Koski et al. 2005; Lombard et al. 2013b; Koski et al. 2017). These experiments are however difficult to translate to *in situ* POC flux attenuation due to the use of laboratory-formed aggregates, that contain fresh material compared to aggregates in the environment, which contain older material with a lower carbon content (Ploug et al. 2008a).

In this study we investigated the quantitative importance of the dominant mesozooplankton genera *Calanus sp*. and *Pseudocalanus sp*. on POC flux attenuation in three Arctic fjords. Here, downward POC fluxes are high, and can strongly attenuate in the upper 50 m of the water column (Wassmann et al. 2003). We incubated freshly collected copepods with *in situ* collected aggregates to determine aggregate grazing rates, and used video observations to investigate aggregate feeding behaviour. We combined these measurements with vertical profiles of *in situ* zooplankton and aggregate abundances to calculate their impact on flux attenuation.

MATERIAL AND METHODS

All measurements were performed on-board the R/V Helmer Hanssen ARCEx cruise from 17-29 May 2016 in Hornsund, Storfjorden and Erik Eriksen Strait (Fig. 19). These three regions are strongly influenced by Atlantic water from the West Spitsbergen Current (Hornsund), Arctic water (Erik Eriksen Strait), and both Atlantic and Arctic water (Storfjorden).

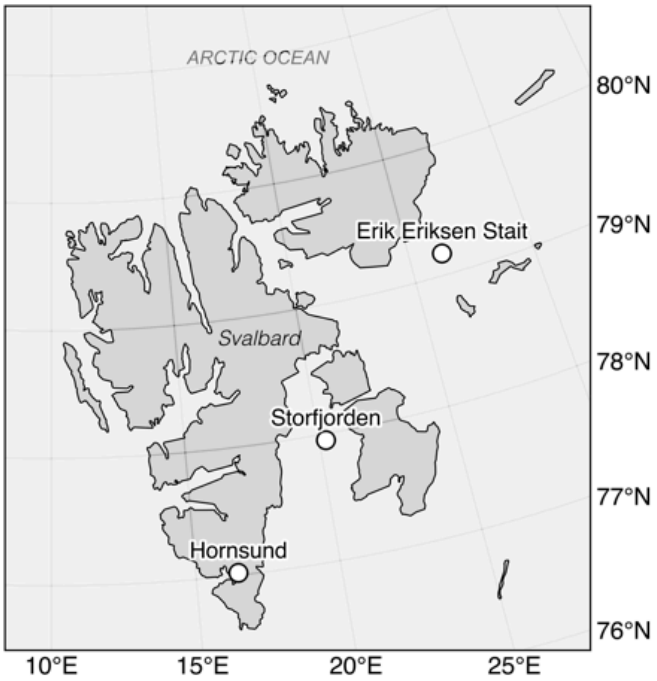

Fig. 19. Overview of the research locations Hornsund, Storfjorden and Erik Eriksen Strait during the Helmer Hanssen ArcEx cruise around Svalbard.

We incubated freshly collected copepods with *in situ* collected aggregates to determine aggregate grazing, and made video recordings to investigate their searching and aggregate feeding behaviour. Incubations and video recordings on *Calanus* were done with copepods and aggregates collected in Hornsund, whereas those on *Pseudocalanus* were done with copepods and aggregates collected in Storfjorden. We used these results to determine their impact on flux attenuation in the three fjords. For this, we determined the abundance of both genera using WP2 and Multinet hauls, the abundance of aggregates in the water column using camera profiles, and POC flux attenuation using drifting sediment traps and camera profiles.

Experiments

Zooplankton collection - Zooplankton was collected using a WP-2 net (200 µm) with a large cod-end to minimize damage to the copepods. The content of the cod-end was directly transferred into several large containers filled with surface water and stored cold. We picked individual copepods with a wide-mouth pipette. Prior to incubations, they were incubated overnight in GF/F filtered water to let them empty their guts. The next morning, we selected healthy and actively swimming copepods and transferred them to either roller tanks for aggregate grazing determination or an aquarium for video recordings of aggregate feeding behavior.

Grazing incubations – Aggregate grazing rate incubations of *Calanus sp.* and *Pseudocalanus sp.* were done in roller tanks (1.15 L, diameter: 14 cm, depth: 7.5 cm), using intact aggregates collected with a Marine Snow Catcher (MSC). Five roller tanks were filled with GF/F filtered water from the MSC, after which carefully four *Calanus* or ten *Pseudocalanus* were added. We collected similar types, sizes and amounts of aggregates from the MSC in ten petri dishes. We removed all copepod fecal pellets from the petri dishes and photographed each petri dish for aggregate size determinations. The content of five petri dishes was filtered on a pre-combusted GF/F filter and used as start POC measurement. The aggregates in the remaining five petri dishes were added to the five roller tanks, which were carefully topped with GF/F filtered water, and closed with silicone stoppers. The roller tanks were incubated on a roller table that rotated with 1 round per min for 24 hours in darkness at *in situ* temperature (0°C). At the end of the incubation we gently picked each copepod and ensured that it was alive before we fixed it in 4% formalin solution for later species confirmation. All visible aggregates from one roller tank were carefully transferred to a petri dish using a wide-bore pipette, whereas the remaining particles and fecal pellets were gently up-concentrated by gravity filtration through a 5 µm mesh. All fecal pellets were separated from the aggregates and particles using a thin mouth pipette, and collected in a petri dish. The produced fecal pellets and remaining aggregates were photographed for size and abundance determinations, after which all aggregates from the five roller tanks were pooled and filtered on a pre-combusted GF/F filter and all produced fecal pellets were pooled and filtered on another for POC determination.

POC and PON determination - The filters were dried at 40°C for 24 hours, fumed with 37% HCL to remove inorganic carbon, and analyzed with a GC elemental analyzer (Elementar vario EL III) to obtain the total POC and particulate organic nitrogen (PON). We corrected for eventual contamination using the measured POC values of blank filters. Images of aggregates filtered at the start and end of the incubations were analyzed with ImageJ to determine the size of each individual aggregate. The image was converted to 8-bit, the background removed by subtracting a copy that was equalized with a Gaussian Blur (200 px radius), and a threshold was applied to identify particles from the background. We calculated the equivalent spherical diameter (ESD) from the projected area of each aggregate. POC concentrations were calculated by fitting a volumetric POC relationship to the aggregate volumes (after Alldredge 1998): $POC = a \times V^b$, where the POC content of an aggregate is in µg C, the volume V is in mm^3, b is fixed to 0.5, and a is fitted to the data. The volumetric relationship of aggregates filtered at the start of the experiment was applied to aggregates added to the roller tanks to obtain the start aggregate POC concentration for each roller tank (POC_{start}), whereas the volumetric relationship of aggregates filtered at the end of the experiment was used to calculate the end aggregate POC concentration (POC_{end}). Carbon ingestion from aggregate feeding was estimated by dividing the carbon loss per roller tank by the number of copepods and the incubation time.

Video recordings - The video recordings were done in an aquarium with two Basler acA1300-30gc cameras (1 Mpx, IR-filter removed) recording simultaneously from the front and side of the aquarium, which was illuminated with two infrared-backlights (MBJ DBL plate, 880 nm, and custom-build plate with Vishay LEDs, 850 nm). One of the cameras was fixed and used to determine the swimming speed of the copepods, and the size and sinking velocity of the settling aggregates, whereas the other was attached to a stand that allowed movements in x-, y- and z- directions in order to keep individual aggregates in focus while they sank through the aquarium. All video recordings were done in darkness, with only infrared illumination, at *in situ* water temperature (0°C). The aquarium was filled with GF/F filtered seawater from the MSC. Copepods were allowed one-hour acclimatization time in the aquarium prior to filming. Aggregates were first placed in a petri dish containing the same seawater as in the aquarium to ensure that the temperature and salinity of the pore water in the aggregates was similar to that in the aquarium. In a video sequence, one aggregate was gently transferred from the petri dish to the aquarium with a wide bore-pipette, was allowed to sink out of the pipette into the aquarium and followed by the moving

camera during its descent. After 5 minutes the cameras and infrared lights were switched off for 5 minutes to minimize water heating and to dilute eventual chemical trails originating from the sinking aggregate in the aquarium. Thereafter a new video sequence was started.

Video analyses - All video sequences were analyzed frame by frame to detect all copepod-aggregate interactions. We identified four main responses when the copepods encountered sinking aggregates: attachment, avoidance, rejection and no reaction. Attachment was defined as a copepod that attached to the aggregate for longer than a second. Rejection was defined as a copepod that attached to an aggregate for a period shorter than one second whereupon it either detached or, for small aggregates, 'kicked' the aggregate away from its feeding appendages. Avoidance was defined as a copepod that swam towards an aggregate but changed its swimming direction in the vicinity of the aggregate to avoid encounter. No reaction was defined as a copepod that was close to an aggregate without showing any visible reaction to the presence of the aggregate. This also included copepods that were swimming into an aggregate, while not changing their course or attaching. All other sinking aggregates that were not close to a copepod are defined as 'other'. For each action, the sensing distance (distance at which a reaction was observed) and position of the copepod relative to the aggregate (above, below, beside) was recorded together with impact of the encounter (e.g. whether the aggregate settling was altered or if the aggregate was fragmented). Additionally, we recorded the duration of each attachment and any change in aggregate volume caused by the attachment. Aggregate size was determined by measuring the x- and y-axis of the aggregate in a frame of fixed camera. The shorter of the two axes was used as z-axis to calculate the volume of an aggregate assuming an ellipsoid form:

$$V = \frac{\frac{4}{3}\pi\ x\,y\,z}{8} \quad (1)$$

and equivalent spherical diameter (ESD) using this volume:

$$ESD = 2 \times \left(\frac{3}{4}V \times \frac{1}{\pi}\right)^{\frac{1}{3}} \quad (2)$$

Aggregate sinking velocity was determined using the fixed camera only, by analyzing its track in ImageJ using the plugin MTrackJ. The total vertical track line length was divided by the number of frames of the track and multiplied with the frame rate (frames s^{-1}) to obtain the sinking velocity. For aggregates that were interacted with, where possible size

and sinking velocity were determined before the interaction. We tested for statistical differences in aggregate size and sinking velocities between the *Calanus* and *Pseudocalanus* video recordings with a non-parametric Wilcoxon rank sum test using R (R Core Team et al. 2016).

Table 4. Overview of the deployments of the marine snow catcher (MSC), WP2-net, sediment trap, in-situ camera (ISC), and multinet (MN).

Location	Device	Date	Depth	Notes
Hornsund	MSC	19.05.2016	20m	Calanus experiments
	WP2	19.05.2016	90m	Calanus experiments
	WP2	19.05.2016	113m	
	Trap	19.05.2016	20,30,40,60,90m	Anchored
	ISC	19.05.2016	122m	
	ISC	20.05.2016	95m	
	ISC	20.05.2016	93m	
	ISC	20.05.2016	126m	
	ISC	20.05.2016	112m	
	ISC	20.05.2016	135m	
Erik Eriksen St.	Trap	23.05.2016	30,40,60,90,120,150m	Attached to ice floe
	MN	23.05.2016	25,50,100,150,250m	
	ISC	23.05.2016	263m	
	ISC	23.05.2016	262m	
	ISC	23.05.2016	235m	
	ISC	23.05.2016	251m	
	ISC	23.05.2016	61m	
Storfjorden	MSC	21.05.2016	25m	Pseudocalanus experiments
	WP2	21.05.2016	95m	Pseudocalanus experiments
	WP2	21.05.2016	95m	
	ISC	21.05.2016	86m	

Calculating *in situ* zooplankton aggregate feeding

Zooplankton abundance - We used a Hydrobios Midi-Multinet (200 µm mesh-size) with five nets to determine vertical composition and abundance of zooplankton at depth-intervals in the Erik Eriksen Strait (Table 4). However, due to a malfunction of the Multinet, we had to use a WP-2 net (200 µm mesh-size) in Hornsund and Storfjorden. Since the WP-2 only consists of one net, we were not able to determine vertical distribution at these stations and did one vertical net haul through the full water column. The flow-meter on the multinet showed that the filter-efficiency was 0.77 and we assumed that the WP-2 had a similar filter-efficiency. The multinet showed that zooplankton abundance was not evenly distributed through the water column and 72% of all *Calanus* and 69% of all *Pseudocalanus* resided in the upper 25 m. We therefore assumed that this was similar for the WP-2 nets from Hornsund and Storfjorden. All zooplankton samples were fixed in 4% formalin and counted in the home laboratory. Biomass was estimated using literature values for the dry weight of specific copepod developmental stages (Richter 1994). *Calanus hyperboreus, C.*

glacialis, and *C. finmarchicus* were differentiated based on their prosome length (Arnkværn et al. 2005).

In situ aggregate size and abundance - The vertical aggregate abundance and size-distribution was measured with an *In situ* Camera (ISC) in Hornsund, Storfjorden and Erik Eriksen Strait. The ISC is a camera system that is illuminated by an infrared backlight, which samples a water volume of 20 ml every 15 cm through the water column. The pixel size was 24 µm, resulting in quantitative detection of particles larger than ESD~100 µm. The ISC was connected to a SeaBird 19 CTD that was equipped with a fluorescence sensor, a turbidity sensor, and an oxygen sensor. We processed the images with the Imaging Processing Toolbox in Matlab (The Mathworks) to characterize individual particles. The size of a particle was determined from its area and converted into ESD. Detected particles were sorted into logarithmically spaced size bins based on their ESDs. The particle size distributions (n_C) were calculated from the particle number concentration (ΔN_C) within a given size range (Δd) of each image:

$$n_c = \frac{\Delta N_C}{\Delta d} \qquad [\#\ m^{-3}\ cm^{-1}] \qquad (3)$$

We binned 10 images and obtained a vertical depth-resolution of ~1.5 m.

POC fluxes and attenuation from sediment traps - We deployed drifting sediment traps in Hornsund and the Erik Eriksen Strait. The sediment trap cylinders (KC Denmark A/S, Ø 7.2 cm, 45 cm long) were deployed at 20, 30, 40, 60, and 90 m in Hornsund and at 30, 40, 60, 90, 120, and 150 m depth in Erik Eriksen Strait. Each collection depth had at trap station equipped with four sediment trap cylinders. The deployment time was 20 h and 50 min in Hornsund and 23 h in Erik Eriksen Strait. We transferred the content from the four trap cylinders at each collection depth into a carboy immediately after recovery and stored the carboys at 0°C in darkness for a maximum of 6 hours until filtration. We subsampled the exported material from the carboys to determine POC and PON fluxes from each collection depth. This was done by filtering the subsamples onto pre-combusted GF/F filters in triplicates within 6 hours after the sediment trap array was retrieved. The filters were immediately frozen at -20°C until arrival to the laboratory where the samples were dried for 48 h at 50°C, fumed with fuming HCl for 24 h to remove carbonates, and analyzed with a GC elemental analyzer (Elementar vario EL III). We used the POC flux from 30 and 60 m (F_{30} and F_{60}, respectively) to calculate the fractional loss in carbon flux between the two depths. This was calculated by $1\text{-}F_{60}/F_{30}$. This approach assumes that the settling aggregates

sank vertically through the water column and that the flux at 60 m was directly comparable to that at 30 m.

Volumetric POC relationships – After the first deployment of the traps, they were redeployed at the same location while one cylinder was equipped with an insert filled with a viscous gel (TissueTek, OCT, cryogel from Sakura Finetek) that preserved the size and three-dimensional structure of the embedded particles and aggregates (following the procedures of Wiedmann et al. 2014). The second deployment was kept to two and three hours in Hornsund and Erik Eriksen Strait, respectively. After recovery, the cylinder of each depth without gel was transferred to one carboy and analyzed in the same way as the cylinders of the first deployment. The gel traps were gently removed from the collection cylinder and frozen until imaging in the home laboratory. The images were analyzed as described in Wiedmann et al. (2014) to obtain determination of size, abundance, and types of the collected particles and aggregates. A volumetric POC relationship was fitted to all collected aggregates in the gel in the same way as described for the grazing incubations, using the total POC content of the cylinder that was deployed together with the gel insert. As there was no gel trap deployed in Storfjorden, we used the volumetric POC relationship of the MSC aggregates from the *Pseudocalanus* incubation, which was within the range of those determined for the gel traps.

POC attenuation from ISC - We used the vertical particle profiles obtained with the ISC to calculate POC concentration profiles. This was calculated by applying the volumetric POC relationships to the different particle size bins, and summing all bins for each depth. To identify the depth interval in which the highest POC degradation took place, we plotted the POC concentration over depth and identified the POC peak (POC_{peak}, between 5 and 20 m) and the depth from which the POC concentrations remains quasi constant with increasing depth (POC_{low}, 18-25m below the peak POC). The fractional POC loss through this depth interval was calculated by $1\text{-}POC_{low}/POC_{peak}$.

Encounter and ingestion rates - Encounter and ingestion rates for *Calanus* and *Pseudocalanus* were calculated as described in Koski et al. 2005 with slight adaptations, using parameters obtained from the incubations and video recordings. The encounter kernel β describes the volume of water a copepod can search per time for a given aggregate radius:

$$\beta(r) = v \times \pi \times \left(\frac{s}{2} \times l \times r\right)^2 \quad (4)$$

where v is the average swimming speed (including pause events), s is the total antennae length of a copepod, l the detection distance at which the copepod can recognize a sinking aggregate, and r the radius of the sinking aggregate. Using β, the numbers of copepods that a sinking aggregate with radius r encounters during its descent through a water column of depth z is:

$$E(r) = \beta(r) \times C \times \frac{z}{u(r)} \quad (5)$$

where C is the average copepod concentration over depth z, and $u(r)$ the size-specific aggregate sinking velocity. The fractional degradation (κ) caused by copepod feeding of an aggregate that sinks to depth z is:

$$\kappa(r) = \frac{E(r) \times \alpha \times i \times \delta}{POC(r)} \quad (6)$$

where α is the fraction of encounters that lead to attachment, δ is the time a copepod spends on an aggregate, i is the carbon ingestion rate of a copepod when feeding on an aggregate and $POC(r)$ is the size-specific POC-content of the aggregate. All input parameters were directly obtained from the video recordings and the incubations. For δ we averaged the attachment times, as there was no relation between aggregate size and time spend on the aggregate. We assume therefore that the ingestion (i) is a sigmoid function of size:

$$i = \frac{a}{1 + e^{\frac{b-r}{c}}} \quad (7)$$

To fit the parameters a, b, and c for i, we first calculated i_{calc} by assuming that κ was constant for different aggregate sizes and used the overall fractional degradation found from the roller tank incubations as a value for κ. We then fitted a sigmoid curve to the i_{calc} values against aggregate sizes using the nonlinear least-squares method in R (nls) and used the resulting fit to determine the size-specific i for each of the investigated copepod species and aggregate types.

Calculating POC attenuation by zooplankton - Using the previously fitted parameters, the concentration of *Pseudocalanus* and *Calanus* in the upper 25m, the depth interval *z* per ISC cast, and the POC_{peak} from the ISC cast, we calculated the *in situ* encounter kernel β, the number of encounters E, and the fraction degradation κ. The POC that is degraded per bin by zooplankton (POC_{zoo}) is κ multiplied with the start POC (POC_{peak}) per bin. The fraction of POC that is degraded by zooplankton:

$$\kappa_{tot} = 1 - \frac{\Sigma POC_{zoo}}{\Sigma POC_{peak}} \quad (8)$$

where both POC values are summed over the size bins. We also estimated the microbial degradation, assuming the carbon-specific degradation is 0.03 d^{-1} (Morata and Seuthe 2014; Belcher et al. 2016):

$$\kappa_{micro}(r) = 1 - e^{-\frac{0.03}{u(r)} * z} \quad (9)$$

RESULTS

Experiments

Aggregate feeding rates – We performed aggregate feeding incubations with *Calanus sp.,* containing a mixture of different stages of *Calanus glacialis* and *Calanus hyperboreus* with an average prosome length of 3 mm, and with *Pseudocalanus sp.*, containing only adult females with an average prosome length of 0.85 mm. The average ingestion rate of *Calanus* was three times higher than *Pseudocalanus* (13.4 ± 4.34 and 5.79±2.17 µg C ind^{-1} d^{-1} respectively). Also the fecal pellet production rate was three times higher for *Calanus* compared to *Pseudocalanus* (13.9 and 4.59 µg C ind^{-1} d^{-1}). The aggregate C/N ratios increased from 10.3 to 13.8 during the *Calanus* incubation and 8.4 to 8.9 during the *Pseudocalanus* incubation (Fig. 20). The C/N ratios of the produced fecal pellets were with 19.4 for *Calanus* and 18.1 for *Pseudocalanus* much higher than that of the incubated aggregates (Fig. 20).

Aggregate size, sinking velocity and interactions – We made video-recordings of copepods and sinking aggregates to determine aggregate feeding behavior and measure aggregate sizes and sinking velocities. Aggregates from the *Calanus* and *Pseudocalanus* experiments were similar-sized, with an average equivalent spherical diameter (ESD) of 0.35±0.27 mm and 0.39±0.28 mm respectively (Wilcoxon rank sum test, $p=0.37$). Sinking velocities in the *Calanus* experiment were higher than in the *Pseudocalanus* experiment (Wilcoxon rank sum test, $p<0.01$), which is possibly caused by the higher dry weight of the aggregates used

for the *Calanus* experiments (13.3 mg DW per mg C compared to 3.62 mg DW per mg C), indicating a difference in aggregate ballasting. *Pseudocalanus* reacted to more aggregates in its vicinity than *Calanus*, and only 6% of the aggregates within 0.5 body-length from the *Pseudocalanus* did not result in a behavior response, compared to 48% for *Calanus*. We observed two clear ingestion events for *Calanus* with one small slow-sinking aggregate (ESD 0.1 mm, SV 5.9 m d^{-1}) and one larger (ESD 0.3 mm, SV 58 m d^{-1}). During these two events *Calanus* attached to the aggregates for 2.3 s and 67.5 s, respectively. Four attachments resulted in rejection within one second after attaching (ESD 0.15-0.22 mm, SV 3-17 m d^{-1}).

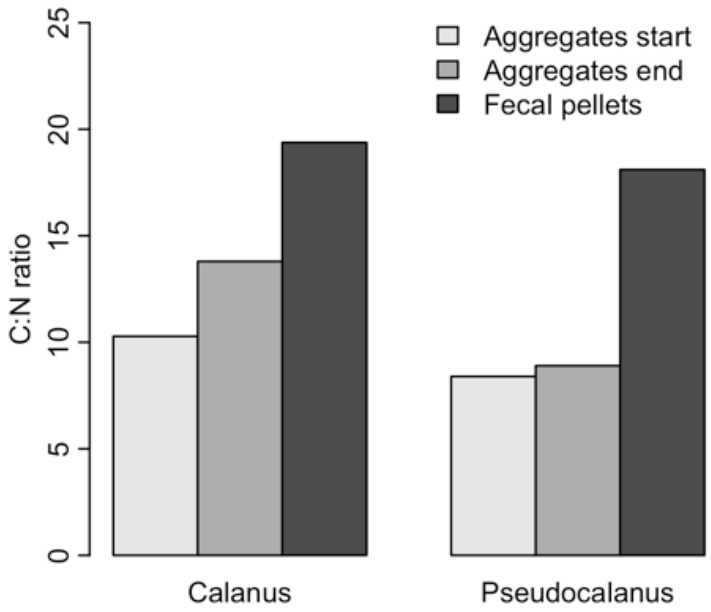

Fig. 20. C:N ratios of aggregates before the incubations, aggregates after the incubations, and produced fecal pellets during the incubations.

Seven aggregates were actively avoided, of which four had sinking velocities faster than 100 m d^{-1}. In contrast, *Pseudocalanus* attached more frequently to aggregates, with 26 recorded attachments lasting longer than one second (ESD 0.06-0.83 mm, SV 0.8-58 m d^{-1}), with an average attachment time of 12 s (sd 14.5, min: 1s, max: 66s). *Pseudocalanus* actively avoided 21 aggregates (ESD 0.1-1.22 mm, SV 2.7-96 m d^{-1}), and rejected four aggregates directly upon attachment (ESD 0.04-0.55 mm, SV 3-48 m d^{-1}).

Detection distance - The two observed *Calanus* attachments were established by copepods that approached the aggregate from aside, and detected the aggregate at a distance of 0.69 mm (Fig. 21). The aggregates that were avoided were in a similar proximity (0.67 mm), although when the copepod was swimming above the sinking aggregate this distance was

slightly larger (0.95 ± 0.69 mm). *Calanus* was observed to swim into aggregates without attaching, thereby sometimes fragmenting the aggregates. Most of the *Pseudocalanus* attachments occurred when the copepod was filter feeding and the aggregate sank into the feeding current from above, whereupon the filter feeding activity would be interrupted and the copepod would attach to the aggregate by grapping it with the mandibles (Fig. 21). The average detection distance for these events was 0.46 ± 0.40 mm, whereas the detection distance for copepods that approached aggregates from above or aside was 1.08 mm ± 0.85 and 0.78 mm ± 0.43, respectively. Avoidance events occurred within similar reaction distances as observed for the attachment events. One exception was a copepod swimming 13.4 mm above the aggregate, who followed the track of the sinking aggregate but avoided it from a distance of 0.96 mm (ESD 0.81, SV 84 m d^{-1}) (Fig. 21). Additionally, four aggregates were rejected within one second upon attachment.

Calculating *in situ* zooplankton aggregate feeding

Zooplankton abundances – *Pseudocalanus* and *Calanus* made up the majority of the biomass at all three stations with 85%, 88%, and 95% of the total zooplankton biomass in Hornsund, Storfjorden, and Erik Eriksen Strait, respectively. In terms of abundance the two genera contributed 16%, 4.9%, and 6% of the total zooplankton abundance, respectively. *Calanus sp*. concentrations in the upper 25 m were 86, 495 and 208 ind. m^{-3}, whereas *Pseudocalanus sp*. concentrations were 255, 33 and 126 ind. m^{-3} in Hornsund, Storfjorden, and Erik Eriksen Strait. The total zooplankton abundance was highest at Erik Eriksen Strait, where 93% of the abundance consisted of calanoid nauplii. The lowest zooplankton abundance was observed at Hornsund, where half of the zooplankton consisted of barnacle nauplii. At Storfjorden barnacle and calanoid nauplii together made up 72% of the total zooplankton abundance.

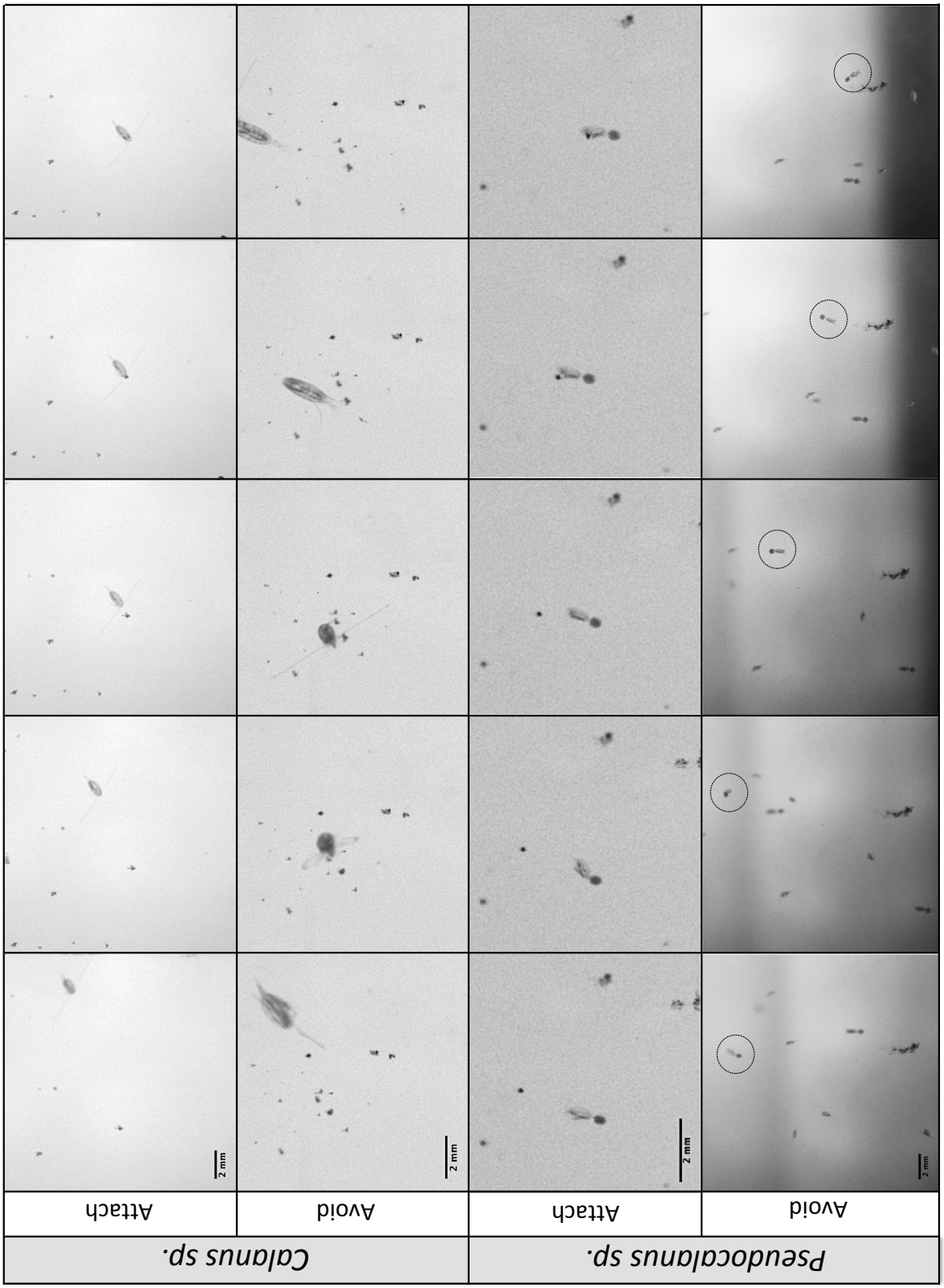

Fig. 21. Stills from videos with interactions between copepods and sinking aggregates. Upper: Calanus sp. swims from the side towards an aggregate and attaches to it. Second: Calanus sp. swims, changes course, touches an aggregate with its swimming legs (3rd photo), and jumps away. Third: Pseudocalanus sp. female is filter feeding, jumps, swims towards the sinking aggregate, attaches to the aggregate with its swimming legs, and sinks while feeding. Lower: Pseudocalanus sp. (circle) swims back and forth 13mm above a sinking aggregate, follows its trail down, but swims away from the aggregate when in the vicinity.

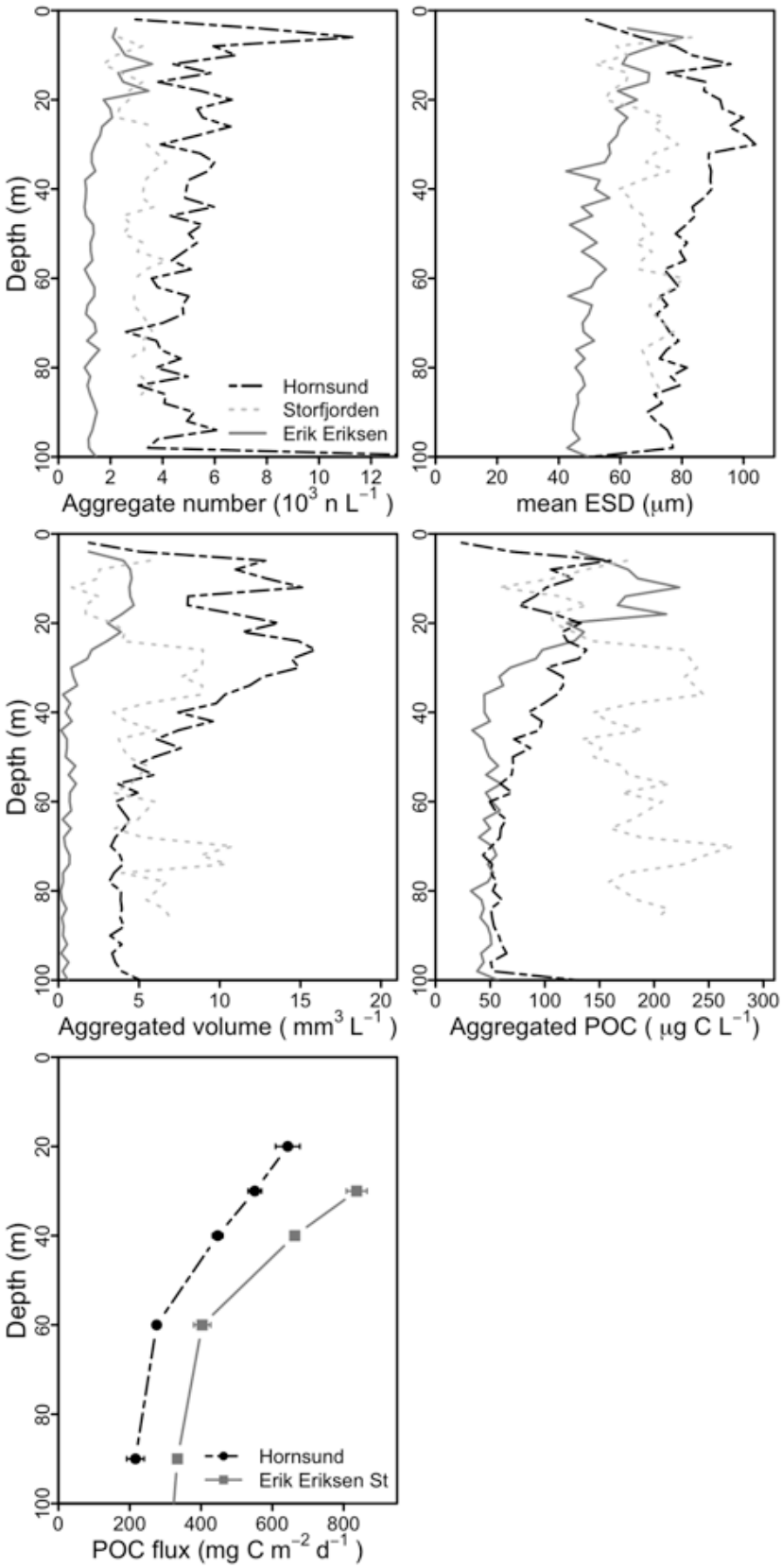

Fig. 22. Averaged depth profiles of the stations Erik Eriksen Strait (5 profiles), Hornsund (6 profiles) and Storfjorden (1 profile), and POC fluxes from the sediment traps. a.) number of aggregates; b.) ESD; c.) total aggregated volume; d.) total aggregated POC; and e.) POC fluxes, average ± sd.

Aggregate abundances and flux attenuation – We determined *in situ* aggregate abundance and size-distribution from 12 vertical profiles done with the In-Situ Camera (ISC). The total number of aggregates, the mean aggregate size, and the total aggregated volume was highest at Hornsund, followed by Storfjorden, and lowest at Erik Eriksen Strait (Fig. 22). At all three locations the total aggregated volume showed strong attenuation in the upper 50 m. We used the volumetric POC ratios to calculate the total aggregated volume into total aggregated POC concentrations. This showed a decrease in POC concentration in the upper 50 m at all stations: by 46 ± 16% (number of profiles *n*=6) at Hornsund, by 39% at Storfjorden (*n*=1), and by 55 ± 21% at Erik Eriksen Strait (*n*=5). In contrast to the total aggregated volume obtained from the ISC, POC fluxes obtained from the drifting sediment traps were higher at Erik Eriksen Strait compared to Hornsund (Fig. 22). The POC flux attenuation between 30-60 m was 50% at Hornsund and 58% at Erik Eriksen Strait.

Calculating in situ aggregate feeding – Using the parameters obtained from the experiments in combination with the zooplankton and aggregate abundance measurements (Table 5), we calculated the contribution to POC flux attenuation in the upper 50 m by *Calanus*, *Pseudocalanus* and microbes at the three stations using equations 3-8 (Fig. 23), and compared these values to the observed POC flux attenuation measured from sediment traps and camera profiles.

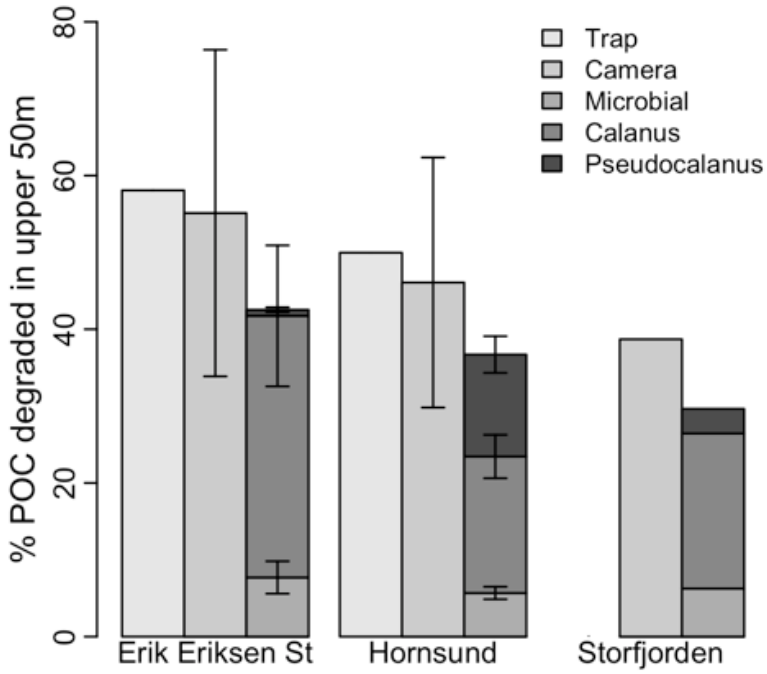

Fig. 23. POC degradation in the upper 50m from drifting sediment traps (light), estimated from camera profiles (light grey), calculated microbial degradation based on a C-specific degradation of 0.03 d-1 (darker grey), and calculated Calanus (dark grey) and Pseudocalanus degradation (dark).

Table 5. Parameters obtained from the experiments and *in situ* measurements used for calculating *in situ* aggregate feeding. Sinking velocity was obtained from the video recordings of aggregates from Storfjorden, the antenna length, detection distance, swimming velocity, the fraction of interactions that leads to an attachment, and the time spend on an aggregate were determined in the video recordings, the ingestion rates were fitted to the incubation experiments using the previous parameters, and the POC content of an aggregate was determined from the sediment traps at Erik Eriksen St and Hornsund, and the MSC at Storfjorden.

Parameter		unit	Calanus	Pseudocalanus
Sinking velocity	sv	m d^{-1} (ESD:mm)	$48*ESD^{0.85}$	
Antenna length	h	mm	5.7	1.7
Detection distance	l	mm	0.69	0.69
Swimming velocity	v	mm s^{-1}	1.21	0.89
Fraction attachments	f		0.07	0.49
Time on aggregate	δ	s	35	12
Ingestion rate	i	µg C s^{-1} (r:mm)	$\frac{0.117}{1+e^{\frac{0.697-r}{0.161}}}$	$\frac{0.0322}{1+e^{\frac{0.379-r}{0.0966}}}$
POC content		µg C (vol:mm^3)		
Erik Eriksen St			$4.29*vol^{0.5}$	
Hornsund			$0.84*vol^{0.5}$	
Storfjorden			$3.19*vol^{0.5}$	

Observed POC flux attenuation from the sediment traps was 58% and 50% at Erik Eriksen Strait and Hornsund respectively. The camera profiles showed a POC flux decrease of 55±21% at Erik Eriksen Strait, 46±16% at Hornsund, and 39% at Storfjorden. The combined contribution by *Calanus*, *Pseudocalanus*, and microbes was 43% at Erik Eriksen Strait, 37% at Hornsund, and 30% at Storfjorden, which accounted for 77%, 76% and 77% of the observed POC flux attenuation respectively. *Calanus* aggregate feeding alone accounted for 38-62% of the POC flux decrease, whereas *Pseudocalanus* aggregate feeding accounted for 1.5-29%, and microbial degradation for 12-16% at the three stations. The observed POC flux loss between the sediment traps at 30 and 60 m was 436 mg C m^{-2} d^{-1} at Erik Eriksen Strait and 276 mg C m^{-2} d^{-1} at Hornsund. The integrated aggregate feeding rate for the upper 50 m for *Calanus* was 269 mg C m^{-2} d^{-1} at Erik Eriksen Strait, and 102 mg C m^{-2} d^{-1} at Hornsund, while *Pseudocalanus* integrated aggregate feeding rates were 6.3 and 76 mg C m^{-2} d^{-1} at these stations respectively.

Size-specific aggregate-loss in the upper 50 m – Our calculations suggested that grazing on and degradation of small slow-sinking aggregates (ESD <0.2mm) made up the majority of the POC flux attenuation. Compared to the observed POC concentration at 50 m from the ISC profiles, our calculations caused a stronger decline in small aggregates and only a limited decline in large aggregates (Fig. 24). This discrepancy between the calculated and observed POC size-spectra suggests aggregate fragmentation, which converts large aggregates into two or more small aggregates.

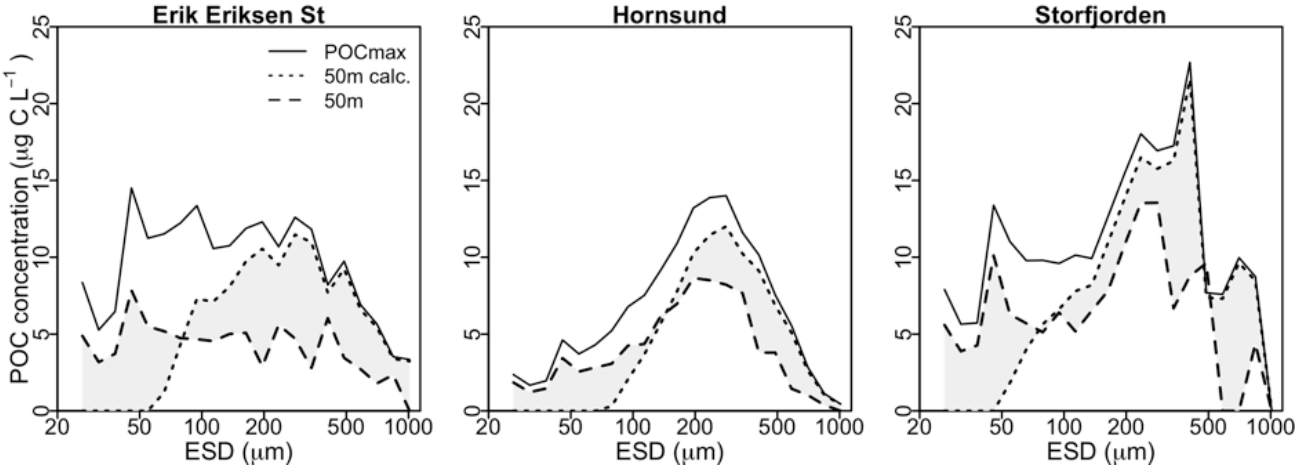

Fig. 24. Average POC distribution for different particle size classes at Erik Eriksen Strait, Hornsund and Storfjorden. Continuous lines show the POCmax values from the ISC profiles, used as input in the calculations, dotted black lines show the calculated values at 50 m, based on microbial degradation and Calanus and Pseudocalanus aggregate feeding, and black dashed lines show the measured values at 50 m from the ISC profiles. Grey shaded area indicates differences between observed and calculated POC concentration at 50 m.

DISCUSSION

We observed that the dominant Arctic zooplankton genera *Calanus sp*. and *Pseudocalanus sp*. were able to detect and feed on sinking aggregates, which contributed significantly to POC flux attenuation. From direct video recordings, we observed that *Pseudocalanus* attached to 45% of the sinking aggregates within detection distance, whereas *Calanus* only attached to 7%. However, *Calanus* is much larger, has larger antennae and a higher swimming velocity than *Pseudocalanus*, resulting in a larger volume of water it can search per time. Therefore the probability of finding an aggregate is higher for *Calanus* than for *Pseudocalanus*. This was also evident from the grazing incubations, where *Calanus* ingested three-fold more aggregated POC than *Pseudocalanus*.

Both species primarily attached to aggregates that were within a distance of half a body length, suggesting that detection was via the hydromechanical signals generated by the sinking aggregates (Visser 2001). On one occasion, *Pseudocalanus* detected an aggregate sinking 13 mm below and followed its sinking path (Fig. 21). This indicates that besides hydromechanical signals, *Pseudocalanus* can detect chemical trails originating from the sinking aggregate, a trait that has previously only been directly observed for the calanoid copepod *Temora longicornis* (Lombard et al. 2013b). As this detection did not lead to an aggregate capture, and all other encounters were based on detection upon close distance, we assume that the use of hydromechanical signals was the main mechanism for aggregate detection by *Calanus* and *Pseudocalanus*.

We calculated that aggregate gazing by *Calanus* and *Pseudocalanus* contributed to 60-67% of the POC flux attenuation. Additionally, microbial degradation was responsible for 12-16% of the observed flux attenuation, when assuming an aggregate carbon-specific microbial degradation of 0.03 d^{-1} measured in polar seas (Morata and Seuthe 2014; Belcher et al. 2016). Hence we could explain 77% of the total POC flux attenuation in the upper 50 m of the water column with microbial degradation and aggregate grazing by *Calanus* and *Pseudocalanus* alone.

We investigated whether the remaining 23% of the measured flux attenuation could be attributed to other zooplankton. The most abundant zooplankton at the three stations were barnacle and calanoid nauplii, although they contributed only little to the total zooplankton biomass. To investigate their potential aggregate feeding rates, we performed an aggregate grazing experiment with barnacle nauplii, resulting in the production of 1.5 fecal pellets per individual per day, corresponding to 0.088 µg C ind^{-1} d^{-1}, which is in the range of previously reported values (Turner et al. 2001; Gaonkar and Anil 2010). Assuming that the fecal pellet production was one third of the ingestion rate, barnacle nauplii were responsible for only 0.7-1.2% of the flux attenuation. Calanoid nauplii have been observed to feed actively on particles and fragmented fecal pellets (Green et al. 1992). Using the calanoid nauplii abundance and the aggregate grazing rates from the barnacle nauplii, we estimated that they contributed to only 0.5-2% of the observed flux attenuation. Therefore, despite the high abundances of barnacle and calanoid nauplii, their contribution to flux attenuation was minor. Of the remaining observed zooplankton in the net hauls, only *Microsetella norvegica* (Koski et al. 2005, 2007), *Oncaea sp.* (Green and Dagg 1997; Koski et al. 2017), and euphausiids (Dilling et al. 1998) have previously been observed to feed actively on sinking aggregates. We made several video recordings of euphausiids with sinking aggregates, where we did not observe aggregate feeding. Using previously published aggregate ingestion rates (Dilling et al. 1998), they may have contributed to 0.14-5.9% of the observed flux attenuation. Small copepods, such as *Oncaea sp.* and *Oithona sp.*, may have contributed to <0.01-1.6% of the observed flux attenuation, assuming an aggregate ingestion rate of 1.08 µg C ind^{-1} d^{-1} (Kiørboe 2000). The combined contribution of these zooplankton groups may have been 0.6-9.4% of the total POC flux attenuation.

Aggregate fragmentation was occasionally observed for *Calanus* and *Pseudocalanus*, as well as euphausiids, resulting in smaller and slower-sinking aggregates. The POC size spectra (Fig. 24) showed that the calculations overestimated the loss of small aggregates and

underestimated the loss of large aggregates, suggesting that fragmentation and disaggregation occurred in the upper 50 m of the water column. The lower settling velocities of smaller aggregates increase the residence time in the upper water column, allowing more time for microbial degradation (Iversen and Ploug 2010) and grazing by zooplankton (Iversen and Poulsen 2007; Giering et al. 2014; Mayor et al. 2014) and protozooplankton (Poulsen and Iversen 2008). Therefore, aggregate fragmentation and feeding upon fragments by microorganisms and filter-feeding zooplankton may be an important mechanism in upper ocean flux attenuation, and would explain the discrepancy between our calculated and observed POC size spectra at 50 m (Fig. 24).

Sinking aggregates may be a major food source for *Calanus* and *Pseudocalanus*. The observed aggregate ingestion rates from the incubations were within the range of previously reported grazing rates (Koski et al. 1998; Seuthe et al. 2007; Grote et al. 2015), although on the low side for *Calanus*. We divided total aggregate feeding in the upper 50 m by the aggregate settling velocities to get daily ingestion rates, which resulted in 4.5-66 μg C ind^{-1} d^{-1} for *Calanus*, and 1.2-21 μg C ind^{-1} d^{-1} for *Pseudocalanus*. These values are in the upper range of previously reported ingestion rates (Koski et al. 1998; Seuthe et al. 2007; Grote et al. 2015), which indicates that both species can sustain their carbon demand by aggregate feeding.

The fecal pellets produced during the aggregate feeding experiments had two-fold higher C/N ratios than the aggregates (Fig. 20), indicating that aggregate feeding increase the C/N ratio of sinking material. This offset in C/N ratios between fecal pellets and other particulate matter has previously been observed in the Arctic during summer (Daly et al. 1999). This suggests a preferential uptake of nitrogen relative to carbon, resulting in more carbon export per unit nitrogen within fecal pellets compared to aggregates. The preferential uptake of nitrogen by zooplankton can retain nitrogen in the epipelagic when copepods excrete urea or cause nitrogen release via sloppy feeding (Møller et al. 2003; Saba et al. 2011). Urea directly enhances phytoplankton growth (Eppley et al. 1971) extending the period of primary production and thereby, potentially resulting in a more efficient biological carbon pump compared to a situation with little or no copepod grazing.

Our results show that zooplankton aggregate feeding contributes to POC flux attenuation. We calculated that zooplankton was responsible for 60-67% of the observed flux attenuation, which is higher than previously observed in temperate and subtropical

environments (Steinberg et al. 2008b; Giering et al. 2014). Temperate and polar marine environments are characterized by large phytoplankton, high primary production and high export fluxes, but strong attenuation in the mesopelagic (Berelson 2001; Wassmann et al. 2003). Zooplankton are suggested to play a crucial role in flux attenuation in these ecosystems (Kiørboe 2000; Wexels Riser et al. 2001; Jackson and Checkley Jr 2011; Iversen et al. 2017), as well as in the NW Mediterranean (Stemmann et al. 2004), and the East Atlantic upwelling area (Iversen et al. 2010). Therefore zooplankton seem to act as 'gatekeepers' of the POC flux in regions with strong POC flux attenuation.

ACKNOWLEDGEMENTS

We thank Christiane Lorenzen for the POC measurements and the crew of the R/V Helmer Hanssen for assistance during the cruise. The cruise was funded by 'ARCEx'. This study was supported by the Helmholtz Association, the Alfred Wegener Institute Helmholtz Centre for Polar and Marine Research and the DFG-Research Center/Cluster of Excellence "The Ocean in the Earth System" at MARUM. This publication is supported by the HGF Young Investigator Group SeaPump "Seasonal and regional food web interactions with the biological pump": VH-NG-1000

3. DISCUSSION

The 'biological carbon pump' transports organic material from the surface ocean to the deep, and is driven by the formation of organic matter via primary production, the formation and the sinking of organic particles, and active transport by animals. This process makes the oceans the largest carbon sink on earth and has aided to the sequestration of one third of anthropogenic CO_2 (Sabine et al. 2004). The efficiency of the biological pump depends, amongst others, on the availability and incorporation of ballast minerals, and degradation by microbes and zooplankton. Although these processes have been identified in the lab and explored in the field, their quantitative importance on the carbon flux is still being explored.

To determine the quantitative importance of ballast minerals and zooplankton aggregate feeding on export and attenuation, it is crucial to combine *in situ* measurements with *in situ* experiments. In this thesis *in situ* experiments were used to investigate mechanisms and quantitative effects of ballast minerals and zooplankton on the downward carbon flux. The combination of these experiments with *in situ* measurements gave new insights on 1) the effects of ballast minerals on downward POC fluxes; 2) the quantitative importance of zooplankton aggregate feeding; and 3) the effects of these processes on regional POC flux variation. In the following sections, key findings from this thesis are summarized and their implications are discussed.

3.1 NEW INSIGHTS ON BALLAST MINERALS IN THE BIOLOGICAL CARBON PUMP

HOW DO BALLAST MINERALS INFLUENCE AGGREGATE FORMATION IN A NATURAL PLANKTON COMMUNITY?

Most direct studies on the influence of ballast minerals on organic aggregates have been done in the laboratory using phytoplankton cultures and different ballast minerals (e.g. Hamm, 2002; Passow & De La Rocha, 2006; Iversen & Ploug, 2010). Saharan dust added to a natural plankton community from the Cape Blanc filament caused higher aggregate abundances and sinking velocities (**Manuscript 1**). As a result, dust deposition may cause up to ten-fold higher POC flux, which is greater than observed in previous studies (Ternon et al. 2010; Bressac et al. 2014).

CAN SINKING AGGREGATES SCAVENGE BALLAST MINERALS?

Aggregates formed in the surface ocean off the Mauritanian coast that sunk through suspended Saharan dust were not altered in size, abundance, or sinking velocity, indicating that scavenging didn't occur (**Manuscript 1**). These results are supporting previous observations of aggregates not interacting with suspended minerals in deeper water layers (Iversen et al. 2010). Aggregates from the Cape Blanc filament are already heavily ballasted with lithogenic material in the euphotic zone and may thus not scavenge additional minerals during their descent. Therefore, in areas with high concentrations of lithogenic material, scavenging may predominantly occur in the surface ocean and only play a minor role at depth. In areas with low or intermediate ballast mineral concentrations scavenging may possibly continue to occur at greater depth.

HOW DO BALLAST MINERALS INFLUENCE THE BIOLOGICAL CARBON PUMP?

The results presented in this thesis indicate that the presence of ballast minerals control the magnitude of the POC flux in the Cape Blanc filament. The presence of ballast minerals could explain up to 91% of the variability in carbon export (**Manuscript 2**). This region is ballasted year-round with Saharan dust, biogenic silica and carbonate (Iversen et al. 2010; Friese et al. 2016; Fischer et al. 2016). Ballasting by Saharan dust increased aggregate abundance and sinking velocities (**Manuscript 1**), indicating that these are the crucial parameters for ballasting. A previous study in the Cape Blanc area also showed that Saharan dust deposition increased aggregate abundance while aggregate size remained unaffected (Nowald et al. 2015). Ballast minerals are known to enhance aggregate sinking velocities (Hamm 2002; Passow and De La Rocha 2006; Iversen and Robert 2015). Therefore,

aggregate abundance and sinking velocities seem to be the parameters greatest influenced by the process of aggregate ballasting, resulting in enhanced POC fluxes.

SEASONAL AND INTERANNUAL VARIATIONS IN BALLASTING AT CAPE BLANC

The Cape Blanc filament is located in a strong permanent upwelling zone, and is characterized by weak seasonality. Dust deposition is highest in winter, and upwelling is strongest in spring and at the end of summer. Generally, lithogenic and BSi fluxes are highest in winter, whereas carbonate and POC fluxes peak both in winter and summer (Fischer et al. 2016). In summer, the downward flux consists mostly of coccolithophores, foraminifera and pteropods, while in spring diatoms are most abundant (Fischer et al. 2016; Romero and Fischer 2017).

Manuscript 2 discussed a dataset consisting of one sediment trap in spring, two in summer and fifteen in winter over the years 2012-2017. As the number of traps in other seasons than winter was limiting, seasonal variations were difficult to assess. Only in 2017 traps were deployed in both winter and summer, showing significant differences between seasons (Fig. 25). The two summer traps had low POC and PON fluxes at 100 m and had little to no attenuation over depth, whereas in winter POC and PON fluxes were nearly twice as high at 100 m and attenuated to 400 m. C/N ratios in summer were higher, indicating that the exported material was heavily degraded. In winter, significant degradation took place below the euphotic zone. This difference in POC attenuation and C/N ratios is likely a result of differences in primary production and zooplankton activity. Zooplankton abundance in the Cape Blanc filament is highest in winter compared to summer (Somoue et al. 2005; Glushko and Lidvanov 2012; Beharro et al. 2015), while primary production peaks at the end of winter and the end of summer (Lathuilière et al. 2008). Carbon export is highest in winter as a result of increased Saharan dust input (Fischer et al. 2016) and high primary production, which results in fast-sinking aggregates. The high zooplankton abundance in winter (Somoue et al. 2005; Beharro et al. 2015) may feed on these sinking aggregates and thereby cause strong flux attenuation. In summer primary production is also high but Saharan dust input is lower (Fischer et al. 2016; Friese et al. 2017), which may result in longer retention of slower-sinking aggregates in the euphotic zone. Therefore in summer there is possibly more degradation of organic material in the euphotic zone, resulting in lower carbon export and higher C/N ratios of the exported material.

There were differences in aggregate size and type between aggregates settled in summer and winter. Aggregates in winter were larger, and total aggregated volume was higher. In summer, a larger fraction of the aggregates was recognizable as zooplankton fecal pellets. Interestingly, there were no clear differences in ballasting rates (fraction of POC to total particulate mass) between fluxes measured in winter and summer (Fig. 25). Although deep-sea traps from previous years showed seasonality in BSi, carbonate and lithogenic fluxes (Fischer et al. 2016, 2019), the data from 2017 showed small differences between seasons.

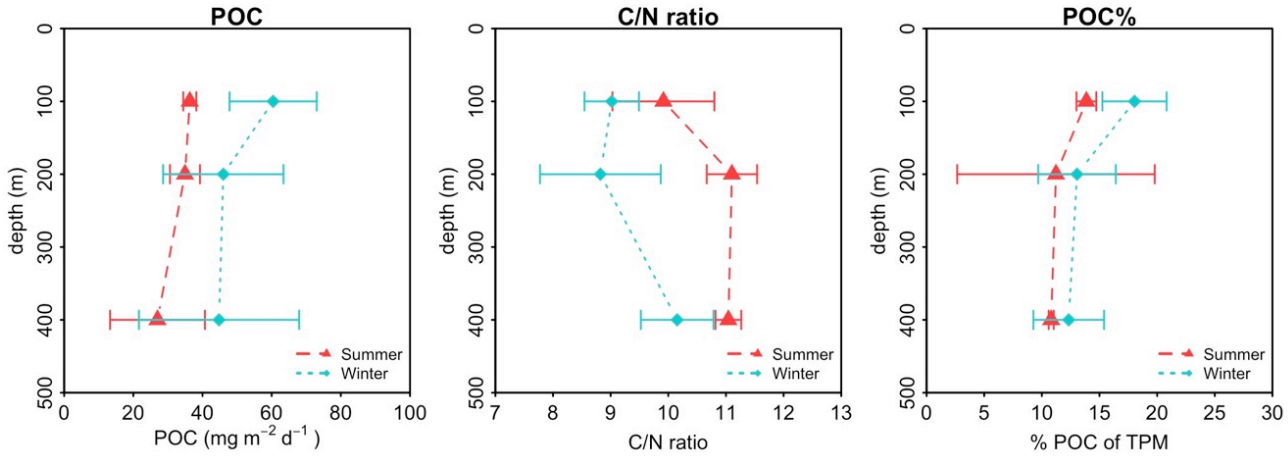

Fig. 25. Average fluxes in summer (red) and winter (blue) of 2017, ± SD. POC fluxes in winter were higher and C/N ratios were lower compared to summer. Ballast ratios (expressed as the fraction POC of total particulate mass) were not significantly different between seasons. Average of winter traps DF15, DF16 and DF17 and of summer traps DF18 and DF19 (see **Manuscript 2**).

Rather than seasonal variation, the dataset presented in **Manuscript 2** revealed interannual variations in ballasting. In winter, there were significant differences in the fraction of POC to total mass flux (POC%) between years (Kruskal-Wallis rank sum test, $p<0.01$). Traps deployed in winter 2013 had significantly lower POC% compared to traps deployed during the winters of 2015-2017 (Fig. 26). Traps deployed during 2013 had the lowest POC% of all traps (ranging between 2.6 and 6.9%), indicating high ballasting of the exported material. In winter 2017 significantly higher POC% were measured compared to the winters of 2012-2014 (Kruskal-Wallis multiple comparison adjusted with Benjamini-Hochberg method). Looking at the POC% for the whole time series, a trend seems to emerge with a shift from relatively high ballasting up to 2014 to lower ballasting from 2015 onwards (Fig. 26). Observed interannual deep-sea flux variations in the Cape Blanc filament can only partially be linked to global interannual oscillations, such as the North Atlantic Oscillation or the El Niño-Southern Oscillation (Fischer et al. 2016). Rather, the area seems to be strongest affected by dust deposition events, that enhance POC export (Iversen et al. 2010;

Fischer et al. 2016; **Manuscript 1**). These dust events are irregular between years, resulting in interannual variation in POC and ballast fluxes. Indeed in 2013 an anomalously high number of dust storms took place compared to previous years (Friese et al. 2017), resulting in extraordinary high carbon fluxes in deep sediment traps (Fischer et al. 2019). This corresponds with the low POC% observed in sediment traps deployed during 2013 (Fig. 26).

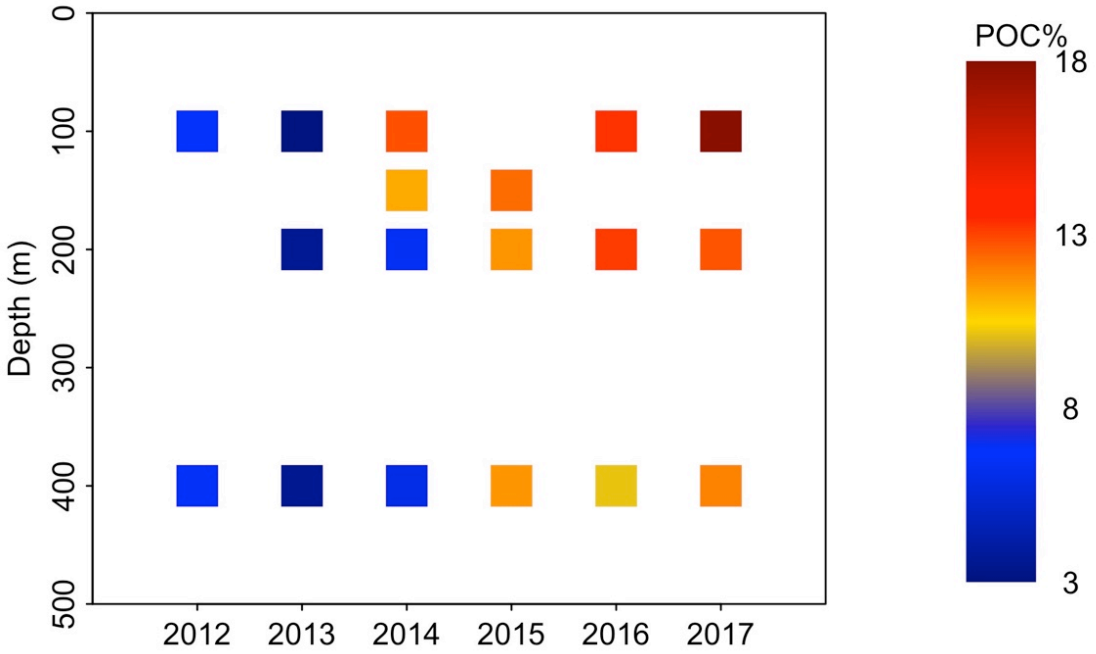

Fig. 26. Overview of the average POC% per year over depth. 2012-2014 had low POC% indicating high ballasting, whereas 2015-2017 had relatively high POC%.

FUTURE OF THE CAPE BLANC FILAMENT

Due to an increased atmospheric CO_2 concentration and anthropogenic activities, the oceans are changing. POC export in the Cape Blanc filament is strongly influenced by dust deposition and upwelling, thus changes in these processes will likely change POC fluxes in the area.

Two contrasting scenarios have been suggested for dust deposition in the future: 1.) increasing desertification and stronger trade winds may lead to higher dust deposition (e.g. Naiman, 1976; Shao et al., 2011); and 2.) Saharan 'greening' in dust source regions may lead to reduced dust deposition (Fontaine et al. 2011; Lucio et al. 2012). It is still debated whether greening or desertification takes place in the Sahara and Sahel. Satellite observations indicate a greening effect in some areas, but this is most likely a result of increased agricultural activity (Dardel et al. 2014; Kusserow 2017). So far, there is no evidence that dust deposition in the Cape Blanc filament has changed between 1988 and 2010, indicating that neither desertification nor greening has altered dust deposition significantly (Fischer et al. 2016).

Due to an increased temperature difference between land and sea, trade winds are expected to increase in intensity. As a result, upwelling intensity and duration are predicted to increase in Eastern Boundary upwelling systems (Bakun 1990; Bakun et al. 2015; Wang et al. 2015). For the Canary Current specifically, whose upwelling drives the formation of the Cape Blanc filament, at latitudes >25 °N upwelling will start earlier and become more intense. Below 21°N (and for the Cape Blanc filament) upwelling is predicted to weaken (Cropper et al. 2014; Wang et al. 2015). A weakened upwelling will bring less nutrients to the surface, which may lead to a reduced primary production and potentially lower POC export. Higher dust deposition rates in the future might therefore not increase POC export, as aggregates are already ballasted up to a maximum capacity (Ternon et al. 2010; **Manuscript 1**). So far, no long-term trends in POC fluxes have been observed, even though there seems to be a slight decrease in chlorophyll-a concentration in the surface waters (Fischer et al. 2016) and a slight decrease in POC fluxes (Fischer et al. 2019).

3.2 NEW INSIGHTS ON ZOOPLANKTON IN THE BIOLOGICAL CARBON PUMP

HOW DOES ZOOPLANKTON FEED ON NATURAL SINKING AGGREGATES?

Previously, feeding on aggregates (laboratory aggregates, fecal pellets and appendicularian houses) has been observed for *Microsetella* and *Oncaea* (Alldredge 1972; Ohtsuka et al. 1993; Koski et al. 2005), *Temora* (Lombard et al. 2013b; Koski et al. 2017), *Pseudocalanus* (Iversen and Poulsen 2007), and euphausiids (Dilling et al. 1998). They detect sinking aggregates randomly, recognize their hydrodynamic signals (Visser 2001), or find and follow a chemical trail (Kiørboe and Thygesen 2001). The ability to recognize chemical trails increases the chance of finding an aggregate, and has so far been only observed for *Temora longicornis* (Lombard et al. 2013b).

In the Arctic, the genera *Calanus* and *Pseudocalanus* were shown to detect and feed on *in situ* aggregates (**Manuscript 3**). *Pseudocalanus* used hydrodynamic and chemical signals to locate these sinking aggregates (**Manuscript 3**). This indicates that *Pseudocalanus* could efficiently locate aggregates, thereby increasing encounter rates. Additionally, *Calanus* and *Pseudocalanus* were observed to fragment sinking aggregates into smaller slower-sinking ones, on which they may feed (**Manuscript 3**, Iversen and Poulsen 2007). Fragmentation indirectly increases microbial degradation, as the fragments sink slower through the water column, thus increasing the attenuation of the POC flux (Lampitt et al. 1990; Mayor et al. 2014).

WHAT IS THE QUANTITATIVE IMPORTANCE OF AGGREGATE DEGRADATION BY ZOOPLANKTON ON THE CARBON FLUX?

Aggregate feeding by *Calanus* and *Pseudocalanus* could explain 60-67% of the observed POC export attenuation in three subarctic fjords (**Manuscript 3**). This quantitative importance of zooplankton aggregate feeding is higher than previously observed in temperate and subtropical environments (Steinberg et al. 2008b; Giering et al. 2014). Zooplankton activity is suggested to play a crucial role in POC flux attenuation for polar waters, as they have high but (seasonal) variable zooplankton abundances that are known to mediate the POC flux (Kiørboe 2000; Wexels Riser et al. 2001; Jackson and Checkley Jr 2011; Iversen et al. 2017; **Manuscript 3**). Observed high POC flux attenuation in the Arctic (e.g. Olli et al. 2007; Wiedmann et al. 2014; **Manuscript 3**) is likely caused by both high aggregate and zooplankton abundances, which increase encounter rates and, therefore, aggregate feeding. Large copepods and other zooplankton have relatively high encounter

rates due to their size and swimming speed (**Manuscript 3**). Therefore they may have a strong impact on flux attenuation, either via fragmentation or aggregate feeding. Smaller copepods have a lower chance of encountering aggregates. However, small copepods as *Microsetella* and *Oncaea* are often observed to reside and feed on aggregates (Koski et al. 2007, 2017; Möller et al. 2012). These copepods may therefore use other mechanisms to enhance encounter rates, such as recognizing chemical trails released from settling aggregates (Lombard et al. 2013b), potentially greatly increasing their impact on the POC flux.

ZOOPLANKTON AGGREGATE FEEDING IN OTHER REGIONS

Zooplankton aggregate feeding may play a major role in POC flux degradation in areas with high zooplankton and aggregate abundance, and either large or specialized zooplankton. Besides Arctic coastal waters, also in the Mediterranean Sea zooplankton aggregate feeding has been suggested to occur (Stemmann et al. 2004). The Mediterranean is a relatively oligotrophic environment with low POC fluxes and zooplankton concentrations. Here, mesozooplankton is suggested to find sinking aggregates from a large distance with the help of chemical cues (Stemmann et al. 2004). So far, there are no direct observations of Mediterranean zooplankton feeding on aggregates. Other locations suggested to have high zooplankton aggregate feeding are the oligotrophic subtropical Pacific Gyre near Hawaii and the northwest subarctic Pacific near Japan (Steinberg et al. 2008b), the Southern Ocean (Iversen et al. 2017; **Manuscript 2**), the temperate Atlantic near Ireland and the Cape Blanc filament (**Manuscript 2**; Iversen et al. 2010).

POC fluxes in the Cape Blanc filament are high, and especially in winter attenuate strongly (Iversen et al. 2010). This high attenuation has been attributed to zooplankton-mediated POC flux degradation (Iversen et al. 2010; **Manuscript 2**). During a cruise at the Cape Blanc filament in 2016 we video-recorded copepods and sinking aggregates (see methods **Manuscript 3**) and observed aggregate feeding (Fig. 27). These observations support the hypothesis that aggregate feeding also occurs in the Cape Blanc filament. Here, the large filter feeder *Paracalanus indicus* and the small copepod *Oncaea media* comprise up to 77% of the zooplankton abundance (Glushko and Lidvanov 2012), and could well be important contributors to aggregate degradation. Little is known about aggregate interactions by *Paracalanus*, but it may fragment aggregates in a similar way as *Calanus* in the Arctic (**Manuscript 3**). In other regions *Oncaea sp*. has been observed to feed on aggregates

(Turner 2004; Koski et al. 2017). Therefore, these zooplankton species may contribute to POC flux attenuation on a similar scale as was measured in the Arctic (**Manuscript 3**).

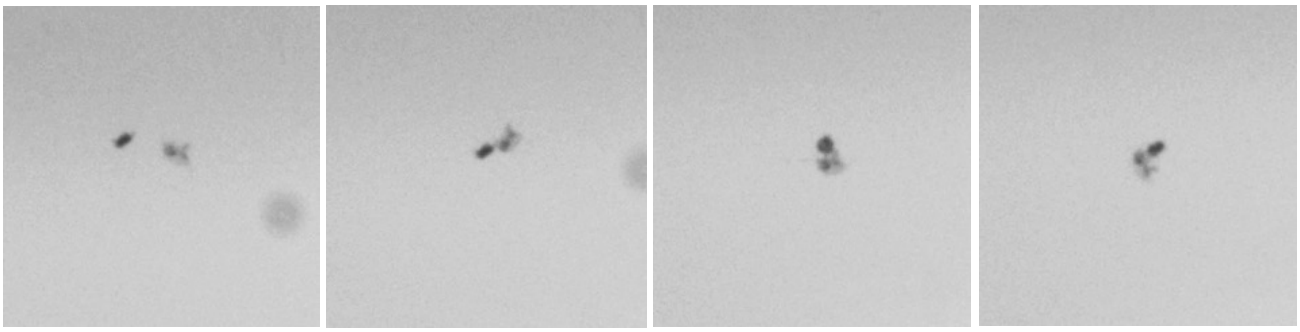

Fig. 27. An unidentified copepod swims to a sinking aggregate (dark), attaches, and feeds while spinning it around. Video recording from cruise POS495 in February 2016 in the Cape Blanc filament.

In the polar, temperate and tropical Atlantic, high POC fluxes at 100 m are often linked to high attenuation between 100 and 400 m (**Manuscript 2**). This suggests that increased primary production and subsequent POC export may stimulate the zooplankton community, leading to increased aggregate feeding and therefore stronger attenuation. This way, zooplankton aggregate feeding may buffer POC export, resulting in less variation in POC fluxes below 100 m (**Manuscript 2**).

FUTURE OF ARCTIC POC EXPORT

Climate change is expected to have the strongest effect on polar regions. In the Arctic, between 1958 and 2018 sea ice thickness has decreased by 66% and the area covered by multi-year ice has halved (Kwok 2018). This drastic change in sea-ice cover has profound effects on primary production and POC export. Between 1998 and 2012, primary production in the Arctic Ocean has increased by 30% (Arrigo and van Dijken 2015). As a result of earlier sea-ice breakup, primary production will start earlier and continue over longer time periods (Wassmann and Reigstad 2011). However, higher primary production may not directly lead to higher POC export, as phytoplankton size is expected to shift from large diatoms to small picoplankton (Li et al. 2009), resulting in lower aggregation and slower sinking velocities of aggregates.

Over the last decades in the Arctic, primary production has been extremely high at the beginning of the spring, while the heterotrophic community (i.e. zooplankton) was still relatively small and unable to degrade the massive amount of newly fixed POC (Wassmann and Reigstad 2011). This resulted in a high POC export in early spring. However, as the productive season will extend, the heterotrophic community is able to better keep up with

primary production rates (Vaqué et al. 2019), resulting in a higher degradation in the euphotic zone and thus lower POC export (Wassmann and Reigstad 2011). As a result of higher degradation in the surface, the remaining sinking aggregates may contain less nitrogen and phosphorus (Hoppe et al. 1993; Piontek et al. 2009) which renders them less nutritious for zooplankton living at depth. As the number and quality of aggregates may decrease with climate change, the quantitative importance of aggregate feeding by zooplankton may be compromised in the future.

3.3 CONCLUSIONS

Processes that affect the POC flux are primary production, aggregate formation and sinking, microbial degradation, fecal pellet production, zooplankton feeding, and ballasting. In this thesis the effect of ballasting and zooplankton aggregate grazing was investigated. I could show that these two processes are of varying importance between geographical regions, seasons and years. The magnitude of POC fluxes is controlled by primary production and the presence of ballast minerals, whereas attenuation is controlled by microbial and zooplankton degradation. Especially zooplankton-mediated degradation can cause intense but variable POC flux attenuation on temporal and geographical scales, and may even function as a buffer for POC fluxes at greater depth. The understanding of these processes is fundamental for improving and validating global carbon export models. It is therefore necessary to continue quantifying these processes in the field, thereby refining the parameterization of the biological carbon pump. Ultimately, this will enable us to improve our understanding of CO_2 sequestration in today's oceans and better predict this ocean service in the future.

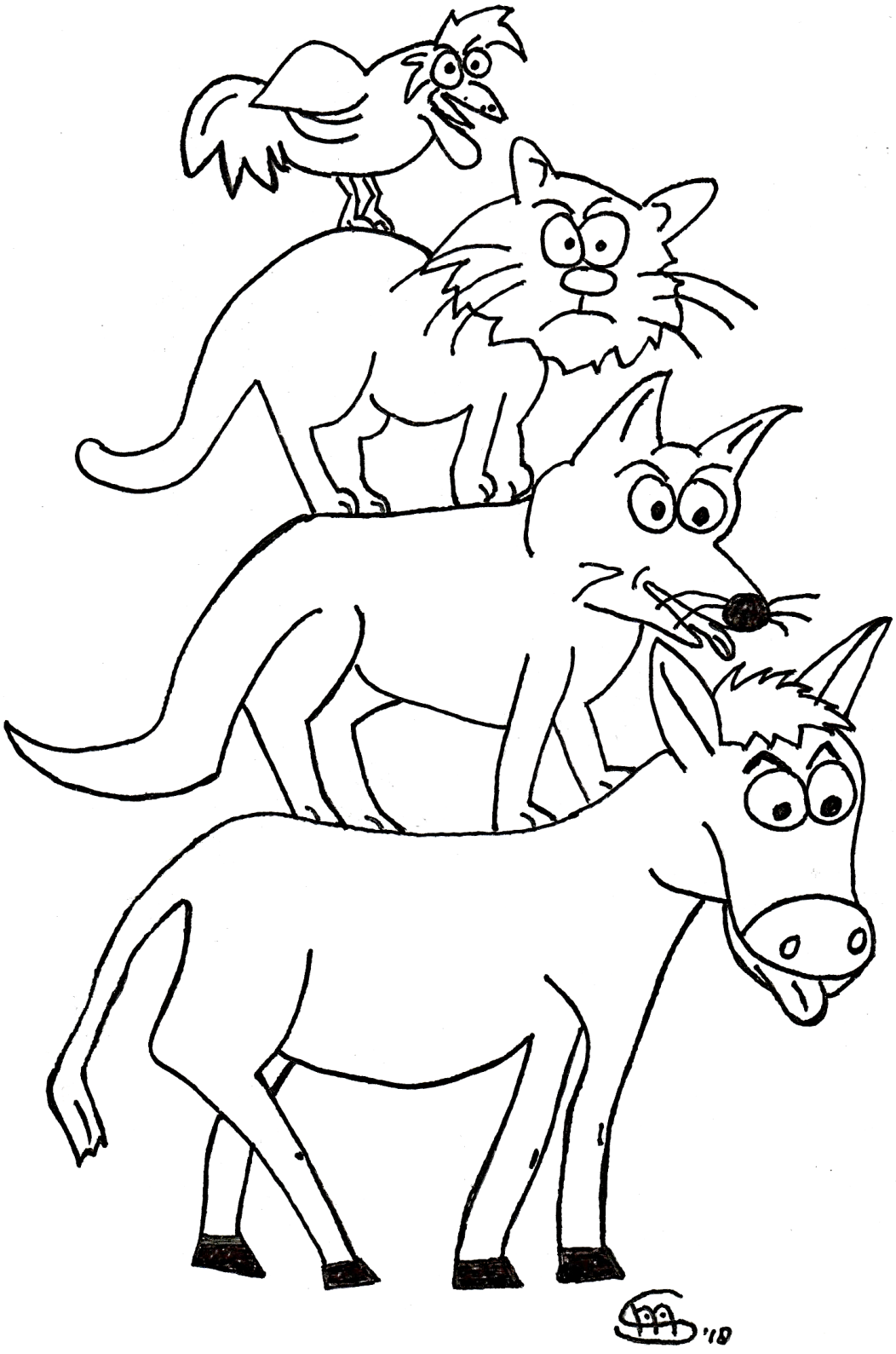

ACKNOWLEDGEMENTS

First, I would like to thank my PhD supervisor dr. Morten Iversen for his support and hard work. I am grateful for your enthusiasm, support, our lively discussions, the pimientos and jamon, the music and the fun we had on the cruises we did together. It has been a pleasure to work with someone so creative and dedicated but also so open for crazy ideas and lively brainstorm sessions.

Second, I would like to thank Christian Konrad and Clara Flintrop for the much-needed structure and chaos, the coffees and chats, the science- and nonscience-discussions, the cruise planning, packing and execution, the conferences, the experience of teaching, supervision and coaching of students together, and all the things that made the SeaPump group. Thanks to Stefan for the post-its, teas, chats, podcasts, lunches, and sharing an office with me.

Special thanks to all the people that helped with the cruises, measurements and analyses: Captains and crews of FS Poseidon, FS Maria S. Merian, FS Polarstern and FF Helmer Hanssen; Marco Klann, Götz Ruhland, Nico Nowald, Gerhard Fisher for the Poseidon cruises and drift trap deployments; Lili Hufnagel, Alessandra Cani, and Christiane Lorenzen for filtrations and C/N/BSi measurements; Ingrid Wiedmann, Nicole Hildebrandt, and Barbara Niehoff for the Helmer Hanssen cruise and zooplankton counts. Thanks to Lionel Guidi and Michal Kucera for being reviewers on this thesis and the defense. Thanks to Gerhard Fischer for the many brainstorm sessions and discussions. A big thanks to Niels, Lili, Stefan and Kathi, for proofreading this thesis and translating the summary.

To my friends in Bremen, thanks for all the fun, food and craft nights we shared. Thanks to Stefan, Christian, Anna, Laura, Clara, Lili, Sebastian, Anja, Ron, Kathi, Alven, Kathy, Sebastian, Anika, Simon and Svenja for being the friends I could always count on. To my friends and family in the Netherlands, thanks for the visits and the distractions, and supporting me these past years. To Hester, Ans, Jorn, Marcel, thanks for keeping me with two feet on the ground. Marcel, thanks for the great drawing!

To my sisters Gabriëlle and Madelinde and my parents Arjen and Erna, thanks for the many visits and the smuggled Dutch delicacies, the support and many video calls, and the coffees and lunches at the kitchen table to help me finish this thesis. And to Niels for being my "klankbord", for the support and belief until the very end, and for simply being the best boyfriend in the world.

REFERENCES

Alldredge, A. 1998. The carbon, nitrogen and mass content of marine snow as a function of aggregate size. Deep-Sea Res. I **45**: 529–541.

Alldredge, A. 2005. The contribution of discarded appendicularian houses to the flux of particulate organic carbon from oceanic surface waters, p. 315–332. *In* G. Gorsky [ed.], Response of Marine Ecosystems to Global Change: Ecological Impact of Appendicularians. GB Science Publishers- Éditions scientifiques.

Alldredge, A., and C. Gotschalk. 1988. In situ settling behavior of marine snow. Limnol. Ocean. **33**: 339–351.

Alldredge, A. L. 1972. Abandoned larvacean houses: a unique food source in the pelagic environment. Science **177**: 885–887. doi:10.1126/science.177.4052.885

Alldredge, A. L., and G. A. Jackson. 1995. Aggregation in marine systems. Deep-Sea Res. II **42**: 1–7.

Alldredge, A. L., U. Passow, and B. E. Logan. 1993. The abundance and significance of a class of large, transparent organic particles in the ocean. Deep-Sea Res. I **40**: 1131–1140.

Alldredge, A. L., and M. W. Silver. 1988. Characteristics, dynamics and significance of marine snow. Prog. Oceanogr. **20**: 41–82.

Alonso-González, I. J., J. Arístegui, C. Lee, A. Sanchez-Vidal, A. Calafat, J. Fabrés, P. Sangrá, and E. Mason. 2013. Carbon Dynamics within Cyclonic Eddies: Insights from a Biomarker Study D.A. Campbell [ed.]. PLoS One **8**: e82447. doi:10.1371/journal.pone.0082447

Anderson, L. A., and J. L. Sarmiento. 1994. Redfield ratios of remineralization determined by nutrient data analysis. Glob. Biogeochem. Cy. **8**: 65–80. doi:10.1029/93GB03318

Armstrong, R. A., C. Lee, J. I. Hedges, S. Honjo, and S. G. Wakeham. 2002. A new, mechanistic model for organic carbon fluxes in the ocean based on the quantitative association of POC with ballast minerals. Deep-Sea Res. I **49**: 219–236.

Arnkværn, G., M. Daase, and K. Eiane. 2005. Dynamics of coexisting Calanus finmarchicus, Calanus glacialis and Calanus hyperboreus populations in a high-Arctic fjord. Polar Biol. **28**: 528–538. doi:10.1007/s00300-005-0715-8

Arrigo, K. R. 2007. Carbon cycle: marine manipulations. Nature **450**: 491–492. doi:10.1038/450491a

Arrigo, K. R., and G. L. van Dijken. 2015. Continued increases in Arctic Ocean primary production. Prog. Oceanogr. **136**: 60–70. doi:10.1016/J.POCEAN.2015.05.002

Azam, F., T. Fenchel, J. Field, J. Gray, L. Meyer-Reil, and F. Thingstad. 1983. The ecological role of water column microbes in the sea. Mar. Ecol. Prog. Ser. **10**: 257–263. doi:10.2307/24814647

Azetsu-Scott, K., and U. Passow. 2004. Ascending marine particles: Significance of transparent exopolymer particles (TEP) in the upper ocean. Limnol. Oceanogr. **49**: 741–748.

Bakun, A. 1990. Coastal Ocean Upwelling. Science **247**: 198–201.

Bakun, A., B. A. Black, S. J. Bograd, M. García-Reyes, A. J. Miller, R. R. Rykaczewski, and W. J. Sydeman. 2015. Anticipated Effects of Climate Change on Coastal Upwelling Ecosystems. Curr. Clim. Chang. Reports **1**: 85–93. doi:10.1007/s40641-015-0008-4

Bathmann, U. V, T. T. Noji, M. Voss, and R. Peinert. 1987. Copepod fecal pellets: Abundance, sedimentation and content at a permanent station in the Norwegian Sea in May/June 1986. Mar. Ecol. Prog. Ser. Oldend. **38**: 45–51.

Beharro, A., L. Somoue, S. Hernández-León, and L. Valdés. 2015. Zooplankton in the Canary Current Large Marine Ecosystem, p. 183–195. *In* L. Valdés and I. Déniz-González [eds.], Oceanographic and biological featurs in the Canary Current Large Marine Ecosystem. IOC-UNESC.

Behrenfeld, M. J., and P. G. Falkowski. 1997. Photosynthetic rates derived from satellite-based chlorophyll concentration. Limnol. Oceanogr. **42**: 1–20.

Belcher, A., M. H. Iversen, C. Manno, S. A. Henson, G. A. Tarling, and R. Sanders. 2016. The role of particle associated microbes in remineralization of fecal pellets in the upper mesopelagic of the Scotia Sea, Antarctica. Limnol. Oceanogr. **61**: 1049–1064. doi:10.1002/lno.10269

Belcher, A., C. Manno, S. Thorpe, and G. Tarling. 2018. Acantharian cysts: high flux occurrence in the bathypelagic zone of the Scotia Sea, Southern Ocean. Mar. Biol. **165**: 117. doi:10.1007/s00227-018-3376-1

Berelson, W. M. 2001. The Flux of Particulate Organic Carbon Into the Ocean Interior: A comparison of Four U.S. JGOFS Regional Studies. Oceanography **14**: 59–67.

Boyd, P. W., N. D. Sherry, J. A. Berges, and others. 1999. Transformations of biogenic particulates from the pelagic to the deep ocean realm. Deep-Sea Res. II **46**: 2761–2792.

Bressac, M., C. Guieu, D. Doxaran, F. Bourrin, K. Desboeufs, N. Leblond, and C. Ridame. 2014. Quantification of the lithogenic carbon pump following a simulated dust-deposition event in large mesocosms. Biogeosciences **11**: 1007–1020.

Buesseler, K. O. 1998. The decoupling of production and particle export in the surface ocean. Glob. Biogeochem. Cy. **12**: 297–310. doi:10.1029/97GB03366

Buesseler, K. O., and P. Boyd. 2009. Shedding light on processes that control particle export and flux attenuation in the twilight zone of the open ocean. Limnol. Oceanogr. **54**: 1210–1232.

Burd, A. B., and G. A. Jackson. 2009. Particle Aggregation. Ann. Rev. Mar. Sci. **1**: 65:90.

Van Camp, L., L. Nykjaer, E. Mittelstaedt, and P. Schlittenhardt. 1991. Upwelling and boundary circulation off Northwest Africa as depicted by infrared and visible satellite observations. Prog. Oceanogr. **26**: 357–402.

Canadell, J. G., C. Le Quéré, M. R. Raupach, and others. 2007. Contributions to accelerating atmospheric CO2 growth from economic activities, carbon intensity, and efficiency of natural sinks. Proc. Nat. Ac. Sci. USA **104**: 18866–18870.

Carr, M. E. 2002. Estimations of potential productivity in Eastern Boundary Currents using remote sensing. Deep-Sea Res. I **49**: 59–80.

Chavez, F. P., M. Messié, J. Timothy Pennington, and J. T. Pennington. 2011. Marine Primary Production in Relation to Climate Variability and Change. Ann. Rev. Mar. Sci. **3**: 227–260. doi:10.1146/annurev.marine.010908.163917

Christiansen, S., H. J. Hoving, F. Schütte, and others. 2018. Particulate matter flux interception in oceanic mesoscale eddies by the polychaete Poeobius sp. Limnol. Oceanogr. **63**: 2093–2109. doi:10.1002/lno.10926

Cropper, T. E., E. Hanna, and G. R. Bigg. 2014. Spatial and temporal seasonal trends in coastal upwelling off Northwest Africa, 1981–2012. Deep-Sea Res. I **86**: 94–111. doi:10.1016/J.DSR.2014.01.007

Dagg, M. 1993. Sinking particles as a possible source of nutrition for the large calanoid copepod Neocalanus cristatus in the subarctic Pacific Ocean. Deep-Sea Res. I **40**: 1431–1445. doi:10.1016/0967-0637(93)90121-I

Daly, K. L., D. W. R. Wallace, W. O. Smith, A. Skoog, R. Lara, M. Gosselin, E. Falck, and P. L. Yager. 1999. Non-Redfield carbon and nitrogen cycling in the Arctic: Effects of ecosystem structure and dynamics. J. Geophys. Res. Ocean. **104**: 3185–3199. doi:10.1029/1998JC900071

Dardel, C., L. Kergoat, P. Hiernaux, E. Mougin, M. Grippa, and C. J. Tucker. 2014. Re-greening Sahel: 30 years of remote sensing data and field observations (Mali, Niger). Remote Sens. Environ. **140**: 350–364. doi:10.1016/J.RSE.2013.09.011

Dickson, R. R. 1986. Nepheloid layers on the continental slope west of Porcupine Bank [E. North Atlantic] Dickson, R.R. and I.N. McCave, 1986. Deep-Sea Res., 33(6A):791–818. Deep Sea Res. Part B. Oceanogr. Lit. Rev. **33**: 1012. doi:10.1016/0198-0254(86)94414-6

Diercks, A. R., and V. L. Asper. 1997. In situ settling speeds of marine snow aggregates below the mixed layer: Black Sea and Gulf of Mexico. Deep-Sea Res. I **44**: 385–398.

Dilling, L., and A. L. Alldredge. 2000. Fragmentation of marine snow by swimming macrozooplankton: A new process impacting carbon cycling in the sea. Deep-Sea Res. I **47**: 1227–1245.

Dilling, L., J. Wilson, D. Steinberg, and A. Alldredge. 1998. Feeding by the euphausiid Euphausia pacifica and the copepod Calanus pacificus on marine snow. Mar. Ecol. Prog. Ser. **170**: 189–201. doi:10.3354/meps170189

Dittmar, T., and G. Kattner. 2003. The biogeochemistry of the river and shelf ecosystem of the Arctic Ocean: A review. Mar. Chem. **83**: 103–120. doi:10.1016/S0304-4203(03)00105-1

Doney, S. C. 2006. The Dangers of Ocean Acidification. Sci. Am. **294**: 58–65.

Ducklow, H. W., S. C. Doney, and D. K. Steinberg. 2009. Contributions of Long-Term Research and Time-Series Observations to Marine Ecology and Biogeochemistry. Ann. Rev. Mar. Sci. **1**: 279–302. doi:10.1146/annurev.marine.010908.163801

Ducklow, H. W., D. K. Steinber, and K. O. Buesseler. 2001. Upper Ocean Carbon Export and the Biological Pump. Oceanography **14**: 50–58.

Dunne, J. P., J. L. Sarmiento, and A. Gnanadesikan. 2007. A synthesis of global particle export from the surface ocean and cycling through the ocean interior and on the seafloor. Glob. Biogeochem. Cy. **21**: GB4006.

Ebersbach, F., and T. W. Trull. 2008. Sinking particle properties from polyacrylamide gels during the Kerguelen Ocean and Plateau compared Study (KEOPS): Zooplankton control of carbon export in an area of persistent natural iron inputs in the Southern Ocean. Limnol. Oceanogr. **53**: 212–224.

Engel, A. 2000. The role of transparent exopolymer particles (TEP) in the increase in apparent particle stickiness (a) during the decline of a diatom bloom. J. Plankton Res. **22**: 485–497.

Engel, A., L. Abramson, J. Szlosek, Z. Liu, G. Steward, D. Hirschberg, and C. Lee. 2009a. Investigating the effect of ballasting by CaCO3 in Emiliania huxleyi, II: Decomposition of particulate organic matter. Deep-Sea Res. I **56**: 1408–1419.

Engel, A., J. Szlosek, L. Abramson, Z. Liu, and C. Lee. 2009b. Investigating the effect of ballasting by CaCO3 in Emiliania huxleyi: I. Formation, settling velocities and physical properties of aggregates. Deep-Sea Res. I **56**: 1396–1407.

Eppley, R. W., A. F. Carlucci, O. Holm-Hansen, D. Kiefer, J. J. McCarthy, E. Venrick, and P. M. Williams. 1971. Phytoplankton growth and composition in shipboard cultures supplied with nitrate, ammonium, or urea as the nitrogen source. Limnol. Oceanogr. **16**: 741–751. doi:10.4319/lo.1971.16.5.0741

Fadeev, E., I. Salter, V. Schourup-Kristensen, and others. 2018. Microbial Communities in the East and West Fram Strait During Sea Ice Melting Season. Front. Mar. Sci. **5**: 429. doi:10.3389/fmars.2018.00429

Fahl, K., and E. Nöting. 2007. Lithogenic and biogenic particle fluxes on the Lomonosov Ridge (central Arctic Ocean) and their relevance for sediment accumulation: Vertical vs. lateral transport. Deep-Sea Res. I **54**: doi:10.1016/j.drs.2007.04.014.

Falkowski, P. G., R. T. Barber, and V. Smetacek. 1998. Biogeochemical controls and feedbacks on ocean primary productivity,.

Fehrenbacher, J. S., A. D. Russell, C. V. Davis, H. J. Spero, E. Chu, and B. Hönisch. 2018. Ba/Ca ratios in the non-spinose planktic foraminifer Neogloboquadrina dutertrei : Evidence for an organic aggregate microhabitat. Geochim. Cosmochim. Acta. doi:10.1016/j.gca.2018.03.008

Field, C. B., M. J. Behrenfeld, J. T. Randerson, and P. Falkowski. 1998. Primary production of the biosphere: Integrating terrestrial and oceanic components. Science **281**: 237–240. doi:10.1126/SCIENCE.281.5374.237

Fischer, G., and G. Karakas. 2009. Sinking rates and ballast composition of particles in the Atlantic Ocean: implications for the organic carbon fluxes to the deep ocean. Biogeosciences **6**: 85–102.

Fischer, G., G. Karakas, M. Blaas, and others. 2009a. Mineral ballast and particle settling rates in the coastal upwelling system off NW Africa and the South Atlantic. Int. J. Earth Sci. **98**: 281–298.

Fischer, G., C. Reuter, G. Karakas, N. Nowald, and G. Wefer. 2009b. Offshore advection of particles within the Cape Blanc filament, Mauritania: Results from observational and modelling studies. Prog. Oceanogr. **83**: 322–330.

Fischer, G., O. Romero, U. Merkel, and others. 2016. Deep ocean mass fluxes in the coastal upwelling off Mauritania from 1988 to 2012: variability on seasonal to decadal timescales. Biogeosciences **13**: 3071–3090.

Fischer, G., O. Romero, E. Toby, and others. 2019. Changes in the dust-influenced biological carbon pump in the Canary Current System: implications from a coastal and an offshore sediment trap record off Cape Blanc, Mauritania. Glob. Biogeochem. Cy. 2019GB006194. doi:10.1029/2019GB006194

Fontaine, B., P. Roucou, M. Gaetani, and R. Marteau. 2011. Recent changes in precipitation, ITCZ convection and northern tropical circulation over North Africa (1979-2007). Int. J. Climatol. **31**: 633–648.

Francois, R., S. Honjo, R. Krishfield, and S. Manganini. 2002. Factors controlling the flux of organic carbon to the bathypelagic zone of the ocean. Glob. Biogeochem. Cy. **16**: 1087.

Friese, C. A., M. M. van der Does, U. Merkel, M. H. Iversen, G. Fischer, and J. B. W. Stuut. 2016. Environmental factors controlling the seasonal variability in particle size distribution of modern Saharan dust deposited off Cape Blanc. Aeolian Res. **22**: 165–179. doi:10.1016/j.aeolia.2016.04.005

Friese, C. A., J. A. van Hateren, C. Vogt, G. Fischer, J.-B. W. Stuut, H. van Hateren, C. Vogt, and G. Fischer. 2017. Seasonal provenance changes of present-day Saharan dust collected on- and offshore Mauritania. Atmos. Chem. Phys. **17**: 10163–10193.

Frignani, M., T. Courp, J. K. Cochran, D. Hirschberg, and L. Vitoria I Codina. 2002. Scavenging rates and particle characteristics in and near the Lacaze-Duthiers submarine canyon, northwest Mediterranean. Cont. Shelf Res. **22**: 2175–2190. doi:10.1016/S0278-4343(02)00078-X

Gaonkar, C. A., and A. C. Anil. 2010. What do barnacle larvae feed on? Implications in biofouling ecology. J. Mar. Biol. Assoc. United Kingdom **90**: 1241–1247. doi:10.1017/S0025315409991238

Gärdes, A., M. H. Iversen, H. Grossart, U. Passow, and M. S. Ullrich. 2010. Diatom-associated bacteria are required for aggregation of Thalassiosira weissflogii. ISME J. 1–10.

Giering, S. L. C., R. Sanders, R. S. Lampitt, and others. 2014. Reconciliation of the carbon budget in the ocean's twilight zone. Nature **507**: 480–483. doi:10.1038/nature13123

Glushko, O. G., and V. V Lidvanov. 2012. Composition and Structure of the Zooplankton in Coastal Waters of Mauritania in Winter. J. Sib. Fed. Univ. Biol. **5**: 136–150.

Goldthwait, S. A., C. A. Carlson, G. K. Henderson, and A. L. Alldredge. 2005. Effects of physical fragmentation on remineralization of marine snow. Mar. Ecol. Prog. Ser. **305**: 59–65.

Goldthwait, S., J. Yen, J. Brown, and A. Alldredge. 2004. Quantification of marine snow fragmentation by swimming euphausiids. Limnol. Oceanogr. **49**: 940–952.

González, H. E., and V. Smetacek. 1994. The possible role of the cyclopoid copepod Oithona in retarding vertical flux of zooplankton faecal material. Mar. Ecol. Prog. Ser. **113**: 233–246.

Goossens, D., and Z. Y. Offer. 2000. Wind tunnel and field calibration of six aeolian dust samplers. Atmos. Environ. **34**: 1043–1057. doi:10.1016/S1352-2310(99)00376-3

Green, E. P., and M. J. Dagg. 1997. Mesozooplankton associations with medium to large marine snow aggregates in the northern Gulf of Mexico. J. Plankton Res. **19**: 435–447.

Green, E. P., R. P. Harris, and A. Duncan. 1992. The production and ingestion of faecal pellets by nauplii of marine calanoid copepods. J. Plankton Res. **14**: 1631–1643.

Grossart, H. P., G. Czub, and M. Simon. 2006. Algae-bacteria interactions and their effects on aggregation and organic matter flux in the sea. Environ. Microbiol. **8**: 1074–1084.

Grossart, H. P., and M. Simon. 1998. Bacterial colonization and microbial decomposition of limnetic organic aggregates (lake snow). Aquat. Microb. Ecol. **15**: 127–140.

Grote, U., A. Pasternak, E. Arashkevich, E. Halvorsen, and A. Nikishina. 2015. Thermal response of ingestion and egestion rates in the Arctic copepod Calanus glacialis and possible metabolic consequences in a warming ocean. Polar Biol. **38**: 1025–1033. doi:10.1007/s00300-015-1664-5

Gruber, N., M. Gloor, S. E. Mikaloff Fletcher, and others. 2009. Oceanic sources, sinks, and transport of atmospheric CO2. Glob. Biogeochem. Cy. **23**: doi:10.1029/2008GB003349.

Hall, I. R., S. Schmidt, I. N. Mccave, and J. L. Reyss. 2000. Particulate matter distribution and Th / U disequilibrium along the Northern Iberian Margin : implications for particulate organic carbon export. Deep. Res. **47**: 557–582.

Hamm, C. E. 2002. Interactive aggregation and sedimentation of diatoms and clay-sized lithogenic material. Limnol. Oceanogr. **47**: 1790–1795.

Hansell, D. A., C. A. Carlson, D. J. Repeta, and R. Schlitzer. 2009. Dissolved organic matter in the ocean. Oceanography **22**: 202–211.

Hedges, J. I. 1992. Global biogeochemical cycles: Progress and problems. Mar. Chem. **39**: 67–93.

Hernández-León, S., M. Gómez, M. Pagazaurtundua, A. Portillo-Hahnefeld, I. Montero, and C. Almeida. 2001. Vertical distribution of zooplankton in Canary Island waters: Implications for export flux. Deep-Sea Res. I **48**: 1071–1092. doi:10.1016/S0967-0637(00)00074-1

Hill, V., and G. Cota. 2005. Spatial patterns of primary production on the shelf, slope and basin of the Western Arctic in 2002. Deep-Sea Res. I **52**: 3344–3354. doi:10.1016/J.DSR2.2005.10.001

Hoppe, H. G., H. W. Ducklow, and B. Karrasch. 1993. Evidence for the dependency of bacterial growth on enzymatic hydrolysis of particulate organic matter in the mesopelagic Ocean. Mar. Ecol. Prog. Ser **93**: 277–283.

Huston, M. A., and S. Wolverton. 2009. The global distribution of net primary production: Resolving the paradox. Ecol. Monogr. **79**: 343–377. doi:10.1890/08-0588.1

IPCC. 2014. Climate Change 2014: Synthesis report. Contribution of Working Groups I, II and III to the Fifth Assessment Report of the Intergovernmental Panel on Climate Change, Core Writing Team, R.K. Pachauri, and L.A. Meyer [eds.].

Ittekkot, V. 1993. The abiotically driven biological pump in the ocean and short-term fluctuations in atmospheric CO2 contents. Glob. Planet. Change **8**: 17–25. doi:10.1016/0921-8181(93)90060-2

Iversen, M. H., N. Nowald, H. Ploug, G. A. Jackson, and G. Fischer. 2010. High resolution profiles of vertical particulate organic matter export off Cape Blanc, Mauritania: Degradation processes and ballasting effects. Deep-Sea Res. I **57**: 771–784.

Iversen, M. H., E. A. Pakhomov, B. P. V. Hunt, H. van der Jagt, D. Wolf-Gladrow, and C. Klaas. 2017. Sinkers or floaters? Contribution from salp pellets to the export flux during a large bloom event in the Southern Ocean. Deep-Sea Res. II **138**: 116–125. doi:10.1016/j.dsr2.2016.12.004

Iversen, M. H., and H. Ploug. 2010. Ballast minerals and the sinking carbon flux in the ocean: Carbon-specific respiration rates and sinking velocity of marine snow aggregates. Biogeosciences **7**: 2613–2624.

Iversen, M. H., and H. Ploug. 2013. Temperature effects on carbon-specific respiration rate and sinking velocity of diatom aggregates - potential implications for deep ocean export processes. Biogeosciences **10**: 4073–4085.

Iversen, M. H., and L. K. Poulsen. 2007. Coprorhexy, coprophagy, and coprochaly in the copepods Calanus helgolandicus, Pseudocalanus elongatus, and Oithona similis. Mar. Ecol. Prog. Ser. **350**: 79–89.

Iversen, M. H., and M. L. Robert. 2015. Ballasting effects of smectite on aggregate formation and export from a natural plankton community. Mar. Chem. **175**: 18–27.

Jackson, G. A. 1993. Flux feeding as a Mechanism for Zooplankton Grazing and Its Implications for Vertical Particulate Flux. Limnol. Oceanogr. **38**: 1328–1331.

Jackson, G. A., and D. M. Checkley Jr. 2011. Particle size distributions in the upper 100 m water column and their implications for animal feeding in the plankton. Deep-Sea Res. I **58**: 283–297. doi:10.1016/j.dsr.2010.12.008

van der Jagt, H., C. Friese, J.-B. W. J.-B. W. Stuut, G. Fischer, and M. H. Iversen. 2018. The ballasting effect of Saharan dust deposition on aggregate dynamics and carbon export: Aggregation, settling, and scavenging potential of marine snow. Limnol. Oceanogr. **63**: 1386–1394. doi:10.1002/lno.10779

Jickells, T. D., Z. S. An, K. K. Andersen, and others. 2005. Global iron connections between desert dust, ocean biogeochemistry, and climate. Science **308**: 67–71.

Karakaş, G., N. Nowald, M. Blaas, and others. 2006. High-resolution modeling of sediment erosion and particle transport across the northwest African shelf. J. Geophys. Res. **111**:

doi:10.1029/2005JC003296. doi:10.1029/2005JC003296

Kiorboe, T. 2008. Particle encounter by advection, p. 57–82. *In* A mechanistic approach to plankton ecology. Princeton University Press.

Kiørboe, T. 2000. Colonization of marine snow aggregates by invertebrate zooplankton: Abundance, scaling, and possible role. Limnol. Oceanogr. **45**: 479–484.

Kiørboe, T., H. P. Grossart, H. Ploug, and K. Tang. 2002. Mechanisms and Rates of Bacterial Colonization of Sinking Aggregates. Appl. Environ. Microbiol. **68**: 3996–4006.

Kiørboe, T., H. P. Grossart, H. Ploug, K. Tang, and B. Auer. 2004. Particle-associated flagellates: swimming patterns, colonization rates, and grazing on attached bacteria. Aquat. Microb. Ecol. **35**: 141–152.

Kiørboe, T., and U. H. Thygesen. 2001. Fluid motion and solute distribution around sinking aggregates. II. Implications for remote detection by colonizing zooplankters. Mar. Ecol. Prog. Ser. **211**: 15–25.

Kiørboe, T., P. Tiselius, B. Mitchell-Innes, J. L. S. Hansen, A. W. Visser, and X. Mari. 1998. Intensive aggregate formation with low vertical flux during an upwelling-induced diatom bloom. Limnol. Oceanogr. **43**: 104–116.

Klaas, C., and D. E. Archer. 2002. Association of sinking organic matter with various types of mineral ballast in the deep sea; implications for the rain ratio. Glob. Biogeochem. Cy. **16**: 1116.

Koroleff, F. 1983. Determination of silicon, p. 174–183. *In* K. Grasshoff, M. Ehrhardt, and K. Kremling [eds.], Methods of Seawater Analysis. Verlag Chemie.

Korte, L. F., G.-J. A. Brummer, M. van der Does, and others. 2017. Downward particle fluxes of biogenic matter and Saharan dust across the equatorial North Atlantic. Atmos. Chem. Phys. **17**: 6023–6040. doi:10.5194/acp-17-6023-2017

Koski, M., J. Boutorh, and C. De La Rocha. 2017. Feeding on dispersed vs. aggregated particles: The effect of zooplankton feeding behavior on vertical flux. PLoS One **12**. doi:10.1371/journal.pone.0177958

Koski, M., W. K. Breteler, and N. Schogt. 1998. Effect of food quality on rate of growth and development of the pelagic copepod Pseudocalanus elongatus (Copepoda, Calanoida). Mar. Ecol. Prog. Ser. **170**: 169–187.

Koski, M., T. Kiørboe, and K. Takahashi. 2005. Benthic life in the pelagic: Aggregate encounter and degradation rates by pelagic harpacticoid copepods. Limnol. Oceanogr. **50**: 1254–1263.

Koski, M., E. F. Moller, M. Maar, and A. W. Visser. 2007. The fate of discarded appendicularian houses: degradation by the copepod, Microsetella norvegica, and other agents. J. Plankton Res. **29**: 641–654.

Kusserow, H. 2017. Desertification, resilience, and re-greening in the African Sahel-a matter of the observation period? Earth Syst. Dyn. **8**: 1141–1170. doi:10.5194/esd-8-1141-2017

Kwok, R. 2018. Arctic sea ice thickness, volume, and multiyear ice coverage: losses and coupled

variability (1958–2018). Environ. Res. Lett. **13**: 105005. doi:10.1088/1748-9326/aae3ec

Kwon, E. Y., F. Primeau, and J. L. Sarmiento. 2009. The impact of remineralization depth on the air-sea carbon balance. Nat. Geosci. **2**: doi:10.1038/NGEO612. doi:10.1038/NGEO612

De La Rocha, C. L., and U. Passow. 2007. Factors influencing the sinking of POC and the efficiency of the biological carbon pump. Deep-Sea Res. I **54**: 639–658. doi:10.1016/j.dsr2.2007.01.004

Lam, P. J., and J. K. B. Bishop. 2007. High biomass, low export regimes in the Southern Ocean. Deep-Sea Res. II **54**: 601–638.

Lampitt, R. S., E. P. Achterberg, T. R. Anderson, and others. 2008. Ocean Fertilization: A Potential Means of Geoengineering? Phil. Trans. R. Soc. A **366**: 3919–3945.

Lampitt, R. S., W. R. Hilier, P. G. Challenor, W. R. Hillier, and P. G. Challenor. 1993. Seasonal and diel variation in the open ocean concentration of marine snow aggregates. Nature **362**: 737–739. doi:10.1038/362737a0

Lampitt, R. S., T. Noji, and B. V Bodungen. 1990. What happens to zooplankton fecal pellets? Implications for material flux. Mar. Biol **104**: 15–23.

Lampitt, R. S., I. Salter, and D. Johns. 2009. Radiolaria: Major exporters of organic carbon to the deep ocean. Glob. Biogeochem. Cy. **23**: doi:10.1029/2008GB003221. doi:10.1029/2008GB003221

Lathuilière, C., V. Echevin, and M. Lévy. 2008. Seasonal and intraseasonal surface chlorophyll-a variability along the northwest African coast. J. Geophys. Res. **113**: C05007. doi:10.1029/2007JC004433

Lee, C., M. L. Peterson, S. G. Wakeham, and others. 2009. Particulate organic matter and ballast fluxes measured using time-series and settling velocity sediment traps in the northwestern Mediterranean Sea. Deep-Sea Res. I **56**: 1420–1436.

Legendre, L., and R. B. Rivkin. 2002. Fluxes of carbon in the upper ocean: regulation by food-web control nodes. Mar. Ecol. Ser. **242**: 95–109.

Li, W. K. W., F. A. McLaughlin, C. Lovejoy, and E. C. Carmack. 2009. Smallest algae thrive as the Arctic Ocean freshens. Science **326**: 539. doi:10.1126/science.1179798

Li, X., and B. E. Logan. 1997. Collision Frequencies between Fractal Aggregates and Small Particles in a Turbulently Sheared Fluid. Environ. Sci. Technol. **31**: 1237–1242.

Li, X. Y., and B. E. Logan. 2000. Settling and coagulation behaviour of fractal aggregates. Water Sci. Technol. **42**: 253–258.

Lombard, F., L. Guidi, and T. Kiørboe. 2013a. Effect of Type and Concentration of Ballasting Particles on Sinking Rate of Marine Snow Produced by the Appendicularian Oikopleura dioica B.R. MacKenzie [ed.]. PLoS One **8**: e75676. doi:10.1371/journal.pone.0075676. doi:10.1371/journal.pone.0075676

Lombard, F., and T. Kiørboe. 2010. Marine snow originating form appendicularian houses: Age-dependent settling characteristics. Deep-Sea Res. I **57**: 1304–1313;

doi:10.1016/j.dsr.2010.06.008.

Lombard, F., M. Koski, and T. Kiørboe. 2013b. Copepods use chemical trails to find sinking marine snow aggregates. Limnol. Ocean. **58**: 185–192.

Longhurst, A. R., and W. Glen Harrison. 1988. Vertical nitrogen flux from the oceanic photic zone by diel migrant zooplankton and nekton. Deep Sea Res. Part A. Oceanogr. Res. Pap. **35**: 881–889. doi:10.1016/0198-0149(88)90065-9

Lucio, P. S., L. C. B. Molion, C. de A. Valadão, F. C. Conde, A. M. Ramos, and M. L. Dias de Melo. 2012. Dynamical Outlines of the Rainfall Variability and the ITCZ Role over the West Sahel. Atmos. Clim. Sci. **02**: 337–350.

Lutz, M., K. Caldeira, R. Dunbar, and M. J. Behrenfeld. 2007. Seasonal rhythms of net primary production and particulate organic carbon flux to depth describe the efficiency of biological pump in the global ocean. J. Geophys. Res. **112**: DOI: 10.1029/2006JC003706.

Maher, B. A., J. M. Prospero, D. Mackie, D. Gaiero, P. P. Hesse, and Y. Balkanski. 2010. Global connections between aeolian dust, climate and ocean biogeochemistry at the present day and at the last glacial maximum. Earth-Science Rev. **99**: 61–97.

Marsay, C. M., R. J. Sanders, S. A. Henson, K. Pabortsava, E. P. Achterberg, and R. S. Lampitt. 2015. Attenuation of sinking particulate organic carbon flux through the mesopelagic ocean. Proc. Natl. Acad. Sci. **112**: 1089–1094. doi:10.1073/pnas.1415311112

Martin, J. H., G. A. Knauer, D. M. Karl, and W. W. Broenkow. 1987. VERTEX: carbon cycling in the northeast Pacific. Deep. Res. **34**: 267–285.

Mayor, D. J., R. Sanders, S. L. C. Giering, and T. R. Anderson. 2014. Microbial gardening in the ocean's twilight zone: Detritivorous metazoans benefit from fragmenting, rather than ingesting, sinking detritus: Fragmentation of refractory detritus by zooplankton beneath the euphotic zone stimulates the harvestable productio. Bioessays 1–6. doi:10.1002/bies.201400100

McCarthy, J. J., and J. C. Goldman. 1979. Nitrogenous nutrition of marine phytoplankton in nutrient-depleted waters. Science **203**: 670–672. doi:10.1126/science.203.4381.670

McDonnell, A. M. P., and K. O. Buesseler. 2010. Variability in the average sinking velocities of marine particles. Limnol. Ocean. **55**: doi:10.4319/lo.2010.55.5.0000.

McTainsh, G., and C. Strong. 2007. The role of aeolian dust in ecosystems. Geomorphology **89**: 39–54.

Mendez, M. J., R. Funk, and D. E. Buschiazzo. 2011. Field wind erosion measurements with Big Spring Number Eight (BSNE) and Modified Wilson and Cook (MWAC) samplers. Geomorphology **129**: 43–48.

Messié, M., and F. P. Chavez. 2015. Seasonal regulation of primary production in eastern boundary upwelling systems. Prog. Oceanogr. **134**: 1–18. doi:10.1016/J.POCEAN.2014.10.011

Mestre, M., E. Borrull, Mm. Sala, and J. M. Gasol. 2017. Patterns of bacterial diversity in the marine planktonic particulate matter continuum. ISME J. **11**: 999–1010. doi:10.1038/ismej.2016.166

Møller, E. F., P. Thor, and T. G. Nielsen. 2003. Production of DOC by Calanus finmarchicus, C. glacialis and C.hyperboreus through sloppy feeding and leakage from fecal pellets. Mar. Ecol. Prog. Ser. **262**: 185–191.

Möller, K. O., M. S. John, A. Temming, and others. 2012. Marine snow, zooplankton and thin layers: Indications of a trophic link from small-scale sampling with the Video Plankton Recorder. Mar. Ecol. Prog. Ser. **468**: 57–69. doi:10.3354/meps09984

Morata, N., and L. Seuthe. 2014. Importance of bacteria and protozooplankton for faecal pellet degradation. Oceanologia **56**: 565–581. doi:10.5697/oc.56-3.565

Muller-Krager, F. R., R. Varela, R. Thunell, H. Zhang, C. Hu, and J. Walsh. 2005. The importance of continental margins in the global carbon cycle. Geophys. Res. Lett. **32**: doi:10.1029/2004GL021346.

Naiman, R. J. 1976. Primary production, standing stock, and export of organic matter in a Mohave Desert thermal stream. Limnol. Ocean. **21**: 60–73.

Neuer, S., R. Davenport, T. Freudenthal, G. Wefer, O. Llinás, M.-J. Rueda, D. K. Steinberg, and D. M. Karl. 2002a. Differences in the biological carbon pump at three subtropical ocean sites. Geophys. Res. Lett. **29**: 32-1-32–4. doi:10.1029/2002GL015393

Neuer, S., T. Freudenthal, R. Davenport, O. Llinas, and M. J. Rueda. 2002b. Seasonality of surface water properties and particle flux along a productivity gradient off NW Africa. Deep-Sea Res. II **49**: 3561–3576.

Noji, T. T., K. W. Estep, F. MacIntyre, and F. Norrbin. 1991. Image analysis of faecal material grazed upon by three species of copepods: Evidence for coprorhexy, coprophagy and coprochaly. J. Mar. Biol. Assoc. UK **71**: 465–480.

Noji, T. T., F. Rey, L. A. Miller, K. Yngve Børsheim, and J. Urban-Rich. 1999. Fate of biogenic carbon in the upper 200 m of the central Greenland Sea. Deep-Sea Res. I **46**: 1497–1509. doi:10.1016/S0967-0645(99)00032-6

Nowald, N., M. H. Iversen, G. Fischer, V. Ratmeyer, and G. Wefer. 2015. Time series of in-situ particle properties and sediment trap fluxes in the coastal upwelling filament off Cape Blanc, Mauritania. Prog. Oceanogr. **137**: 1–11.

Ohtsuka, S., N. Kubo, M. Okada, and K. Gushima. 1993. Attachment and feeding of pelagic copepods on larvacean houses. J. Oceanogr. **49**: 115–120. doi:10.1007/BF02234012

Olli, K., P. Wassmann, M. Reigstad, and others. 2007. The fate of production in the central Arctic Ocean-top-down regulation by zooplankton expatriates? Prog. Oceanogr. **72**: 84–113. doi:10.1016/j.pocean.2006.08.002

Pabi, S., G. L. van Dijken, and K. R. Arrigo. 2008. Primary production in the Arctic Ocean, 1998-2006. J. Geophys. Res. Ocean. **113**: C08005. doi:10.1029/2007JC004578

Pabortsava, K., R. S. Lampitt, J. Benson, and others. 2017. Carbon sequestration in the deep Atlantic enhanced by Saharan dust. Nat. Geosci. **10**: 189–194. doi:10.1038/ngeo2899

Packard, T. T., and M. Gómez. 2013. Modeling vertical carbon flux from zooplankton respiration. Prog. Oceanogr. **110**: 59–68. doi:10.1016/j.pocean.2013.01.003

Passow, U. 2002. Transparent exopolymer particles (TEP) in aquatic environments. Prog. Oceanogr. **55**: 287–333.

Passow, U. 2004. Switching perspectives; do mineral fluxes determine particulate organic carbon fluxes or vice versa? Geochem. Geophys. Geosyst. **5**: Q04002.

Passow, U., and C. A. Carlson. 2012. The biological pump in a high CO2 world. Mar. Ecol. Prog. Ser. **470**: 249–271.

Passow, U., and C. L. De La Rocha. 2006. Accumulation of mineral ballast on organic aggregates. Glob. Biogeochem. Cy. **20**: GB1013.

Piontek, J., N. Händel, G. Langer, J. Wohlers, U. Riebesell, and A. Engel. 2009. Effects of rising temperature on the formation and microbial degradation of marine diatom aggregates. Aquat Microb Ecol **54**: 305–318.

Ploug, H., and H. P. Grossart. 2000. Bacterial growth and grazing on diatom aggregates: Respiratory carbon turnover as a function of aggregate size and sinking velocity. Limnol. Oceanogr. **45**: 1467–1475.

Ploug, H., S. Hietanen, and J. Kuparinen. 2002. Diffusion and advection within and around sinking, porous diatom aggregates. Limnol. Ocean. **47**: 1129–1136.

Ploug, H., M. H. Iversen, and G. Fischer. 2008a. Ballast, sinking velocity, and apparent diffusivity within marine snow and zooplankton fecal pellets: Implications for substrate turnover by attached bacteria. Limnol. Oceanogr. **53**: 1878–1886.

Ploug, H., M. H. Iversen, M. Koski, and E. T. Buitenhuis. 2008b. Production, oxygen respiration rates, and sinking velocity of copepod fecal pellets: Direct measurements of ballasting by opal and calcite. Limnol. Oceanogr. **53**: 469–476.

Ploug, H., and B. B. Jørgensen. 1999. A net-jet flow system for mass transfer and microsensor studies of sinking aggregates. Mar. Ecol. Prog. Ser. **176**: 279–290.

Pomeroy, L. R. 1974. The Ocean's Food Web, A Changing Paradigm. Bioscience **24**: 499–504. doi:10.2307/1296885

Poulsen, L. K., and M. H. Iversen. 2008. Degradation of copepod fecal pellets: key role of protozooplankton. Mar. Ecol. Prog. Ser. **367**: 1–13. doi:10.3354/meps07611

Poulsen, L. K., and T. Kiørboe. 2005. Coprophagy and coprorhexy in the copepods Acartia tonas and Temora longicornis: clearance rates and feeding behaviour. Mar. Ecol. Prog. Ser. **299**: 217–227.

R Core Team, R Development Core Team, and R Core Team. 2016. R: A language and environment for statistical computing, R.D.C. Team [ed.]. R Foundation for Statistical Computing.

Ratmeyer, V., G. Fischer, and G. Wefer. 1999. Lithogenic particle fluxes and grain size distributions in the deep ocean off Northwest Africa: Implications for seasonal changes of aeolian dust input

and downward transport. Deep-Sea Res. I **46**: 1289–1337.

Raven, J. A., and P. G. Falkowski. 1999. Oceanic sinks for atmospheric CO2. Plant, Cell Environ. **22**: 741–755.

Reigstad, M., and P. Wassmann. 2007. Does Phaeocystis spp. contribute significantly to vertical export of organic carbon? Biogeochemistry **83**: 217–234. doi:10.1007/978-1-4020-6214-8_16

Reigstad, M., C. Wexels Riser, P. Wassmann, and T. Ratkova. 2008. Vertical export of particulate organic carbon: Attenuation, composition and loss rates in the northern Barent Sea. Deep-Sea Res. I **55**: 2308–2319.

Richter, C. 1994. Regional and seasonal variability in the vertical distribution of mesozooplankton in the Greenland Sea,.

Ridame, C., J. Dekaezemacker, C. Guieu, S. Bonnet, S. L'Helguen, and F. Malien. 2014. Contrasted Saharan dust events in LNLC environments: impact on nutrient dynamics and primary production. Biogeosciences **11**: 4783–4800.

Riley, J. S., R. Sanders, C. Marsay, F. A. C. Le Moigne, E. P. Achterberg, and A. J. Poulton. 2012. The relative contribution of fast and slow sinking particles to ocean carbon export. Glob. Biogeochem. Cy. **26**: GB1026.

Roca-Martí, M., V. Puigcorbé, M. H. Iversen, M. Rutgers Van Der Loeff, C. Klaas, W. Cheah, A. Bracher, and P. Masqué. 2017. High particulate organic carbon export during the decline of a vast diatom bloom in the Atlantic sector of the Southern Ocean.doi:10.1016/j.dsr2.2015.12.007

Romero, O. E., and G. Fischer. 2017. Shift in the species composition of the diatom community in the eutrophic Mauritanian coastal upwelling: Results from a multi-year sediment trap experiment (2003–2010). Prog. Oceanogr. **159**: 31–44. doi:10.1016/J.POCEAN.2017.09.010

Saba, G. K., D. K. Steinberg, and D. A. Bronk. 2011. The relative importance of sloppy feeding, excretion, and fecal pellet leaching in the release of dissolved carbon and nitrogen by Acartia tonsa copepods. J. Exp. Mar. Bio. Ecol. **404**: 47–56. doi:10.1016/J.JEMBE.2011.04.013

Sabine, C. L., R. A. Feely, N. Gruber, and others. 2004. The Oceanic Sink for Anthropogenic CO2. Science **305**: 367–371.

Sabine, C. L., and T. Tanhua. 2010. Estimation of anthropogenic CO2 intentories in the ocean. Ann. Rev. Mar. Sci. **2**: 175–198.

Sakshaug, E. 2004. Primary and Secondary Production in the Arctic Seas, p. 57–81. *In* The Organic Carbon Cycle in the Arctic Ocean. Springer Berlin Heidelberg.

Sampei, M., H. Sasaki, A. Forest, and L. Fortier. 2012. A substantial export flux of particulate organic carbon linked to sinking dead copepods during winter 2007-2008 in the Amundsen Gulf (southeastern Beaufort Sea, Arctic Ocean). Limnol. Oceanogr. **57**: 90–96. doi:10.4319/lo.2012.57.1.0090

Sato, R., Y. Tanaka, and T. Ishimaru. 2001. House Production by Oikopleura dioica (Tunicata, Appendicularia) Under Laboratory Conditions. J. Plankton Res. **23**: 415–423.

doi:10.1093/plankt/23.4.415

Schmidt, K., C. De La Rocha, M. Gallinari, and G. Cortese. 2014. Not all calcite ballast is created equal: differing effects of foraminiferan and coccolith calcite on the formation and sinking of aggregates. Biogeosciences **11**: 135–145.

Schnetzer, A., and D. K. Steinberg. 2002. Active transport of particulate organic carbon and nitrogen by vertically migrating zooplankton in the Sargasso Sea. Mar. Ecol. Prog. Ser. **234**: 71–84.

Seuthe, L., G. Darnis, C. W. Riser, P. Wassmann, and L. Fortier. 2007. Winter–spring feeding and metabolism of Arctic copepods: insights from faecal pellet production and respiration measurements in the southeastern Beaufort Sea. Polar Biol. **30**: 427–436. doi:10.1007/s00300-006-0199-1

Shao, Y., K. H. Wyrwoll, A. Chappell, and others. 2011. Dust cycle: An emerging core theme in Earth system science. Aeolian Res. **2**: 181–204.

Siegenthaler, U., and J. L. Sarmiento. 1993. Atmospheric carbon dioxide and the ocean. Nature **365**: 119–125.

Silver, M. W., M. M. Gowing, D. C. Brownlee, and J. O. Corliss. 1984. Ciliated protozoa associated with oceanic sinking detritus. Nature **309**: 246–248. doi:10.1038/309246a0

Simon, M., H. P. Grossart, B. Schweitzer, and H. Ploug. 2002. Microbial ecology of organic aggregates in aquatic ecosystems. Aquat. Microb. Ecol. **28**: 175–211.

Smetacek, V., B. Von Bodungen, B. Knoppers, R. Peinert, F. Pollehne, P. Stegmann, and B. Zeitzschel. 1984. Seasonal stages characterizing the annual cycle of an inshore pelagic system. Rapp. P.-v. Réun. Cons. int. Explor. Mer. **183**: 126–135.

Smetacek, V. S. 1980. Zooplankton standing stock, copepod faecal pellets and particulate detritus in Kiel Bight H.J. Freeland, D.M. Farmer, and C.D. Levings [eds.]. Estuar. Coast. Mar. Sci. **11**: 477–490.

Somoue, L. S., N. Elkhiati, M. Ramdani, T. Lam Hoai, O. Ettahiri, A. Berraho, and T. Do Chi. 2005. Abundance and structure of copepod communities along the Atlantic coast of southern Morocco. Acta Adriat. **46**: 63–76.

Steinberg, D. K., C. A. Carlson, N. R. Bates, S. A. Goldthwait, L. P. Madin, and A. F. Michaels. 2000. Zooplankton vertical migration and the active transport of dissolved organic and inorganic carbon in the Sargasso Sea. Deep-Sea Res. I **47**: 137–158.

Steinberg, D. K., J. S. Cope, S. E. Wilson, and T. Kobari. 2008a. A comparison of mesopelagic mesozooplankton community structure in the subtropical and subarctic North Pacific Ocean. Deep-Sea Res. II **55**: 1615–1635. doi:10.1016/j.dsr2.2008.04.025

Steinberg, D. K., S. A. Goldthwait, and D. A. Hansell. 2002. Zooplankton vertical migration and the active transport of dissolved organic and inorganic nitrogen in the Sargasso Sea. Deep-Sea Res. I **49**: 1445–1461.

Steinberg, D. K., B. A. S. Van Mooy, K. O. Buesseler, P. W. Boyd, T. Kobari, and D. M. Karl. 2008b. Bacterial vs. zooplankton control of sinking particle flux in the ocean's twilight zone. Limnol. Oceanogr. **53**: 1327–1338. doi:10.4319/lo.2008.53.4.1327

Steinberg, D. K., M. W. Silver, C. H. Pilskaln, S. L. Coale, and J. B. Paduan. 1994. Midwater zooplankton communities on pelagic detritus (giant larvacean houses) in Monterey Bay, California. Limnol. Ocean. **39**: 1606–1620.

Stemmann, L., G. A. Jackson, and G. Gorsky. 2004. A vertical model of particle size distributions and fluxes in the midwater column that includes biological and physical processes; Part II, Application to a three year survey in the NW Mediterranean Sea. Deep-Sea Res. I **51**: 885–908. doi:10.1016/j.dsr.2004.03.002

Stemmann, L., M. Picheral, and G. Gorsky. 2000. Diel variation in the vertical distribution of particulate matter (>0.15 mm) in the NW Mediterranean Sea investigated with the Underwater Video Profiler. Deep-Sea Res. I **47**: 505–531. doi:10.1016/S0967-0637(99)00100-4

Stolzenbach, K. D. 1993. Scavenging of small particles by fast-sinking porous aggregates. Deep-Sea Res. I **40**: 359–369.

Svensen, C., C. Wexels Riser, M. Reigstad, and L. Seuthe. 2012. Degradation of copepod faecal pellets in the upper layer: role of microbial community and Calanus finmarchicus. Mar. Ecol. Prog. Ser **462**: 39–49.

Tamburini, C., M. Boutrif, M. Garel, R. R. Colwell, and J. W. Deming. 2013. Prokaryotic responses to hydrostatic pressure in the ocean - a review. Environ. Microbiol. **15**: 1262–1274. doi:10.1111/1462-2920.12084

Tamburini, C., M. Goutx, C. Guigue, and others. 2009. Effects of hydrostatic pressure on microbial alteration of sinking fecal pellets. Deep-Sea Res. I **56**: 1533–1546. doi:10.1016/J.DSR2.2008.12.035

Ternon, E., C. Guieu, M.-D. Löye-Pilot, N. Leblond, E. Bosc, B. Gasser, J. C. Miquel, and J. Martin. 2010. The impact of Saharan dust on the particulate export in the water column of the North Western Mediterranean Sea. Biogeosciences **7**: 809–826.

Thiele, S., B. M. Fuchs, R. Amann, and M. H. Iversen. 2015. Colonization in the Photic Zone and Subsequent Changes during Sinking Determine Bacterial Community Composition in Marine Snow. Appl. Environ. Microbiol. **81**: 1463–1471. doi:10.1128/AEM.02570-14

Turner, J. T. 2002. Zooplankton fecal pellets, marine snow and sinking phytoplankton blooms. Aquat. Microb. Ecol. **27**: 57–102.

Turner, J. T. 2004. The importance of small planktonic copepods and thier roles in pelagic marine food webs. Zool. Stud. **43**: 255–266.

Turner, J. T. 2015. Zooplankton fecal pellets, marine snow, phytodetritus and the ocean's biological pump. Prog. Oceanogr. **130**: 205–248. doi:10.1016/j.pocean.2014.08.005

Turner, J. T., H. Levinsen, T. G. Nielsen, and B. W. Hansen. 2001. Zooplankton feeding ecology:

Grazing on phytoplankton and predation on protozoans by copepod and barnacle nauplii in Disko Bay, West Greenland. Mar. Ecol. Prog. Ser. **221**: 209–219. doi:10.3354/meps221209

Vaqué, D., E. Lara, J. M. Arrieta, and others. 2019. Warming and CO2 Enhance Arctic Heterotrophic Microbial Activity. Front. Microbiol. **10**: 494. doi:10.3389/fmicb.2019.00494

Vinogradov, M. E. 1955. Vertical migrations of zooplankton and their importance for the nutrition of abyssal pelagic fauna. Trans. Inst. Oceanol. **13**: 71–76.

Visser, A. W. 2001. Hydromechanical signals in the plankton. Mar. Ecol. Prog. Ser. **222**: 1–24.

Visser, A. W., and G. A. Jackson. 2004. Characteristics of the chemical plume behind a sinking particle in a turbulent water column. Mar. Ecol. Prog. Ser. **283**: 55–71.

Volk, T., and M. I. Hoffert. 1985. Ocean carbon pumps: analysis of relative strengths and efficiencies in ocean-driven atmospheric CO2 changes, p. 99–110. *In* E.T. Sundquist and W.S. Broecker [eds.], The Carbon Cycle and Atmospheric CO2: Natural Variations Archean to Present. AGU.

Wang, D., T. C. Gouhier, B. A. Menge, and A. R. Ganguly. 2015. Intensification and spatial homogenization of coastal upwelling under climate change. Nature **518**: 390–394. doi:10.1038/nature14235

Wassmann, P., K. Olli, C. Wexels Riser, and C. Svensen. 2003. Ecosystem function, biodiversity and vertical flux regulation in the twillight zone, p. 279–287. *In* G. Wefer, F. Lamy, and F. Mantoura [eds.], Marine Science Frontiers for Europe. Springer-Verlag.

Wassmann, P., and M. Reigstad. 2011. Future Arctic Ocean Seasonal Ice Zones and Implications for Pelagic-Benthic Coupling. Oceanography **24**: 220–231. doi:10.5670/oceanog.2011.74

Wassmann, P., D. Slagstad, and I. Ellingsen. 2010. Primary production and climatic variability in the European sector of the Arctic Ocean prior to 2007: preliminary results. Polar Biol. **33**: 1641–1650. doi:10.1007/s00300-010-0839-3

Wexels Riser, C., P. Wassmann, K. Olli, and E. Arashkevich. 2001. Production, retention and export of zooplankton faecal pellets on and off the Iberian shelf, north-west Spain. Prog. Oceanogr. **51**: 423–441.

Wexels Riser, C., P. Wassmann, K. Olli, A. Pasternak, and E. Arashkevich. 2002. Seasonal variation in production, retention and export of zooplankton faecal pellets in the marginal ice zone and central Barents Sea. J. Mar. Syst. **38**: 175–188. doi:10.1016/S0924-7963(02)00176-8

Wexels Riser, C., P. Wassmann, M. Reigstad, and L. Seuthe. 2008. Vertical flux regulation by zooplankton in the northern Barents Sea during Arctic spring. Deep-Sea Res. I **55**: 2320–2329. doi:10.1016/J.DSR2.2008.05.006

Wiedmann, I., M. Reigstad, A. Sundfjord, and S. Basedow. 2014. Potential drivers of sinking particle's size spectra and vertical flux of particulate organic carbon (POC): Turbulence, phytoplankton, and zooplankton. J. Geophys. Res. Ocean. **119**: 6900–6917. doi:10.1002/2013JC009754

Wigley, T. M. L. 1983. The pre-industrial carbon dioxide level. Clim. Change **5**: 315–320.

doi:10.1007/BF02423528

Wilson, S. J., and R. U. Cooke. 1980. Wind erosion., p. 217–251. *In* M.J. Kirkby and R.P.C. Morgan [eds.], Soil erosion. Wiley.

Wolf, C., M. H. Iversen, C. Klaas, and K. Metfies. 2016. Limited sinking of Phaeocystis during a 12 days sediment trap study. Mol. Ecol. **25**: 3428–3435. doi:10.1111/mec.13697